UNIVERSITY OF SAAD DAHLEB OF BLIDA

Faculty of Engineering Science

Civil Engineering Department

THESIS OF MAGISTER

In Civil Engineering

Specialty: construction

USE OF THREADED BARS IN TENSION AND COMPRESSION ZONE OF BEAM COLUMN CONNECTION

By

BADIS Warda

Graduate committee:

ABED Mohamed	**Professor, USDB**	**President**
HAMMOUTENE Malek	**Professor, ENSP**	**Examiner**
BOURAHLA Noureddine	**Professor, USDB**	**Examiner**
MENADI Belkacem	**MCA, USDB**	**Supervisor**
SETHI Abdalaziz	**MCB, USDB**	**Guest**

Blida, September 2012

ملخص

في هذه الدراسة، استخدمت طريقة الأجزاء المنتهية لتحليل أربعة عشر تجربة استعملت فيها نماذج على شكل حرفT مشدودة إلى عمود كطريقة بديلة لدراسة هذا النوع من الروابط عندما تكون مدعومة بصفائح غير ملحمة لتقوية منطقتي التوتر و الشدة.وذلك باستعمال برنامج الأجزاء المنتهية ABAQUS.

تمت المصادقة على النموذج الغير مدعوم المتحصل عليه بطريقة الأجزاء المنتهية ضد اختيار تجريبي من خلال مقارنة التجريبية الحمولة- التمدد للنموذج و الاختبار التجريبي. وقد تم إدخال تعديلات على النموذج ليعكس منحنى التجربة. تم بعدها إضافة أنواع مختلفة من عناصر شكل حرف U. و البراغي الممتدة. وذلك لتحسين مقاومة الروابط.

استخدمت طريقة الانكسار وتمت مقارنة المقاومات التي قدمتها هذه الطريقة مع تلك التي وردت في السلسلة الثانية من الاختبارات.

كلمات المفاتيح :القوة، الصلابة، الليونة، الرافدة،البراغي الممتدة.

RESUME

Dans cette recherche quatorze modèles en forme de T représentant les zones de traction et compression d'un assemblage par platine d'extrémité ont été développés comme méthode alternative pour étudier le comportement de tels assemblages lorsqu'ils sont localement renforcés avec raidisseurs non soudés. Le logiciel ABAQUS été utilisé.

Le premier modèle d'élément finie représentant l'assemblage par platine d'extrémité non-renforcé a été validé contre un essai expérimental en comparant les courbes force-déplacement. Des ajustements ont été effectués sur le modèle initial pour refléter la courbe expérimentale. Différents type de renforcement ont été ajoutée au modèle de validation tels que les plats ; les éléments en U et les tiges filetée .etc. dans le but d'améliorer la résistance de l'assemblage.

La méthode des lignes de rupture a été utilisée pour déterminer l'effort résistant des différents assemblages étudiée. Ces derniers ont été comparés à ceux donnée par la méthode des éléments finie.

Mot clefs : résistance ; rigidité ; ductilité ; platine d'extrémité ; tiges filetée.

ABSTARCT

In this study, 3D Finite Element Analysis (FEA) of fourteen T-stubs to column connection was developed as an alternative method to study the behavior of such connection, when reinforced locally with non welded stiffeners in the tension and compression zone. The finite element software being used was 'ABAQUS',

A finite element representing unreinforced end plate connection was validated against an experimental test data by comparing force-displacement curves of both finite element model and test data. Adjustments were done on the finite element model to reflect test experimental data curve. To the unreinforced finite element model, different non welded stiffeners such as backing plate, channel reinforcement to threaded bars etc. were added to improve connection strength.

A yield line approach was also presented and the theoretically predicted yield loads were compared with those from the second series of tests.

Keywords: strength, stiffness, ductility, end-plate, threaded bars.

ACKNOWLEDGEMENT

In the name of **ALLAH**, The Most Gracious, most Merciful, with His permission, Alhamdulillah this study has completed.

I would like to express my sincere appreciation to Dr A.A SETHI for his guidance and encouragement during the course of this research. His advice, guidance, concern, and support throughout the project will not be forgotten.

My thanks to the jury members to whom I am very truly grateful for their time and interest to discuss my dissertation.

A great deal of appreciation is conveyed to Dr B. MENADI for his kind help and inspiration during the project.

My thanks are also extended to all lecturers and staff of the Civil Engineering Institute of Saad Dahleb University.

I would like to thank my husband for his endless love, support, and encouragement over this work and also for understanding the sacrifices required in completing this study. His encouragement provided the often needed motivation to push me through the hard times.

My heartfelt gratitude is expressed to my parents for their patience, love, prayers and support. Thanks also to my family and my family in law members for their continually encouragement and support.

My sincere and special thanks also go to my English teacher Mrs. JENNY HENRY KEBIR and to my beloved friends and classmates for being supportive and for their contributions and understanding.

Lastly but not least, thank you to all that have contributed either directly or indirectly in making this study a success.

DEDICATION

I dedicate this modest work to my son

Mohamed

TABLE OF CONTENT

CHAPTER 2 : FINITE ELEMENT MODELING AND ANALYSIS

CHAPTER 3 : THEORITICAL ANALYSIS

CHAPTER 4 : RESULTS AND ANALYSIS

CONCLUSION & RECOMMENDATION

REFERENCES

LIST OF FIGURES

LIST OF TABLES

NOTATION

Б: yield stress.

E: young's Modulus.

$\mathbf{t_f}$: thickness of the column flange.

$\mathbf{t_w}$: thickness of the column web.

h: height of the column.

b: width of the column.

Q: prying force.

B: bolt resisting force.

F: the loading.

α, β: angles between yield lines.

ΔE: total internal energy.

ΔT: external work.

m: distance from the bolt centre line to the edge of the root fillet on the column flange.

n: distance from the bolt centre line to the location of the prying force.

L, a: length of yield lines.

θ: rotation of yield lines.

$\mathbf{m_p}$: plastic moment capacity per unit length of yield line.

$\mathbf{f_{yc}}$: yield stress in the column flange.

$\mathbf{t_{fc}}$: thickness of the column flange.

$\mathbf{f_{bc}}$: yield stress in the backing plate.

$\mathbf{t_{bc}}$: thickness of the backing plate.

$\mathbf{t_p}$: thickness of the welded plate,

$\mathbf{t_w}$**:** thickness of the fillet weld.

$\sum \boldsymbol{\beta_t}$ **:** force in bolts.

$\boldsymbol{\delta}$: plastic deflection.

INTRODUCTION

1 Introduction

End plate bolted connections are primarily used to connect beams to columns or to splice two beams together. They are also used to transfer forces between members of a structure or to its supports. End plate connections are increasingly used as moment resistant connections in steel structures.

An end plate connection consists of a plate welded to end steel beam in the fabrication shop. The end plate is predrilled and then bolted on site to a column flange through corresponding holes using rows of high strength bolts or ordinary black bolts.

End plate connection is usually loaded by a combination of vertical shear force, axial force and a moment. The deformability of this connection type is mostly governed by column flange deformation capacity or end plate deformation and bolts elongation in the tension zone of the connection. This is why t-stub model has been used to model and investigate this zone.

Accurate analyses of such connections are difficult to undertake due to number of component joint and their nonlinear behavior. Bolts, welds, beam, column sections and connection geometry as well as end plate itself can all have a significant effect on the connection performance, and any one of these can cause connection failure.

Combination of simple fabrication techniques and speedy site erection have made bolted end plate connections one of the most popular methods of connecting members in structural steelwork frames.

Although simple in their use, bolted end plate connections are extremely complex in their analysis and behavior. The most accurate procedure of analysis to understand their behavior is to carry out full scale beam column connections and investigate these up to failure. Unfortunately this procedure is very expensive to undertake and needs means and

equipment and also are time consuming. Nevertheless conducting such experiments are necessary and somehow compulsory for research purposes.

Availability of well renowned finite element commercial program such as ABAQUS, ANSYS, LUSAS or PAFEC, etc. Finite element models are nowadays progressively replacing the use of full-scale tests. In full-scale tests it is usually difficult to identify causes behind structural failures, even though extensive strain-gauging instrumentation is used. Finite element models on the other hand are very suitable for making parametric analyses in which the influence of different design parameters on the connection performance can be identified.

ABAQUS is one of the finite element packages which have several features such as nodes contact elements, surface contact elements and material nonlinearity can be applicable to the problem of connection characterization.

2 Statement of problem

The column flange thickness required to resist bolt force often dictates a column section heavier than the one required satisfying strength and stability checks. In order to reduce column section, the column flange is usually reinforced with horizontal stiffener welded between opposing column flanges at beam tension flange level.

Conventional welded stiffener known as horizontal stiffener is difficult to weld by automatic processes and is particularly expensive when used on site in structural upgrading schemes. A more recently suggested form of reinforcement consists of backing plates in form of channel which have been investigated by different researches.

3 Objectives

In this research we will be investigating a new type of stiffeners, proposed by Nip and Surtees [13], by using a system of threaded bars locked against inner flange faces of the column in tension and compression zones. We will also be reviewing and investigating non welded stiffener suggested by **Zoetemeijer** [9], **Sethi** [16], and others.

4 Dissertation Outline

In order to attain the objective described above, the layout of this thesis has been divided in six chapters:

- Chapter one is an introduction to the problem considered in the research project.
- Chapter two

  In this chapter a review of previous work is described. In the first part; review of researches carried out on end plate connection, with an emphasis of their behavior, their use and design. The second part is a review of finite element work done end plate moment connections and finally detailed researches done on stiffened end plate connections are also presented.

- Chapter three

  This Chapter gives a brief description on the finite element software used i.e. **ABAQUS.** This includes a general presentation, geometrical details, material proprieties, loading, boundary conditions and analysis techniques.

  This chapter also describes different details on T-stub finite element models carried out.

- Chapter four

  The yield line theory is introduced to develop an analytical equations that define the resistance load in which the plastic hinges start to produce based on failure mechanisms proposed by some researchers.

- Chapter five

  Chapter five presents the results from the finite element analysis and the yield line method. The overall behavior of the connections and performance is discussed a well as the comparison on the resistance load given by the numerical and theoretical method, with a particular focus on the threaded bars connections.

- Chapter six

  The results are presented and summarized, recommendations are made.

CHAPTER 1

PREVIOUS WORK

1.1 Introduction

Performance of steel buildings depends upon the capacity of its load resisting members, namely, columns, beams, and connection between the members at different levels. The capacity of beam to column connections largely controls the ultimate load resisting capacity of a steel building. The most severe stresses in a connection assembly in steel buildings occur where the beam joins to the column. At this location, the force resultants in the beam must be transferred to the column through the beam to column connections, which are either welded or bolted or both [1]. End plate moment connections are commonly used in steel structure.

The first application of the end plate moment connection was in the early 1960's. The concept of end-plate moment connections was developed from research on tee stub moment connections in the late 1950's. End plate moment connections offer several advantages over tee stub moment connections: savings in material weight, smaller number of detail pieces to handle, cost savings in material [2].

End plate connections allow a great variety of structural solutions by properly modifying the connection structural detail. In particular, both rotational stiffness and flexural resistance can be properly balanced by choosing an appropriate number of bolts and their location, an appropriate end plate thickness and its geometrical configuration [3].

1.2 End plate moment connection

The end plate moment connection consists of a plate shop welded to the end of a beam that is then bolted at site to the connecting member through corresponding holes in column flange using high strength bolts. The connections are used to connect a beam to a column or to splice two beams together as shown in figure 2.1.

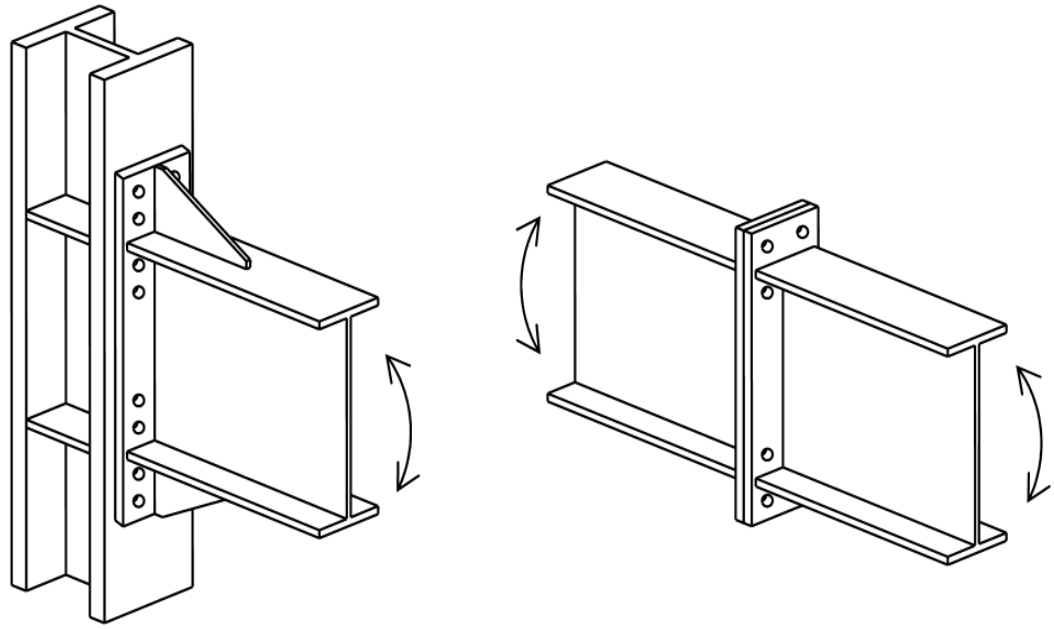

(a) Beam to column connection (b) Beam to beam connection

Figure 1.1: Typical uses for end plate moment connections.

1.3 Types of end plate moment connection

1.3.1 Flush end plate

A flush end plate connection has an end plate that does not extend beyond the outside of the connecting beam flanges as shown in figure 2.2. It can be stiffened or unstiffened. The stiffened configurations have gusset plates welded to the beam web and to the end plate.

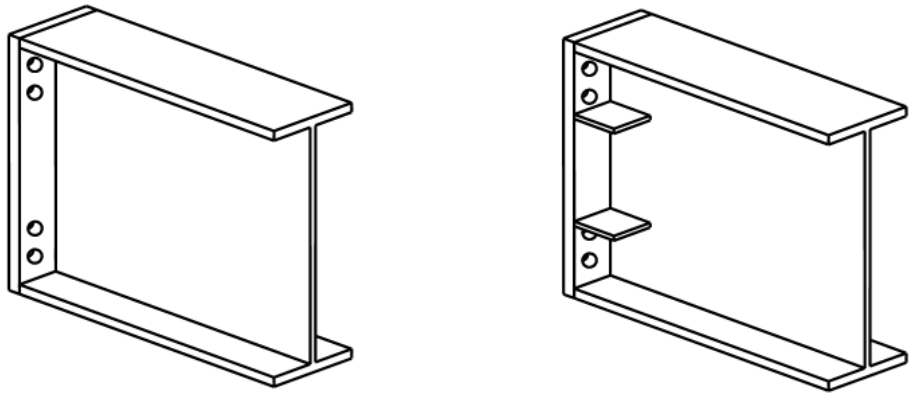

(a) Unstiffened (b) Stiffened

Figure1.2: Flush end plate connections.

1.3.2 Extended end plate

An extended end plate connection has an end plate that extends beyond the outside of the connecting beam flanges. It can be stiffened or unstiffened. The stiffened configurations have a gusset plate welded to the outside of the beam flange and to the end plate. The stiffener is aligned with the web of the connecting beam to strengthen the extended portion of the end plate.

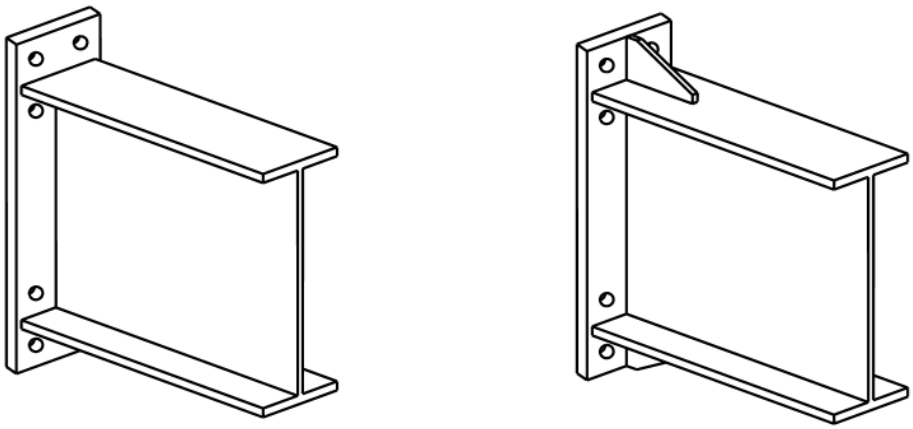

(a) Unstiffened (b) Stiffened

Figure 1.3: Extended End Plate Connections.

1.4 Advantages and disadvantages of end plate moment connection

1.4.1 Advantages

The primary advantage of moment end-plate connections are [4]:

- ✓ The connection is suitable for winter erection in that only field bolting is required.
- ✓ All welding is done in the shop, eliminating problems associated with field welding.
- ✓ Without the need for field welding, the erection process is relatively fast and generally inexpensive.
- ✓ Competitive total installed cost, for most cases.

1.4.2 Disadvantages

The primary disadvantages are that they require precise beam length and bolt hole location tolerances. This problem has been greatly reduced with the increased use of computer controlled fabrication equipment [2].

1.5 Classification of end plate moment connection

Moment end plate connections can be classified as fully restrained, FR, or partially restrained, PR, depending on the type, configuration, and end-plate stiffness [6].

1.5.1 Rigid Connection

Type FR (fully restrained), which is commonly referred as “rigid frame” (continuous frame), considers that connections have enough stiffness to maintain the angles between the connected members. In other words, a full transfer of moment and little or no relative rotation of members within the joint.

Extended moment end plate connection configurations provide sufficient stiffness for fully restrained construction [2].

1.5.2 Semi Rigid Connection

Type PR (partially restrained) assumes that the connections have insufficient stiffness to maintain the angles between the intersecting members. This type of connections requires that the strength, stiffness and ductility characteristics of the connections be considered in the analysis and design [2].

1.6 Behavior of end plate moment connection

The rotational behavior of connections is inherently nonlinear. Such behavior results from a multitude of mechanisms (figure 2.4) that include, in the particular case of bolted end plate beam to column bare steel connections [5] :

- ✓ Web panel zone deformation,
- ✓ Column flange and end plate bending deformations,
- ✓ Combined tension/bending bolt elongation,
- ✓ Beam deformations within the connecting zone,
- ✓ Weld deformations.

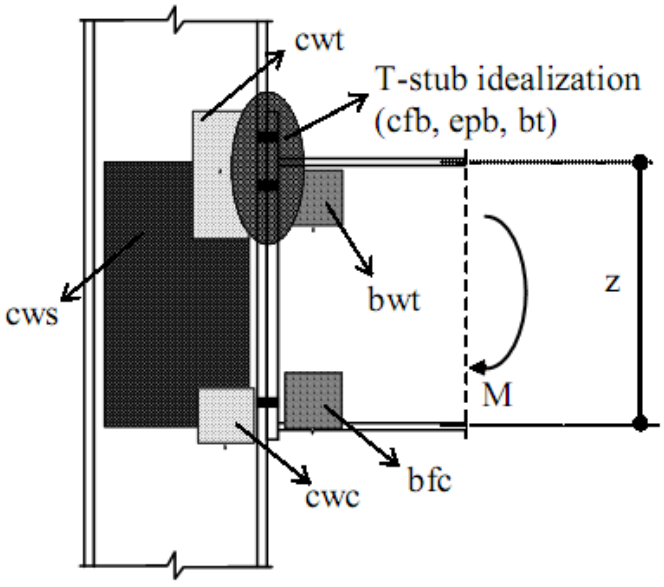

Figure 1.4: Components of bolted end plate connection.

Where:

- ✓ bwt : beam web in tension.
- ✓ bfc : beam flange in compression.
- ✓ bt : bolt in tension.
- ✓ cwt : column web in tension.
- ✓ cws : column web in shear.
- ✓ cwc : column web in compression.
- ✓ cfb : column flange in bending.
- ✓ epb : end plate in bending.

Bolted end plate beam to column connection should exhibit large rotation capacity, ideally characterized by initial yielding of the beams and column web panel zone, followed by yielding of the column flange and/or end plate under tension and elongation of the bolts [5].

1.7 Finite element analysis of end plate connections

The behaviour of end plate moment connections represents a complex problem with a large number of components that affect their behaviour. Due to the limitation of the computer resource, the finite element analysis started with simply 2-D model and linear material properties with static loading. From the late 1970s, the finite element analysis adopted 3-D model to predict accurate the nonlinearity of material and structural behaviour. A large number of studies were conducted [2].

Krishnamurthy and Graddy (1976) [7] did a comparative study to correlate the values of critical displacements and stresses obtained using 2-D and 3-D connection models. Thirteen connections were analyzed. The connections were analyzed elastically, under bolt pretension alone, and under half and full service loads They reported the results of thirteen finite element analyses of 2-D and 3-D end plate connections that showed reasonable correlations.

Packer and Morris(1977) [8] developed an analysis of the column flange failure mechanism relative to experimental observations using curved yield boundaries which accurately predict the column flange yield load in both stiffened and welded plate stiffened

connections. A recommended design approach had developed for only four bolts in the tension regions of the extended end plate connection including bolt size, suitable end plate thickness and column flange strength.

Ahuja et al. (1982) [2] investigated the elastic behavior of the eight bolt extended stiffened end plate moment connection using finite element analysis. **Ghassemieh et al. (1983)** [2] continued the work of Ahuja and included inelastic behavior.

Abolmaali et al. (1984) [2] used finite element analysis to develop a design methodology for the two bolt flush end plate moment connection configuration. Both 2-D and 3-D analyses were conducted to generate correlation coefficients. Finite element 2-D analysis was used to generate regression equations for the design of the connections. The results were adjusted by the correlation coefficients to more closely match the experimental results.

Gendron et. al. (1989) [7] presented a finite element model that takes into account the plasticity and contact in the steel bolted connections, using the finite element program MEF. The 2D model was calibrated against published test results and was shown to correctly predict the behavior of the bolted connection both before and after slip occurrence and can correctly characterize bolt behavior.

Kukreti et al. (1990) [2] used finite element modeling to conduct parametric studies to predict the bolt forces and the end plate stiffness of the eight bolt extended stiffened end-plate moment connection. Regression analysis of the parametric study data resulted in equations for predicting the end plate strength, end plate stiffness, and bolt forces. The predictions were compared to experimental results with reasonable correlation.

Rothert and Gebbeken (1992) [4] reported the study of the numerical tool, finite element modeling method, considering plastic behavior of the end plate moment connection. This study conducts the material nonlinearity, pretension effect, multi-body contact problem, and example of end plate connection. The load-deformation result showed good relationship with experimental result.

Gebbeken et al. (1994) [2] investigated the behavior of the four bolt unstiffened end-plate connection using finite element analysis. The study emphasized modeling of the nonlinear material behavior and the contact between the end plate and the column flange or

the adjacent end plate. Comparisons between the finite element analysis and experimental test results were made.

Sherbourne and Bahaari (1994) [4] developed 3-D finite element model of end plate connections using commercial code "ANSYS". The end plate, beam, column, and stiffeners were represented as plate, plastic quadrilateral shell, elements. The bolt shank was modeled using six spar elements.

Bahaari and Sherbourne (1996) [2] continued their investigation of the four bolt extended unstiffened end-plate connection by considering the effects of connecting the end plate to a stiffened and an unstiffened column flange. 3-D finite element models of the end plate and the column flange were developed using ANSYS. The finite element results were compared with experimental results with good correlation. Once again, it is concluded that 3-D finite element analysis can predict the behavior of end plate connections.

Choi and Chung (1996) [2] investigated the most efficient techniques of modeling four bolt extended unstiffened end plate connections using the finite element method.

Bose et al. (1997) [2] used the finite element method to analyze flush unstiffened end-plate connections. The two and four bolt flush end plate configurations were included in the study. Comparisons with experimental results were made with good correlation.

Bose, Wang, and Sarkar (1997) [4] reported the results of an investigation devoted to the analysis of unstiffened flush end plate bolted connection using the finite element technique. They used the commercial program "LUSAS" to analyze the nonlinear 3-D finite element model. The study included six experimental tests and its results showed good relationship with numerical test results.

Bursi and Jaspart (1998) [4] provided an overview of current developments for estimating the moment-rotation behavior of bolted moment resisting connections. In addition, a methodology for finite element analysis of end plate connections was presented.

Kokan D. (1998) [7] presented a report dealing with the finite element analysis of t -stub connections. A t-stub connection model was developed and a detailed description of

the steps undertaken for the creation of the model was presented. The finite element code ABAQUS was used for modeling of the connection.

Troup et al. (1998) [7] presented a numerical model, based on the finite element method, to predict the moment and rotation characteristics of connections. The finite element analysis of a simple t-stub connection and an extended end plate connection was carried out using ANSYS. The numerical model was calibrated against experimental results from full scale testing of bolted end plate connections. On the basis of the results obtained it was suggested that solid elements were suitable for simple connection problems but shell elements were best suited for more complicated structures like beam to column connections.

Swanson J. A. (1999) [7] investigated the strength, stiffness and ductility behavior of t-stub connections using the finite element code ABAQUS. Three connection models were analyzed. The first model was a 3D solid model incorporating contact with friction and full nonlinear properties. The second connection used 2D plane stress elements to model the stem of the t-stub while the third model used plain strain elements to model a unit width of the t-stub flange. The results obtained from the finite element models matched up quite well with the experimental data. Though the values did not exactly match up due to the various assumptions inherent in the finite element model it helped provide valuable insight to the behavior of t-stub connection.

Bahaari and Sherbourne (2000) [4] conducted 3-D finite element analysis devoted to the analysis of eight bolt extended end plate connections. They used plate, brick and truss elements to create the 3-D finite element model using the commercial program "ANSYS". The model was examined for three experimental case studies in the literature and the results compare well with experimental data in terms of both strength and stiffness.

Mays (2000) [2] used finite element analysis to develop a design procedure for an unstiffened column flange and for the sixteen bolt extended stiffened end plate moment connection. In addition, finite element models were developed and comparisons with experimental results for the four bolt extended unstiffened, eight bolt extended stiffened, and the four bolt wide unstiffened end plate moment connections were made. Good correlation with experimental results was obtained.

Sumner (2003) [4] conducted twenty experimental tests and conducted finite element analysis to develop design procedures for eight extended end plate moment connection configurations. The finite element model used two element types. The solid eight node brick elements were used to model the beam flanges and web and solid twenty node brick elements were used to model the end plate and column flange, and bolts. The analysis considered plasticity effects but the bolt pretension effect was neglected. The finite element results correlated well with the experimental results.

1.8 Reinforced end plate connections

Most of the work on reinforced end plate connections had been undertaken by a number of researchers.

1.8.1 Backing plate reinforced end plate connection

Zoetemeijer (1974) [9] developed a design method for the tension zone of statically loaded bolted beam to column connections based on the plastic behaviour of the flanges and the bolts.

The researcher also presented a formula for determining an effective length for a column flange in tension without stiffening plates between the flanges. The derivation of this formula was based on the analysis of two different collapse mechanisms. One mechanism occurs if bolts failure governs collapse; the second corresponds to the full plastification of the flange.

Experimental tests were performed to insure that the developed design rules would lead to connections that satisfy the limit state of deformation as given in the Dutch regulations for both serviceability and ultimate limit states.

Twenty –eight specimens were tested in order to compare the maximum strength capacity of the connections with the calculated design values.

The developed formulas were in good agreement with test results even when the column flanges were stiffened by a backing plates parallel to the column flanges.

D.B. Moore and P.A.C. Sims (1987) [10] investigated experimentally the influence of backing plates on extended end plate connections by testing, first, a number of t-stubs with backing plates of different lengths and, secondly, a series of cruciform connections augmented with backing plates.

The yield line approach was also presented and the theoretically predicted yield loads were compared with those from the first series of tests. The effect of backing plates on yield load and bolt load was also discussed. Finally the results from the first series of tests are compared with those from the second and the effectiveness of the t-stub idealization discussed.

Although three different modes of failure were possible for this type of connection only failure by yielding of both the column flange and backing plate had been substantiated experimentally. In all cases a 15 mm thick t-stub flange was specifically chosen to ensure failure in the column flange and backing plate assembly.

The tests were divided into three series

- ✓ T-stubs connected to short lengths of column augmented with backing plates,
- ✓ T-stub without backing plates,
- ✓ T-stub with traditional web stiffeners.

The researchers concluded that the t-stub idealization is a good representation of the tension region of an extended end plate beam to column connection with backing plates.

Backing plates are a very effective means of increasing the yield load of an extended end plate connection and provide an alternative to the traditional web stiffener. The variation of length of backing plate has a significant influence on the yield load.

The yield line approach gives a reasonable estimate of the yield load of the column flange backing plate assembly but underestimates the final collapse load .

Grogan and Surtees (1999) [11] conducted a series of fifteen t-stub tests, to investigate the behavior of end plate connections reinforced with angle plates. The angles are bolted to the flanges and web of the column, the effect of varying the thickness, length and angle lateral bolt centers of backing angle was studied.

The t-stub tests were divided into three test pieces:

- ✓ Unreinforced test pieces ,
- ✓ Test pieces reinforced with 10 mm thick traditional welded plate stiffeners,
- ✓ Test pieces with angle reinforcement.

The validity of using t-stubs for connection representation was confirmed by comparison with two conventional cruciform connection tests.

From the conducted tests, it was found that the performance of extended end plate connections in which one or both column flanges have been reinforced with bolted backing angles was found to be far superior to that of traditional welded stiffeners.

Failure loads obtained from tests on angle reinforced whole connection and t-stub specimens have indicated strength improvements of up to 210% beyond the strength of an unreinforced specimen.

It had been demonstrated that the reinforcement may be applied both to semi-rigid and fully rigid connections. Either connection type may be created by selection of an appropriate size of angle reinforcement. Strength and ductility may be controlled by choosing a suitable angle thickness.

Z. Al-Khataba, A. Bouchair (2007) [12] affected a study which aimed to analyse more precisely the behavior of t-stubs reinforced by backing plate using the finite element numerical modeling.

Such a modeling was calibrated in advance, by comparing results obtained by means of 2D and 3D models to the experimental results for elementary t-stubs (not reinforced). It was then used to make a parametrical study and to observe the evolution, during the load until the failure, of various parameters difficult to measure experimentally, such as, the prying forces and the evolution of the contact area under the t-stub flange.

Also, the model was used to make an evaluation of the Eurocode 3 formulae applied to the resistance and the stiffness of elementary t-stubs with available experimental results to calibrate the model. Afterwards, the model is applied to t-stubs reinforced by backing plates to analyze the effect of the backing plate thickness and the bolts preload.

A comparison made between 2D and 3D models allowed the researchers to define the limits of the first model. The 2D model gave satisfactory results for short t-stubs. For

some geometries, only the 3D model with consideration of the contact, the material and the geometrical nonlinearities allowed a faithful representation of the t-stub behavior. This 3D model allowed the description of various phenomena which occur during the load application on the t-stub and gave information which was difficult to obtain experimentally.

The 3D models applied to the t-stubs with backing plates showed that the resistances increase with the thickness of the backing plate. However, as care was taken to exclude any plastification of the web in the T-stub, this increase had an upper limit done by the bolt failure. This corresponded to the failure mode 2(the appearance of one plastic hinge in the flange and to the failure of the bolts in tension) which succeeds the failure mode 1(associated with the failure of the flange by forming of plastic hinges in the flange) and allowed the definition of a thickness “of transition” corresponding to this situation.

The analytical model of the EC3 gave a thickness of backing plate lower than that determined by the finite element model. This showed that a reserve of resistance and ductility exists if the resistances of t-stubs with backing plates are calculated according to the EC3.

The analytical formula proposed by the EC3 applied to the t-stubs with backing plates gave satisfactory results for the resistance in comparison with numerical results which were previously calibrated on the basis of the experimental results. So, numerical models showed that the contribution of the backing plates is interesting. This contribution was more marked if bolts with pretension are used. In that case, the backing plates produce an increase of the plastic resistance and the initial stiffness for all the tested t-stubs.

1.8.2 End plate connections reinforced with threaded bars

Nip and Surtees (2001) [13] developed a new means of providing local column reinforcement in the compression zone of end plate moment connections, using threaded bars. A system of threaded bars is locked against inner flange faces of the column to transmit the horizontal compression force from incoming beams.

Two forms of threaded bar compression stiffening element were used in the tests. The first consists of a short threaded bar with end nuts which fits between, rather than

passes through, the column flanges. The second form also has internal nuts but passes through the flanges to engage outer nuts.

Because of the large number of tests, all involving heavy sections, it was decided to confine testing mainly to compression zone specimens (t-stub specimens). Some tests on full connection specimens were, however, carried out for comparison purposes.

A threaded bar diameter of 24mm was used for most of the tests. Larger sizes of threaded bar were tested both to examine their efficiency as concentrated compression stiffening and to detect potential assembly difficulties.12 tests were studied with different threaded bar configurations.

From the conducted tests, it was shown that threaded bar compression stiffening can be an effective and viable alternative to traditional welded plate stiffening. Tests had confirmed that bearing strengths much in excess of those required for current typical end plate connections are possible.

Use of threaded bar as an effective form of tension stiffening has been considered incidentally because of its application to the whole-connection tests.

Nip and Surtees (2001) [14] on the base of their precedent work mentioned above, they described a general design method for in-line and an off-line compression rod which bears similarity to eurocode 3 approaches for bearing strength of unstiffened girder webs. For the case of in-line stiffeners only, a simple approach based on the relevant BS 5950 clauses for web resistance and strut design may be applied with only slightly more conservative results.

1.8.3 End plate connections reinforced with channels

Tagawa and Gurel [15] proposed a new stiffening method in which bolted channels are used as alternatives to traditional stiffeners. Channel members were installed between the column flanges on both sides. The researchers examined individual t-stubs instead of full connections.

Failure by column flange yielding was considered in this study; in addition, some yield line patterns based on yield line theory were applied to explain plastic behavior of the

column flange and channel flanges. Two different yield patterns based on experimental observations are applied for the column flange and channel stiffener flange.

The t-stubs were divided into three specimens:

- ✓ Test specimen without stiffeners,
- ✓ Test specimen with cold-formed channel stiffeners,
- ✓ Test specimen with hot-rolled channel stiffeners.

For every test specimen, yield loads were estimated using equations with regard to the two failure mechanisms that had been chosen.

The method of stiffening by channels was found to be effective at greatly increasing the yield load of bolted moment connections. Comparison of predicted yield loads with load displacement curves indicated that the failure mechanism based on a yield line approach gives good and reasonable conservative estimates of the yield load for all tests.

Tensile yield loads estimated and obtained from tests indicate strength improvements of 153–204% beyond the strength of the specimen without stiffeners.

The numerous type of stiffeners cited above were also studied by ***Sethi*** [16] *and* ***Aliane*** [17] *and their work are discussed as follows.*

Sethi (1987) [16] affected a theoretical study and an experimental investigation into the reinforcement of the tension flange of en extended end plate connections. New means of stiffening the tension zone of the column flange were proposed instead of traditional horizontal stiffeners. To achieve that:

- ✓ An analytical modeling of the tension zone of the end plate connection had been undertaken.
- ✓ Two series of tests on full size t-stubs/column specimens, representing the tension side of an end plate connection with various reinforcement were carried out.
- ✓ One full size beam to column connection had been tested.

Several variants of the tension zone were analyzed using PAFEK and ABAQUS programs. The influence of the stiffener shape, its thickness and length, the presence of the column web bolts and the welding of the stiffener upon column flange behaviour were studied.

A theoretical analysis of the column flange using yield line theory was performed and proposed formulae had been compared to the finite element results and to the previous work carried out by **Packer** [8].

In the experimental investigation, two series of tests on t-stub column connections were undertaken. The influence of the stiffener shape, thickness and its length upon column flange collapse was studied.

The researcher was found that the most effective way of stiffening the column flange in tension side is by using a backing channel, which can be made from angle plates welded to form a channel. Another alternative is to use angle plates bolted to the column flange.

From the test carried out on the full size beam to column connection, it was found that the angle stiffener could be used to stiffen both the tension and compression zone.

From the theoretical analysis of the column flange, it was found that some proposed patterns were more effective than the others for best prediction of the column collapse.

Aliane (2003) [17] carried out a numerical study using ANSYS software to investigate the influence of various type of reinforcement of the tension and compression zone of the end plate moment connections.

Seventeen tests were undertaken; the tests were divided into four series:

- ✓ The first series of tests contained two t-stub validation specimens chosen from the experimental work of **Sethi** [16] and **Zoetemeijer** [9].
- ✓ Two series of tests on full size t-stubs/column specimens, with different reinforcement were carried out.
- ✓ The fourth series of tests had three full size beams to columns connection. These tests were studied to check the effect of some stiffeners on the compression zone.

Several parameters were analyzed such as prying force and bolt pretension.

A theoretical analysis of the column flange using yield line theory was performed and proposed formulae had been compared to the finite element results.

Aliane found that certain stiffeners lead to an increasing in the prying force which is by itself increases the traction effort on the bolts. This point should be taken during a conception of end plate column connections. The position of the prying force obtained from the numerical results confirmed to the prediction of **Zoetemeijer** [9].

The pretension of the bolts had an effect on the tests whose bolt failure mechanism was a determining factor.

Yield line theory gave reasonable results by comparing them with the finite element yield loads.

The strength improvement of full size beam to column connections was three time 300 % beyond the strength of the unreinforced tests.

1.9 Conclusion

From what was illustrated in this chapter, it can be noted that t-stub models were used from early researches to model the tension zone for end plate moment connection.

But, is the t-stub model able to represent the deformation capacity of the compression zone?

The results found by the investigation of **Nip and Surtees** [13, 14] can prove the effectiveness of using t-stubs model to predict the deformation behavior of the compression zone rather than using full tests.

Based on that, t-stubs models divided into three series of tests will be presented in the next chapter to study their behavior in compression and tension zone after applying different element of reinforcement; these include welded plates, backing plates, channels and threaded bars.

CHAPTER 2
FINITE ELEMENT MODELLING AND ANALYSIS

2.1 Introduction

Design analysis is a process of investigating certain properties of parts, assemblies, or structures. It can be conducted on real objects or on models. The models can be physical or mathematical. Simple mathematical models can be solved analytically, but more complex models require the use of numerical methods. Finite element method (FEM) is one of those numerical methods used to solve complex mathematical models.

In recent research undertaken, finite element analysis was proven to be a successful tool in predicting the behaviour of connections. However, finite element analysis provides only approximate solution and the results still could not be applied in connection design with reasonable confidence. This is because there are various ways to perform discretization and meshing in finite element modeling process and varied analysis results may be obtained.

The total number of elements used and their variation in sizes and types are depending on engineering judgment. Therefore, finite element analysis results are compared with experimental results to determine their efficiency and reliability. A number of powerful finite element software has become commercially available.

This chapter is intended to develop a Finite Element Analysis of a t-stub to column connection using ABAQUS program.

In the first part of this chapter a description of ABAQUS and its capabilities is done. In the second part a description of idealization of tension and compression zone by

this commercial package is cited. In the third part steps of modeling are presented with the geometry of each test .An experimental work was used to calibrate the finite element model.

The dimensions of the connection will follow exactly like the one tested in the laboratory by **Sethi** [16] and the force displacement curve plotted from the result will be compared with the available experimental data. Once a finite element model of a connection is validated with the test results, the calibrated model will be the principal reference model to which different elements of reinforcement will be added.

2.2 Finite element simulation

2.2.1 Analysis software and methodology

Abaqus finite element analysis software was selected for all modeling of this project. It is a general purpose finite element simulation program and was chosen for its ability to model all necessary types of materials and behavior and the ability to solve problems ranging from relatively simple linear analyses to the most challenging nonlinear simulations.

2.2.1.1 Abaqus products

Abaqus consists of two main analysis products Abaqus/Standard and Abaqus/Explicit.

- ✓ Abaqus Standard

Abaqus/Standard is a general purpose analysis product that can solve linear and nonlinear problems by solving a system of equations implicitly at each solution "increment.

- ✓ Abaqus Implicit

Abaqus/Explicit is a special purpose analysis product that uses an explicit dynamic finite element formulation.

- ✓ Abaqus/CAE

Abaqus/CAE is the complete Abaqus environment that includes capabilities for creating Abaqus models, interactively submitting and monitoring Abaqus jobs, and evaluating results.

- ✓ Abaqus/Viewer

Abaqus/Viewer is a subset of Abaqus/CAE that includes just the post-processing functionality.

2.2.1.2 Abaqus basics

A complete Abaqus analysis usually consists of three distinct stages: preprocessing, simulation, and post-processing. These three stages are linked together by files as shown below [18]:

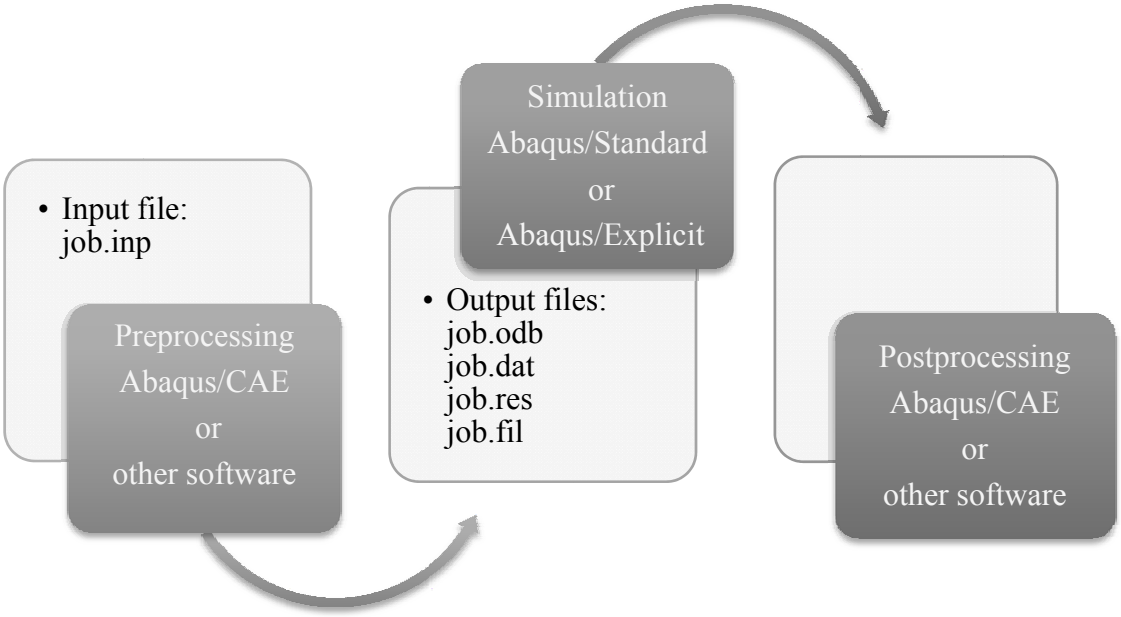

Figure 2.1: Abaqus basics.

✓ Preprocessing (Abaqus/CAE)

In this stage, the model of the physical problem will be defined and an Abaqus input file will be created.

✓ Simulation (Abaqus/Standard or Abaqus/Explicit)

The simulation is the stage in which Abaqus/Standard or Abaqus/Explicit solves the numerical problem defined in the model.

✓ Postprocessing (Abaqus/CAE)

The results can be evaluated once the simulation has been completed. The evaluation is generally done interactively using the Visualization module of Abaqus/CAE or another postprocessor.

Abaqus/CAE was used for all pre and post-processing and the Abaqus/Standard analysis was used to run the analysis. Version 6.9.1 of Abaqus was used (Simulia 2009).

2.2.1.3 Components of an Abaqus analysis model

An Abaqus model is composed of several different components that together describe the physical problem to be analyzed and the results to be obtained. At a minimum the analysis model consists of the following information [18]:

- ✓ Discretized geometry;
- ✓ Element section properties;
- ✓ Material data;
- ✓ Loads and boundary conditions;
- ✓ Analysis type;
- ✓ Output requests.

✓ Discretized geometry

Finite elements and nodes define the basic geometry of the physical structure being modeled in Abaqus. Each element in the model represents a discrete portion of the physical structure, which is, in turn, represented by many interconnected elements. Elements are connected to one another by shared nodes. The collection of all the elements and nodes in a model is called the *mesh*.

✓ Abaqus elements library

Abaqus has an extensive element library to provide a powerful set of tools for solving many different problems [19].

Five aspects of an element characterize its behaviour:

- ✓ Family;
- ✓ Degree of freedom;
- ✓ Number of nodes;
- ✓ Formulation;
- ✓ Integration.

The commonly used element families are shown in the next figure:

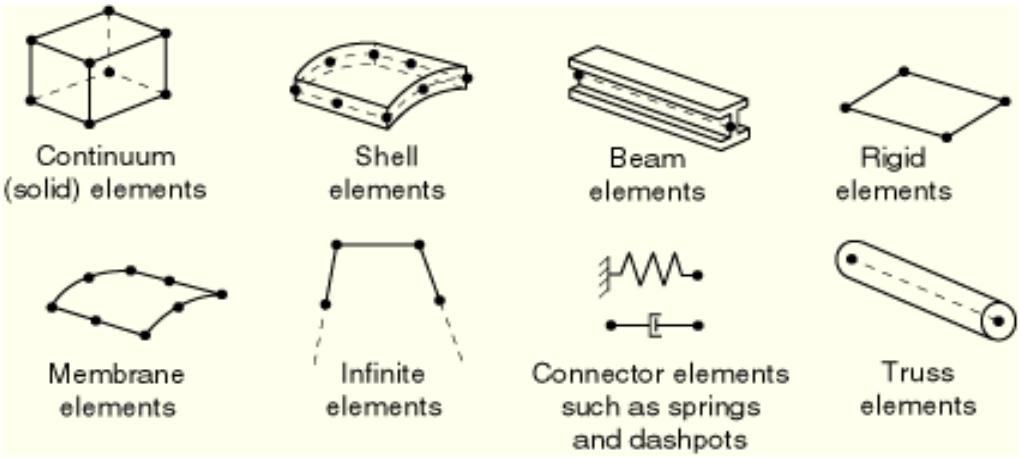

Figure 2.2: Commonly used element families [19].

- ✓ Abaqus material library

The material library in Abaqus is intended to provide comprehensive coverage of linear and nonlinear, isotropic and anisotropic material behaviors.
Material behaviors fall into the following general categories [19]:

- ✓ General properties (material damping, density, thermal expansion);
- ✓ Elastic mechanical properties;
- ✓ Inelastic mechanical properties;
- ✓ Thermal properties;
- ✓ Hydrostatic fluid properties;
- ✓ Mass diffusion properties;
- ✓ Electrical properties; and
- ✓ Pore fluid flow properties.

- ✓ Loads and boundary conditions

The most common forms of loading include [19]:

- ✓ Point loads;
- ✓ Pressure loads on surfaces;
- ✓ body forces, such as the force of gravity; and
- ✓ thermal loads.

Boundary conditions are used to constrain portions of the model to remain fixed (zero displacements) or to move by a prescribed amount (nonzero displacements).

- ✓ Analysis type

Abaqus can carry out many different types of simulations, and provides an extensive selection of analysis techniques. These techniques provide powerful tools for performing an analysis more efficiently and effectively

- ✓ Output requests

An Abaqus simulation can generate a large amount of output. To avoid using excessive disk space, can limit the output to that required for interpreting the results.

2.2.1.4 Abaqus modules

Abaqus/CAE is divided into functional units called modules; each module contains only those tools that are relevant to a specific portion of the modeling task. Abaqus allows selecting a module from the Module list in the context bar, as shown in Figure 2.3. The order of the modules in the menu corresponds to a logical sequence that may be followed to create a model [18].

Figure 2.3: Abaqus modules.

The functionality of each of those modules can be summarized in the next table:

Table 2.1: Abaqus modules and their functionality.

Module	Functionality
Part	The Part module allows creating individual parts by sketching their geometry directly in Abaqus/CAE or by importing their geometry from other geometric modeling programs.
Property	The Property module allows creating section and material definitions and assigns them to regions of parts.
Assembly	The Assembly module is used to create instances of the parts and to position the instances relative to each other in a global coordinate system.
Step	Use the Step module to create and configure analysis steps and associated output requests.
Interaction	In the Interaction module, specify mechanical and thermal interactions between regions of a model or between a region of a model and its surroundings.
Load	The Load module allows to specify loads, boundary conditions and predefined fields
Mesh	The Mesh module contains tools that allow to generate a finite element mesh on an assembly created within Abaqus/CAE
Job	The Job module allows interactively submitting a job for analysis and monitoring its progress.
Visualization	The Visualization module provides graphical display of finite element models and results.
sketch	Sketches are two-dimensional profiles that are used to help form the geometry defining an Abaqus/CAE native part.

2.2.2 Finite element modeling

2.2.2.1 Structural idealization of the tension and compression zone

To investigate the behavior of the tension and compression zone of beam to column connection as shown in the next figure, the column flange and the end plate can be considered to act as an equivalent t-stub with an effective length.

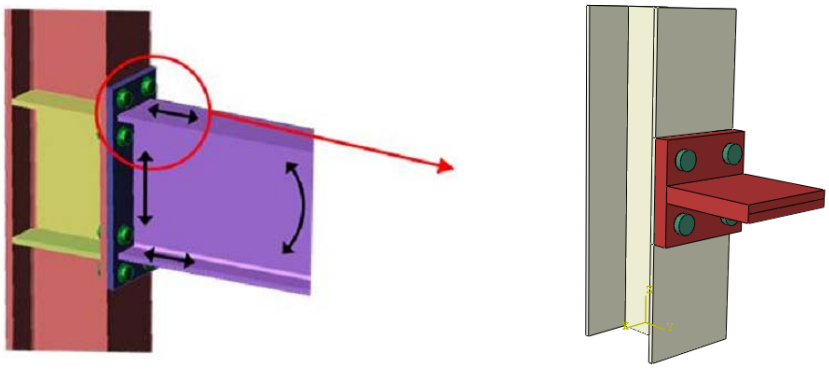

Figure 2.4: Adopted test specimen.

2.2.2.2 Finite element analysis

A three dimensional numerical models are carried out for fourteen t-stub connections divided into three series of tests. Those models started with the creation of single parts such as bolts, t-stub, stiffeners and column, and then assembled these parts into a connection.

2.2.2.3 Units

Abaqus has not a system of units, so it must be chosen by the employer. Units of Newton and millimeter were used for all analysis in this project.

2.2.2.4 Nonlinearity (type of analysis)

There are three sources of nonlinearity in structural static mechanics simulations [19]:

- ✓ Material nonlinearity

  Material nonlinearity is commonly observable in most metals and rubber materials. Steel has a fairly linear stress/strain relationship at low strain values; but at higher

strains such a relationship becomes highly non linear due to material yielding, at which point the response becomes irreversible.

- ✓ Boundary nonlinearity

  Boundary nonlinearity occurs if the boundary conditions change during the analysis.

- ✓ Geometry nonlinearity

  The third source of nonlinearity is related to changes in the geometry of the model during the analysis. Geometric nonlinearity occurs whenever the magnitude of the displacements affects the response of the structure.

2.2.2.5 Type of element

All the parts were modeled using C3D8R witch refer to continuum three dimensional 8-noded brick element with reduced order integration. This element has three degrees of freedom at each node, translations in the nodal x, y, & z [19].

The solid (or continuum) elements in Abaqus can be used for linear analysis and for complex nonlinear analyses involving contact, plasticity, and large deformations [19].

Reduced integration reduces running time, especially in three dimensions [19].

2.2.2.6 Material properties

The material properties for the various components of steel connections were determined according to stress-strain relationships obtained in standard tensile tests of steel, the material proprieties for the column and t-stub are presented in the next table,

Table 2.2: Material proprieties.

	column		T-stub	
	flange	web	flange	web
Yield stress Б (N/mm^2)	319	326	260	240
Young's Modulus E (N/mm^2)	$205*10^3$	$205*10^3$	$205*10^3$	$205*10^3$

It is clear from the table that the steel used was S275 for t-stub and S355 was used for UC sections.

The steel used for the stiffeners is S355. All the bolts were M20 grade 8.8 used in 2 mm clearance holes.

The nominal material properties are summarized in the next table.

Table 2.3: Material Properties of stiffeners steel and bolts steel.

Material type	Yield stress (N/mm^2)	Ultimate stress (N/mm^2)	Young's modulus (N/mm^2)	Poisson ratio
S355	355	550	$205*10^3$	0.3
M20	640	800	$205*10^3$	0.3

2.2.2.7 Contact modeling

In numerical simulations, the realistic representation of the contacts between joints components has a major effect on the performance of the connection and its response [20]. Many engineering problems involve contact between two or more components [19]; the interfacing forces that are developed when two parts come into contact transmit the applied forces [21]. In these problems a force normal to the contacting surfaces acts on the two bodies when they touch each other. If there is friction between the surfaces, shear forces may be created that resist the tangential motion (sliding) of the bodies. The general aim of contact simulations is to identify the areas on the surfaces that are in contact and to calculate the contact pressures generated [18].

Interaction between surfaces

- ✓ Behavior normal to the surfaces

  The distance separating two surfaces is called the clearance. The contact constraint is applied in Abaqus when the clearance between two surfaces becomes zero. There is no limit in the contact formulation on the magnitude of contact pressure that can be transmitted between the surfaces. The surfaces separate when the contact

pressure between them becomes zero or negative, and the constraint is removed. This behavior, referred to as “hard” contact, is the default contact behavior in Abaqus and is summarized in the contact pressure-clearance relationship shown in figure 2.5[19].

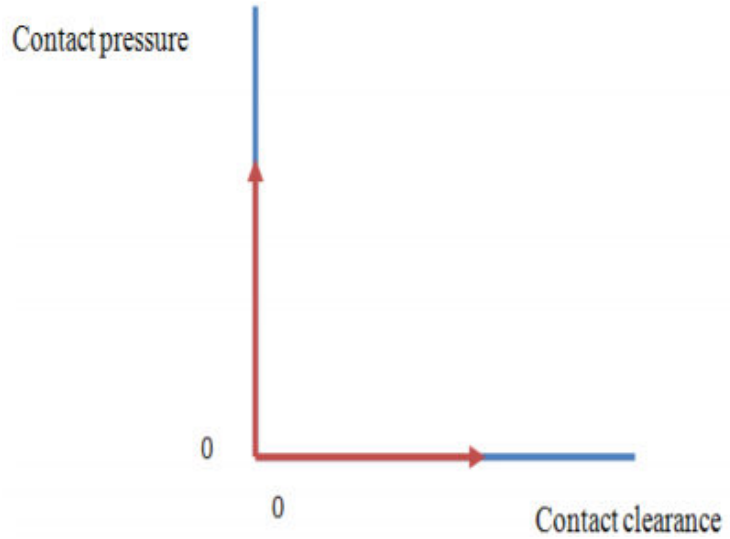

Figure 2.5: Contact pressure-clearance relationship for “hard” contact.

✓ Sliding of the surfaces

An Abaqus analysis also must calculate the relative sliding of the two surfaces. This can be a very complex calculation; therefore, Abaqus makes a distinction between analyses where the magnitude of sliding is small and those where the magnitude of sliding may be finite. It is much less expensive computationally to model problems where the sliding between the surfaces is small [19].

✓ Frictional behavior

When surfaces are in contact, they usually transmit shear as well as normal forces across their interface. Thus, the analysis may need to take frictional forces, which resist the relative sliding of the surfaces, into account. *Coulomb friction* is a common friction model used to describe the interaction of contacting surfaces. The model characterizes the frictional behavior between the surfaces using a coefficient of friction μ [19].

- ✓ Defining contact between two separate surfaces

  A surface-to-surface contact definition can be used to model contact interactions between specific surfaces in a model. When a contact pair contains two surfaces, the two surfaces are not allowed to include any of the same nodes and you must choose which surface will be the slave and which will be the master. The selection of master and slave surfaces is discussed in detail. For simple contact pairs consisting of two deformable surfaces, the following basic guidelines can be used [18]:

  - ✓ The larger of the two surfaces should act as the master surface;
  - ✓ If the surfaces are of comparable size, the surface on the stiffer body should act as the master surface;
  - ✓ If the surfaces are of comparable size and stiffness, the surface with the coarser mesh should act as the master surface.

- ✓ Tie constraint

  Tie constraints are used to tie together two surfaces for the duration of a simulation. Each node on the slave surface is constrained to have the same motion as the point on the master surface to which it is closest. For a structural analysis this means the translational (and, optionally, the rotational) degrees of freedom are constrained [18].

The main question that must be answered before starting the modeling is: does the contact simulation vary if the load was a force of traction or compression?

Jerome Montgomery [22] was discussed the representation of the contact depending on the performance of the bolts, the author considered two cases:

- ✓ bolt under flange separation

  When a load tries to separate a bolted flange joint, the job of the bolts is to hold the flange together as shown in figure 2.6. With increasing load the parts will separate, so in the numerical simulation, where the contact element are used, the surfaces that are in contact must be able to separate. So, the contact elements are not

required for the contact surface between flange and head/nut of the bolts. These surfaces can be glued (tied) together which means that the head contact can share the same surface as the top flange, and the nut contact can share the same surface as the bottom flange. The contact elements are required at the horizontal joint between the top and bottom flange.

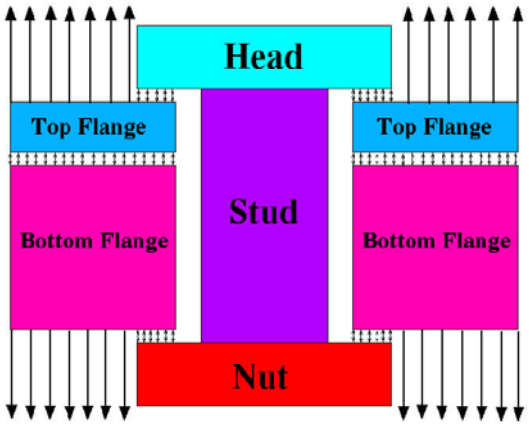

Figure 2.6: Bolt under flange separation.

✓ Bolt under flange compression

When a flange is under compression, there is no load on the bolt. In this case, the head and nut contact must be able to separate from the flanges, whereas, the horizontal joint contact can share the same surface. The surfaces where the top flange and bottom flange meet (horizontal joint contact surface) can be glued together.

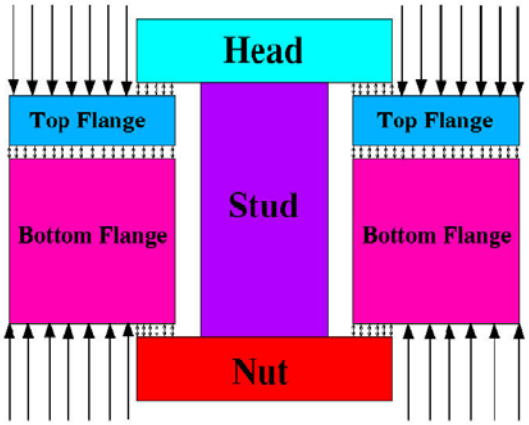

Figure 2.7: Bolt under flange compression.

As results:

- ✓ Surface-to-surface contact was considered for all the contacts in the connections to fully transfer the load applied to the supporting members. the contact surfaces of the bolt shank, bolt head and bolt nut are always modeled as master surfaces in this research (as the bolt is of stiffer material), in the contact between the column and t-stub, the column face is always the master surface in the numerical model because the columns is of a higher grade steel (S355) compared with the end plates which is S275. In the contact between the column and the stiffeners, the column face is the master surface. Whereas the surfaces interfacing master surfaces are defined as slave surfaces.

- ✓ The connection between the flange and the web of the column was assumed to be rigid, so was the connection between flange and the web of the t-stub (the process of welding was not modeled).

- ✓ Frictional contact was considered for the tangential contact between:
  - ✓ The t-stub and the column flange and between the different stiffeners used and the column flange, with traction force.
  - ✓ The bolt head/nut and t-stub/column/stiffeners, with compression force.

  Friction coefficient μ varies generally from 0.25 to 0.3. In this research the value of μ was taken 0.3.

- ✓ The tangential contact between the bolt hole and the bolt shank is considered to be frictionless. The normal contact was considered as hard.

- ✓ Tie constraint is used for the connection of :

  - ✓ The bolt head/nut to the t-stub/column/stiffener, with traction force.
  - ✓ The t-stub to the column flange and the stiffeners to the column flange, with compression force.

2.2.2.8 Boundary condition and loading

Both the ends of the column are fully restrained. The load application has been effected in one load step.

Different types of material properties and boundary conditions such as contact and friction considered in the study make the problem highly non linear, leading to non-convergence of the solution. It is overcome by using the nonlinear analysis option of ABAQUS, in which for a nonlinear analysis, it automatically chooses appropriate load increments and convergence tolerances. Not only does it choose the values for these parameters, it also continually adjusts them during the analysis to ensure that an accurate solution is obtained efficiently [20]. Although, a fixed time increment of 0.01 was chosen in most analysis.

2.2.2.9 Mesh convergence

As an initial step, a finite element analysis requires meshing of the model. In other words, the model is divided into a number of small elements, and after loading, stress and strain are calculated at integration points of these small elements. An important step in finite element modeling is the selection of the mesh density [21]. As far as the stability limit is concerned, it is advantageous to keep the element size as large as possible during the analysis. However, coarse meshes in a model can produce inaccurate numerical results [23]. Moreover, the numerical solution for a model is required to create a unique value as the mesh density increases during the solution procedure. So the mesh of a numerical model is said to be converged, when further mesh refinement yields a negligible change in the analysis .

An adequate number of elements were used in the models to obtain the convergence of results.

It should be noted that the number of elements used depend on the number of elements used for the validation test.

2.3 Steps of modeling

A series of fourteen t-stub end plate connections are undertaken. To achieve the objectives of this work, the modeling of these tests were divided into three steps as shown in figure 2.8.

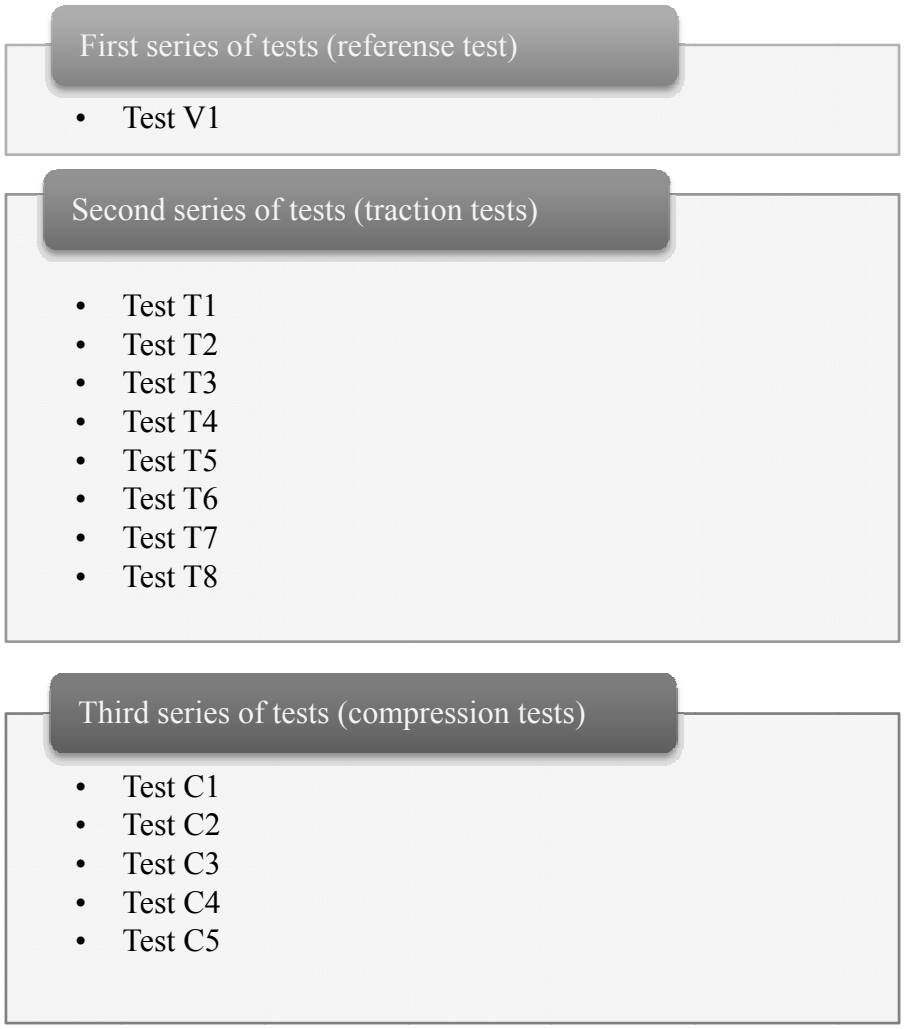

Figure 2.8: Steps of modeling.

2.3.1 First series of tests

For this step three aims were to be met:

- ✓ To develop a finite element model identified test V1, based on the specimen test of the experimental study presented by **Sethi** [16];
- ✓ To find a force-displacement curve characteristics and mode of failure for the finite element model;
- ✓ To validate the finite element model by comparing the results to the experiment test.

2.3.2 Second series of tests

These tests are a combination of a reference test T1 and different element of reinforcement added as shown in table 2.4.

Table 2.4: Second series tests list.

Step	Identification test	stiffener
2	T1	Without
	T2	Welded plates
	T3	Backing plates
	T4	Channels
	T5	Threaded bars
	T6	Threaded bars + Welded plate
	T7	Threaded bars + Backing plate
	T8	Threaded bars + Channels

The reference test T1 is a t-stub bolted to a column which refer to a tension zone of beam to column connection, the details of this test used are based on the validation test V1.
The main objectives are:

- ✓ The determination of the flexural yield load in which the plastic hinges develop;
- ✓ The observation of the mode of failure of the connection and the behavior of each of its components;
- ✓ Examination of the behavior of threaded bars on tension zone.

2.3.2 Third series of tests

The main objective of this step is to study the behavior of the threaded bars in compression zone therefore a series of five tests are take in charge, tests are identified C1, C2, C3, C4, C5, these tests are identical to tests T1, T5, T6, T7, T8 respectively with application of compression force (table 2.5).

Table 2.5: Third series tests list.

Step	Identification test	stiffener
3	C1	Without
	C2	Threaded bars
	C3	Threaded bars + Welded plate
	C4	Threaded bars + Backing plate
	C5	Threaded bars + Channels

2.4 Size and geometry of the tests

For all the tests, the size of the column used is UC 152×152×23 kg where its dimensions are illustrated in table 3.6. The thickness of the t-stub is 24 mm. The flange of the t-stub is bolted to the flange of the column by two rows of high strength bolts, two bolts by row. The size of the bolts is M20 grade 8.8.

Table 2.6: Dimension of the column.

Identification	Dimension (mm)
t_f	6.8
t_w	6.1
h	152.4
b	152.2

Where:

- ✓ t_f : is the thickness of the flange.
- ✓ t_w : is the thickness of the web.
- ✓ h : is the height.
- ✓ b : is the width.

Typical geometry of each test will be given in the following sections.

✓ Numerical test V1

The connection selected for the current study was tested by **Sethi** [16], consists as cited earlier of a t-stub bolted by two rows high strength bolts to the flange of a column (figure 2.9), The size of the column used was UC 152×152×23 kg, the size of the bolts used was M20 grade 8.8 and 24 mm was the thickness of the t-stub.

The boundary conditions for the column ends were considered as fully restrained. The loading was applied to the web of the t-stub.

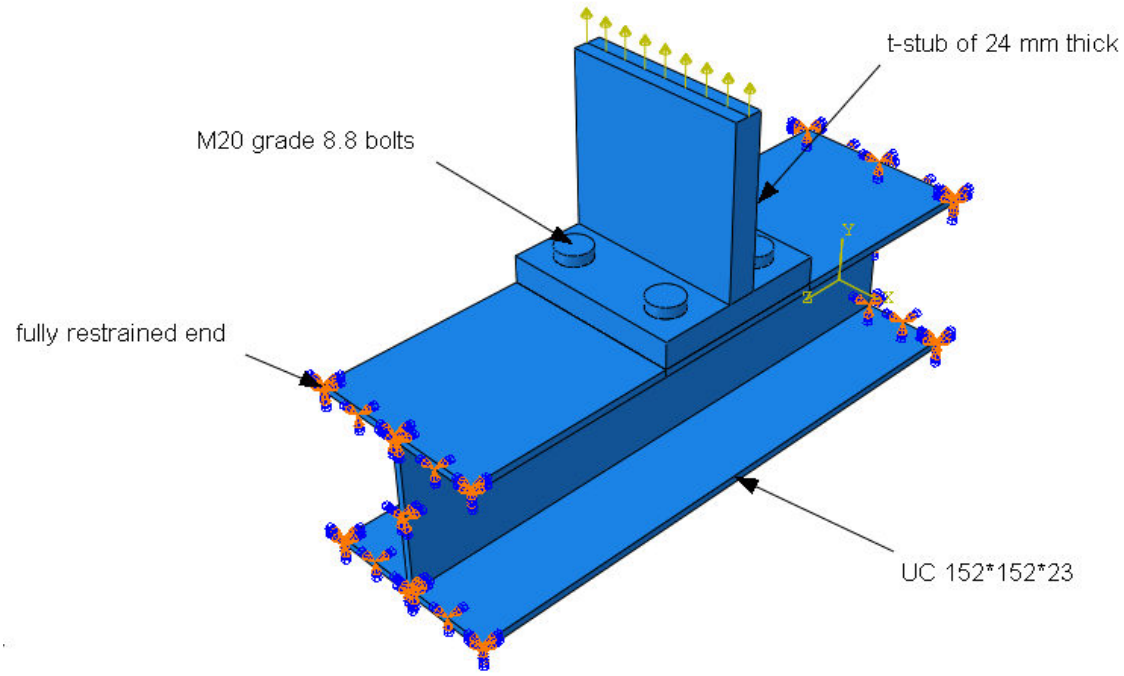

Figure 2.9: Experimental test connection.

✓ Numerical test T1

The test T1, the reference test, has the same components as the validation test. The typical geometry of this test is shown in figure 2.10.

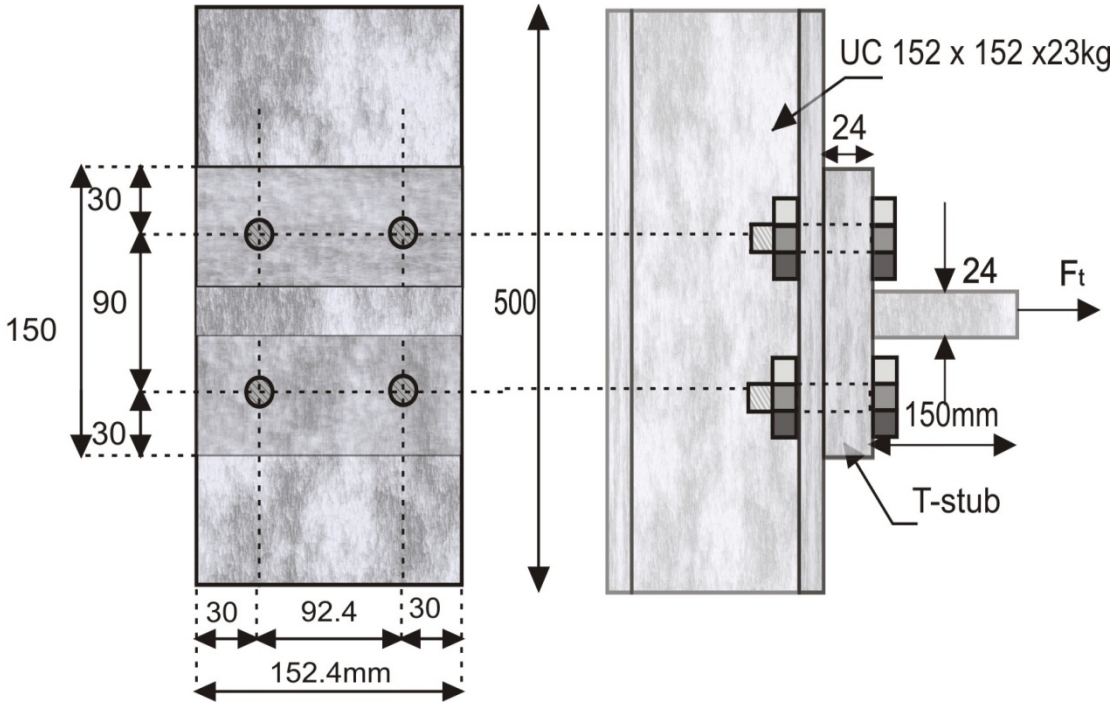

Figure 2.10: Typical geometry for the numerical test T1.

✓ Numerical test T2

In this test an horizontal plate is welded to the web of the column, as shown in figure 2.11. The thickness of the plate is 10 mm.

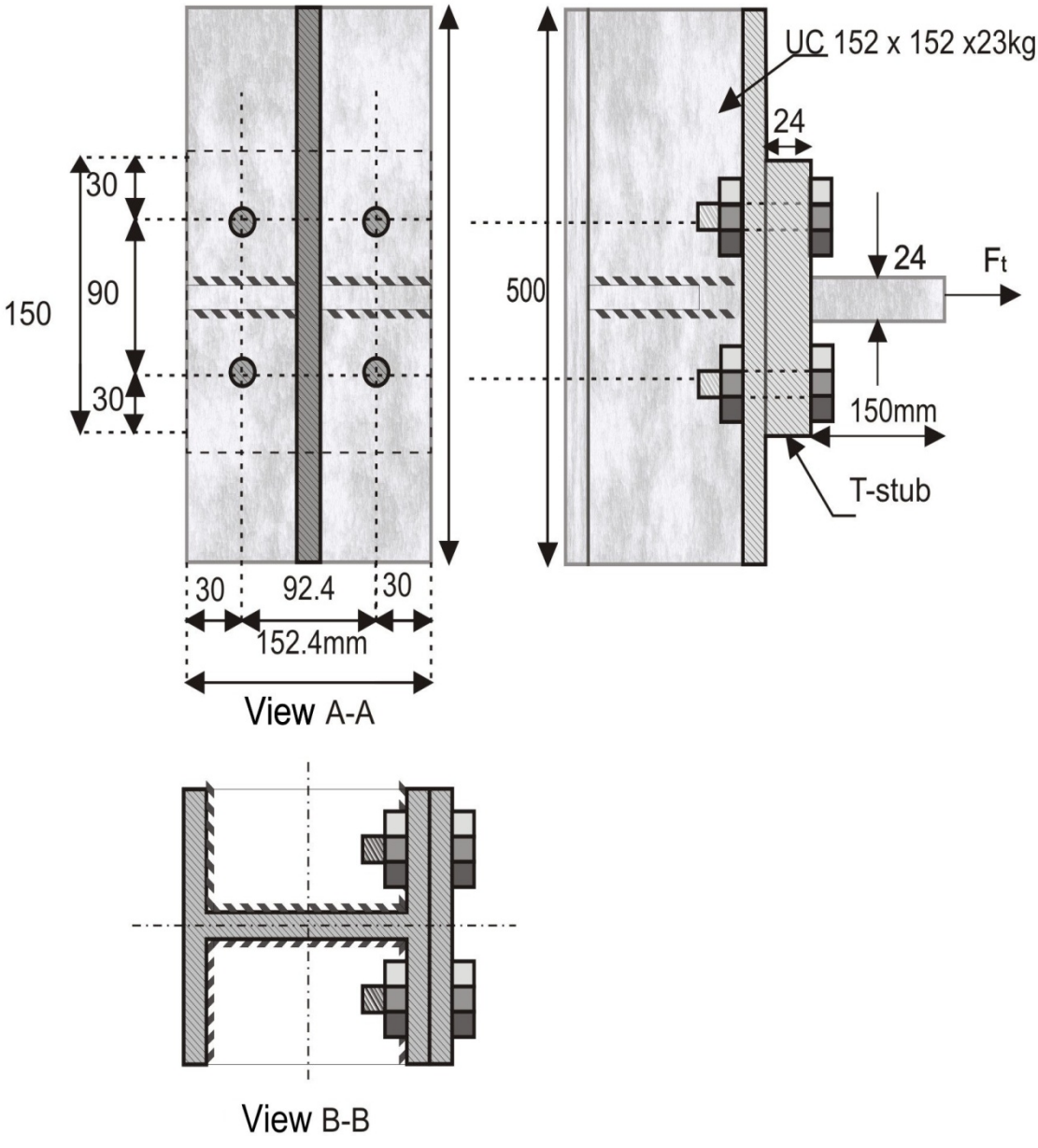

Figure 2.11: Typical geometry for the numerical test T2.

✓ Numerical test T3

The test T3 is a combination of the reference test and a vertical plate that has a thickness of 10 mm and 220 mm high, this plate is bolted to the flange of the column that is itself bolted to the t-stub as presented in figure 2.12.

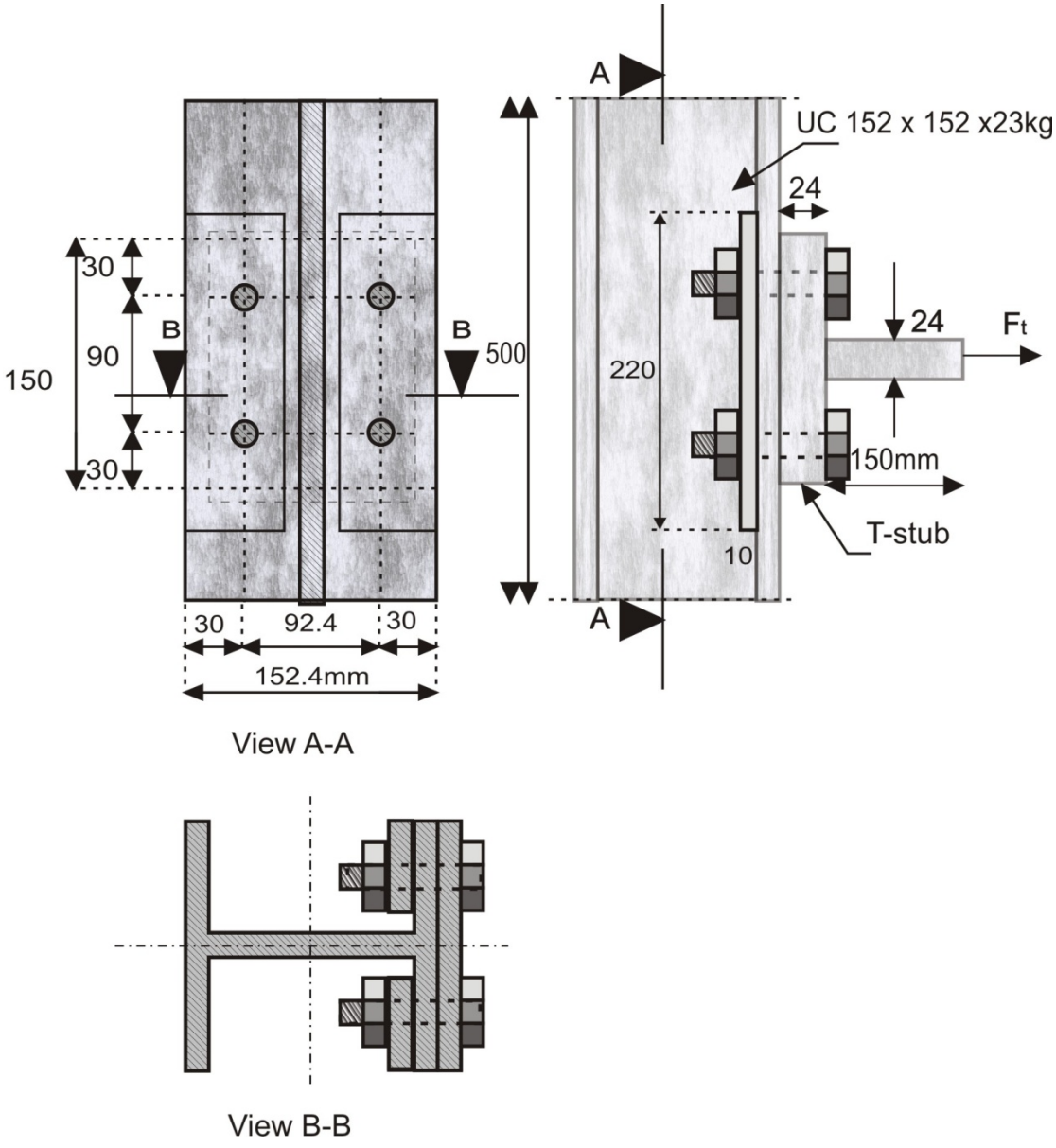

Figure 2.12: Typical geometry for the numerical test T3.

✓ Numerical test T4

The test T4 is the test of reference plus an element of reinforcement that has U-shaped, this element which called channel is bolted to the two flanges of the column. Figure 2.13 illustrates that the base of this element is directed towards the exterior.

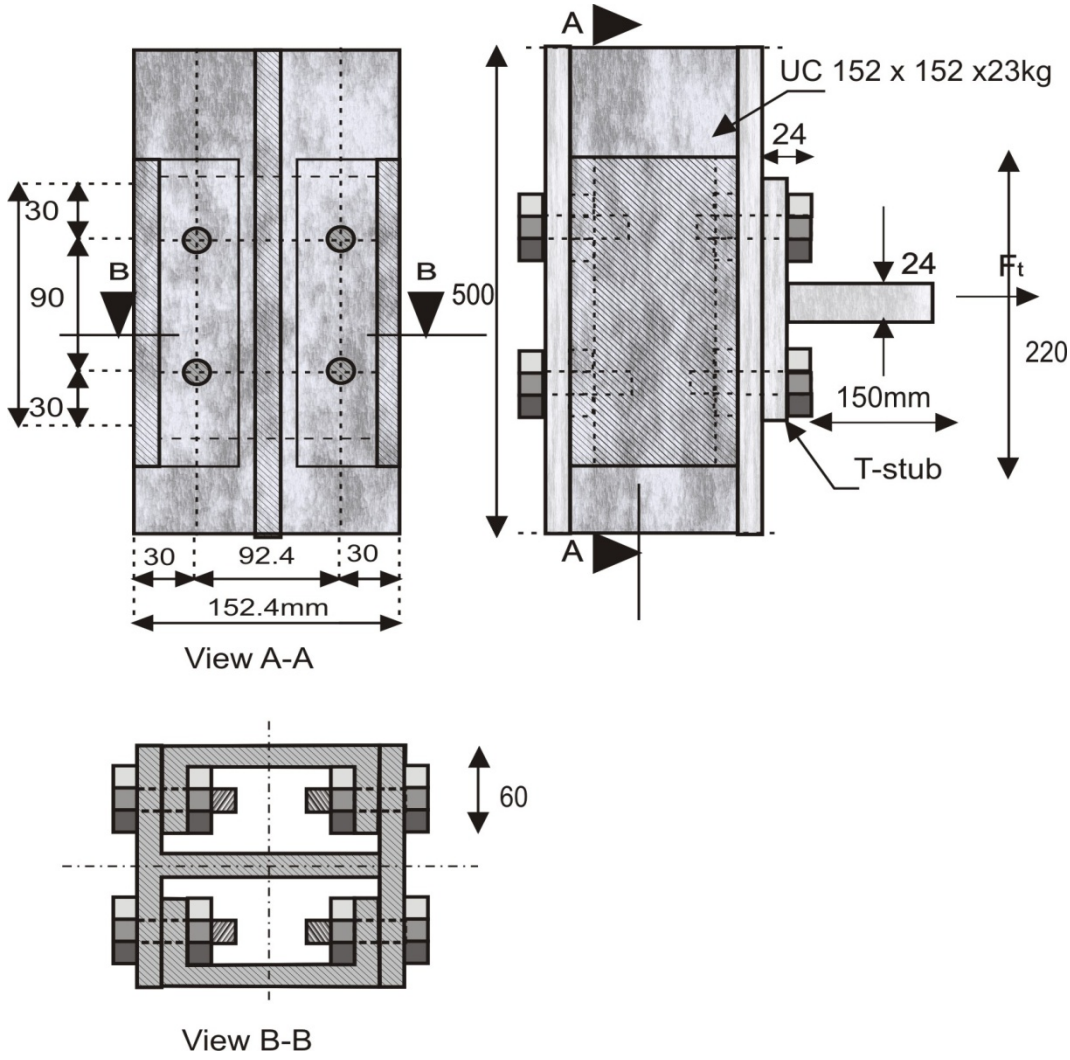

Figure 2.13: Typical geometry for the numerical test T4.

This element was placed in this manner in order to facilitate the fixing of the beams which can exist in the other direction. But the major disadvantage of this reinforcement is the difficulty of the installation of the bolts.

The most practical solution with this problem is the use of extended bolts between the flanges of the column.

✓ Numerical test T5

In this test a new type of reinforcement is suggested named threaded bar , the reinforcement is new in its form, is carried out by prolonging the bolts used in order to connect the two flanges of the column as referred in figure 2.14 .

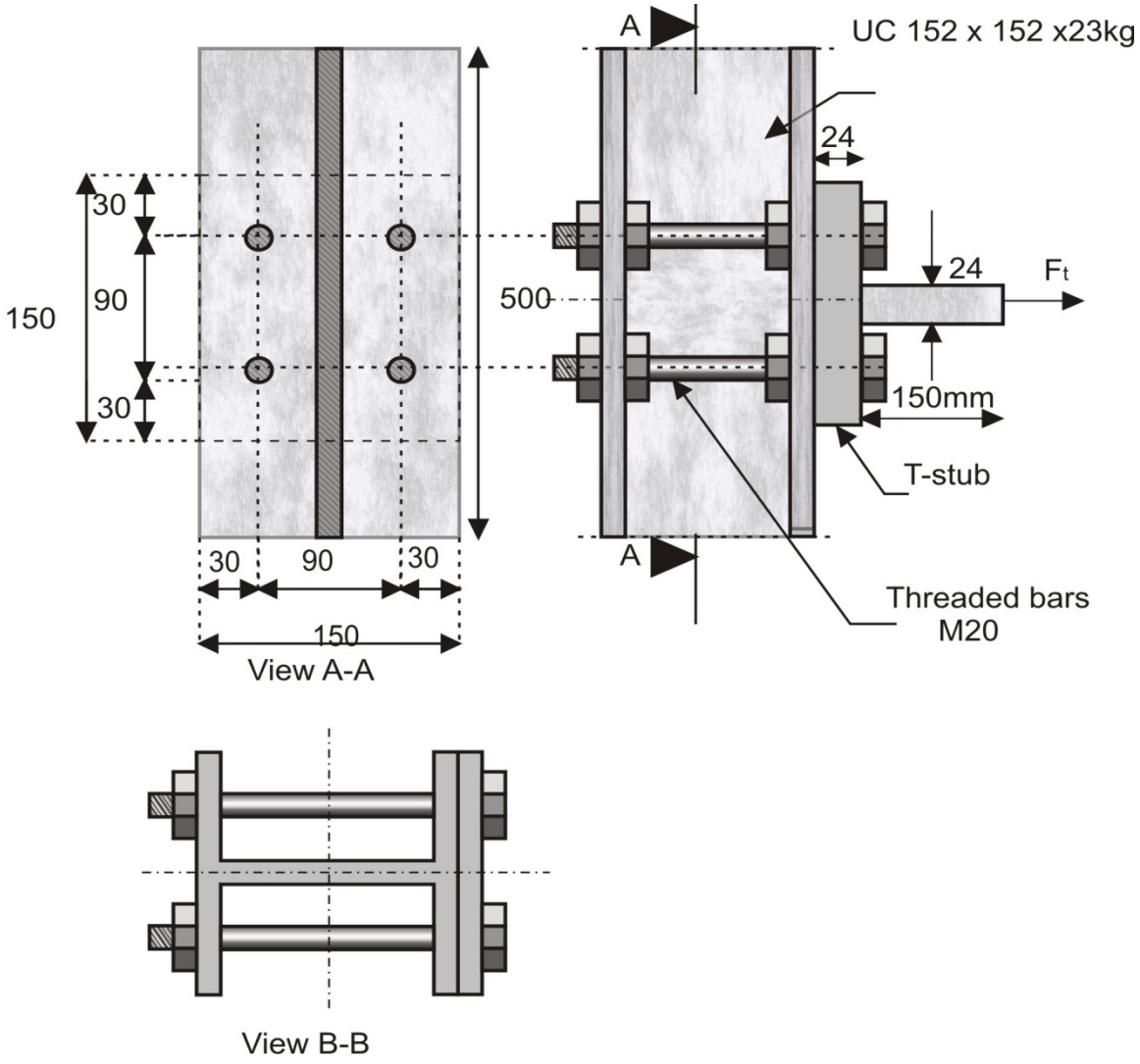

Figure 2.14: Typical geometry for the numerical test T5.

The study is focused on this type reinforcement so a particular attention will be given to its behavior in order to obtain more information about its performance and to compare its behavior with the other elements of reinforcement.

Thus the next three tests are combining between the stiffeners used previously and the threaded bars.

✓ Numerical test T6

In this test threaded bars and welded plate are used together.

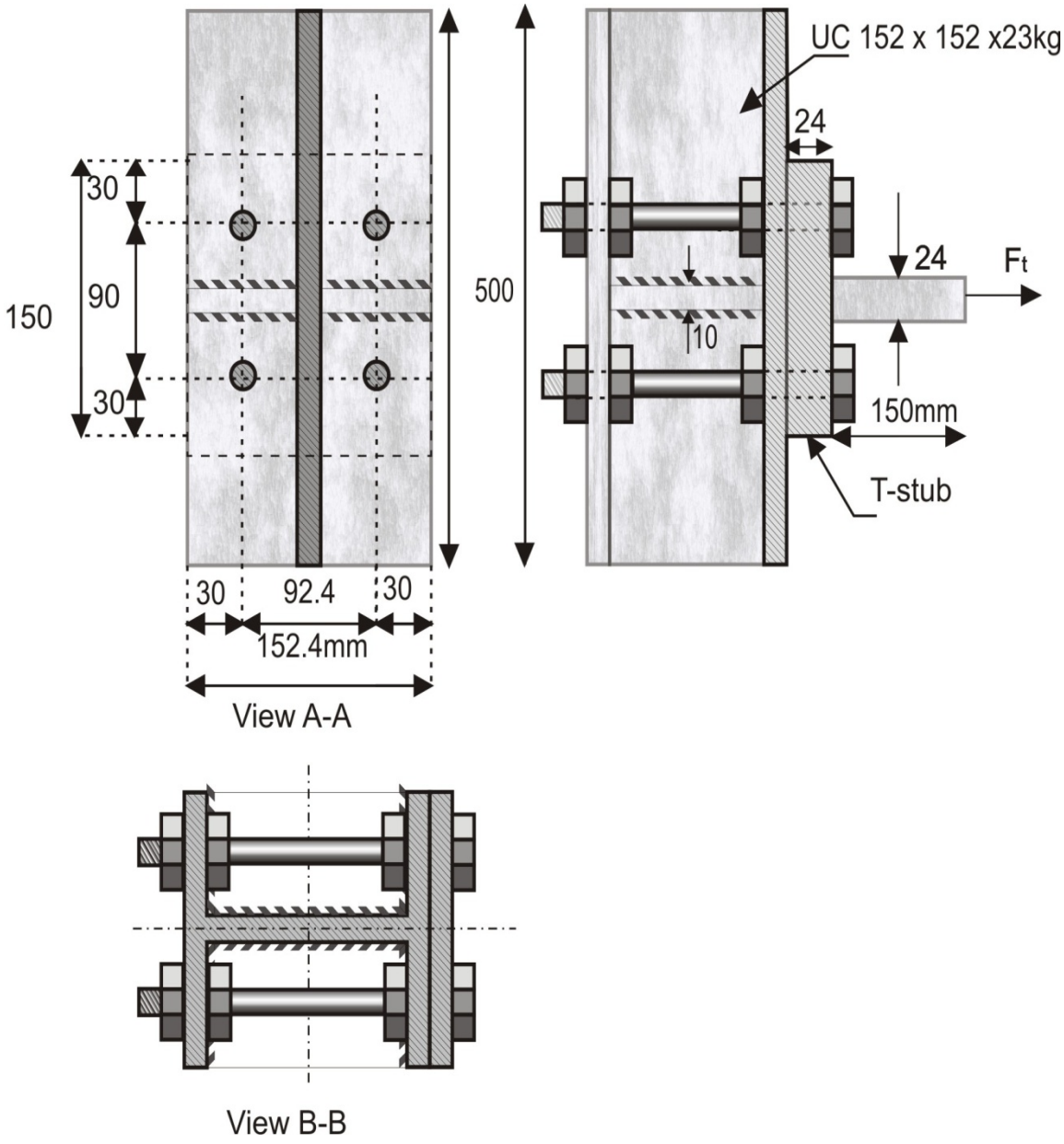

Figure 2.15: Typical geometry for the numerical test T6.

✓ Numerical test T7

In this test threaded bars and backing plate are used together.

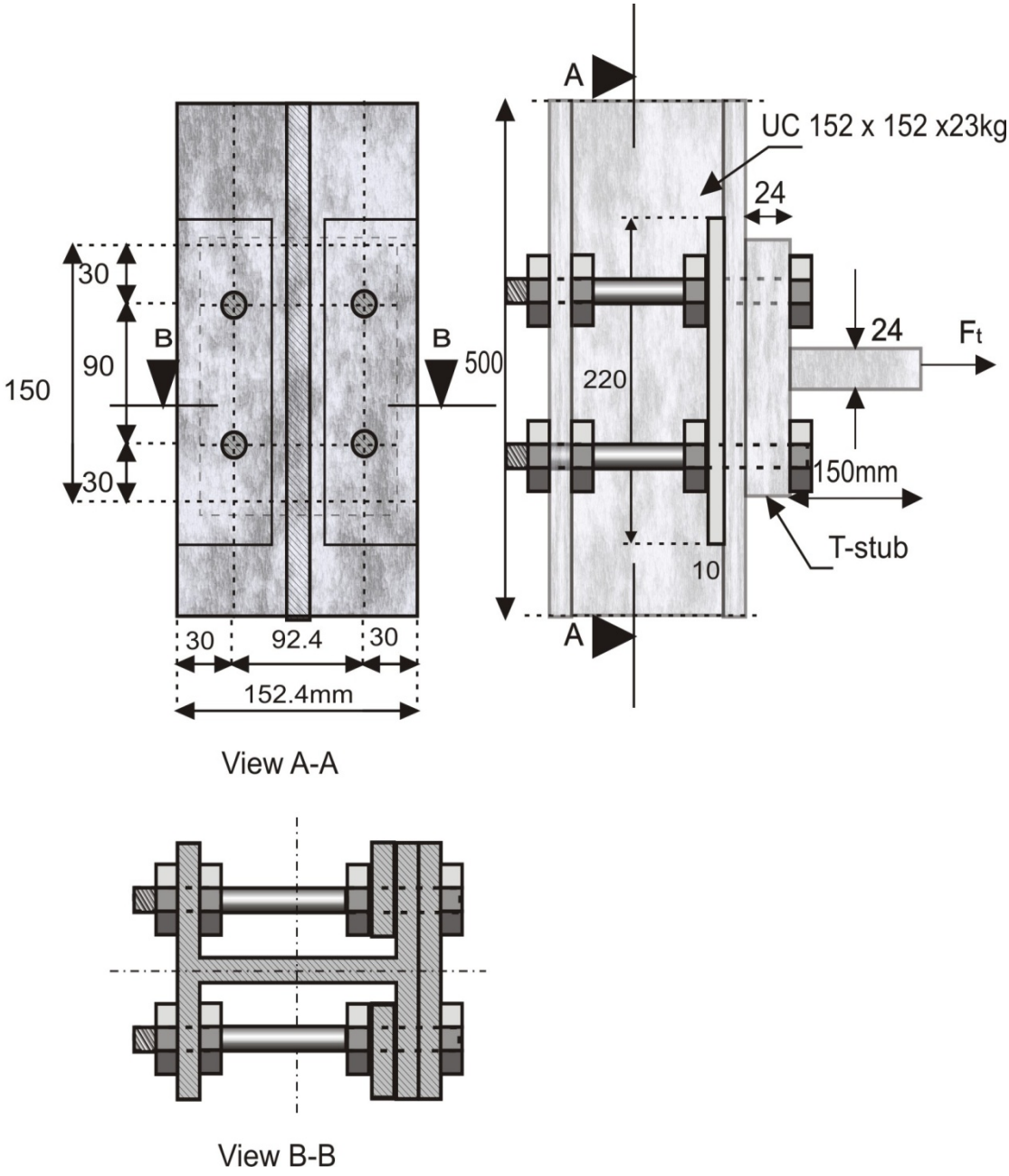

Figure 2.16: Typical geometry for the numerical test T7.

✓ Numerical test T8

In this test threaded bars and channels are used together.

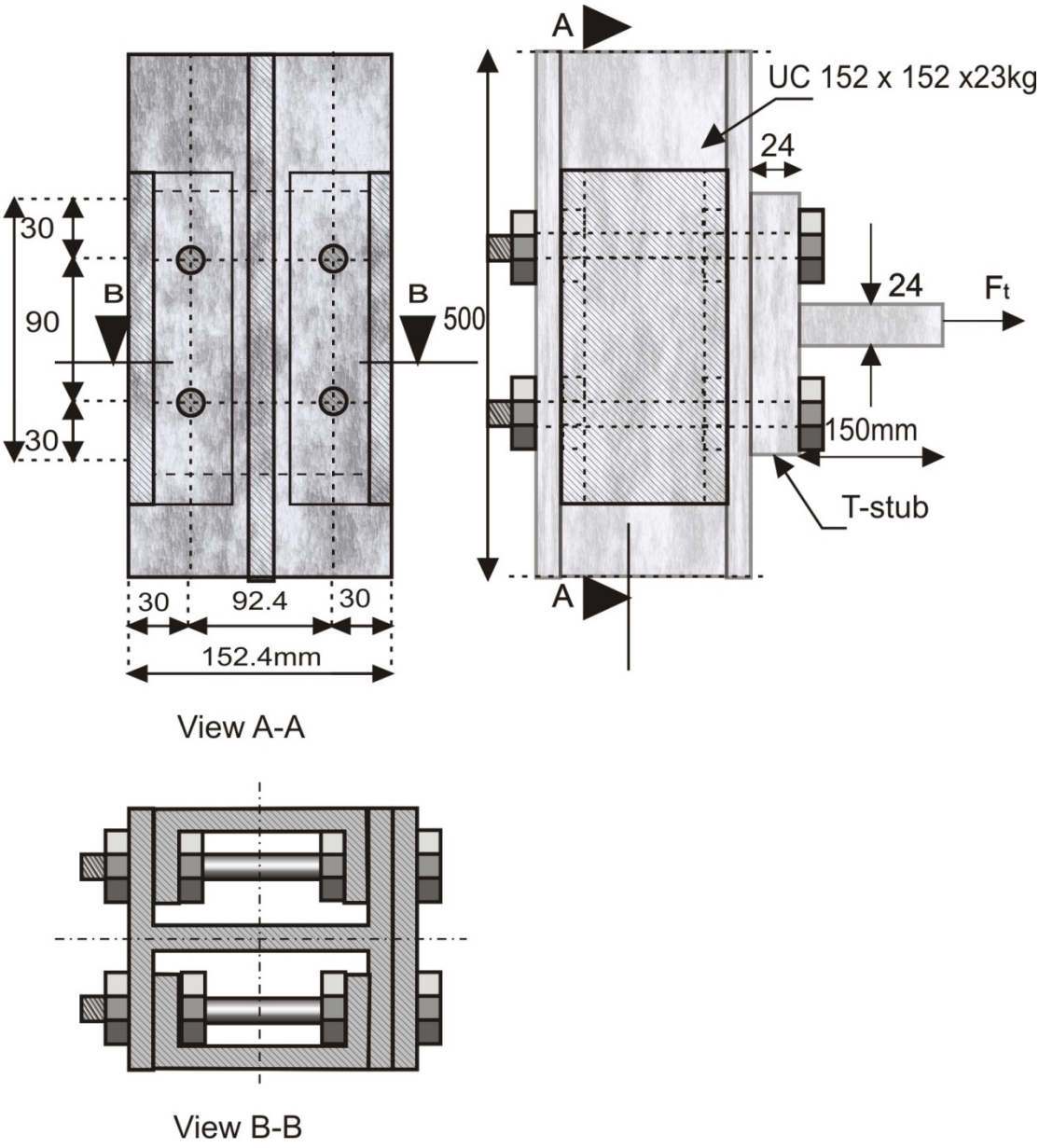

Figure 2.17: Typical geometry for the numerical test T8.

✓ Numerical test C1 to C5

The numerical tests C1 to C5 are identical to the numerical tests T1 and T5 to T8 respectively.

The meshing adopted for the tests is presented in the following figures.

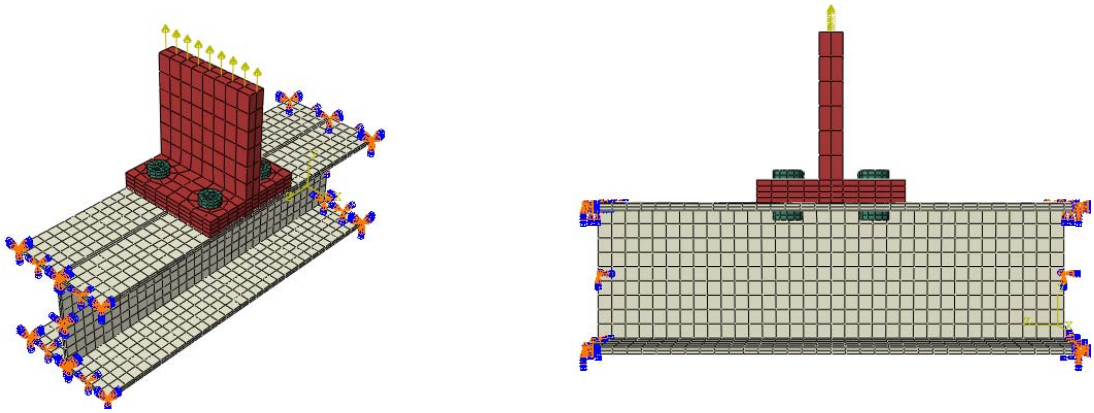

Figure 2.18: Numerical model for the validation test.

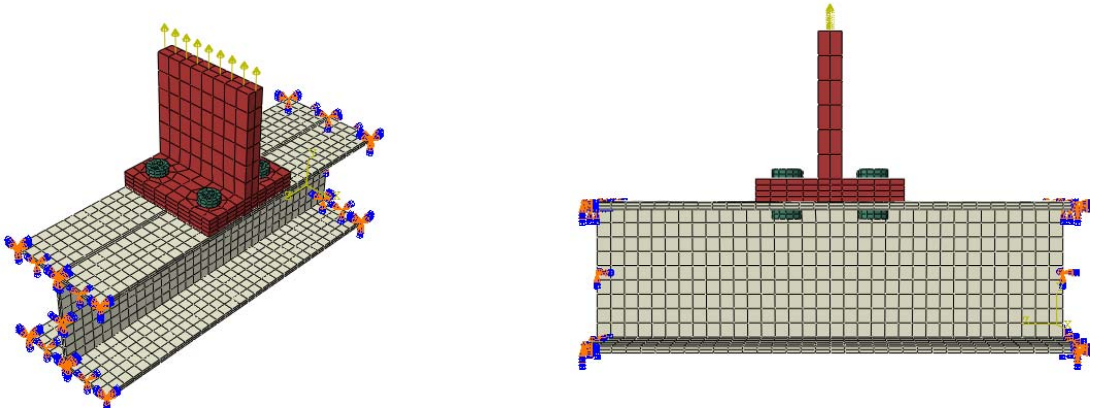

Figure 2.19: Numerical model for the numerical test T1.

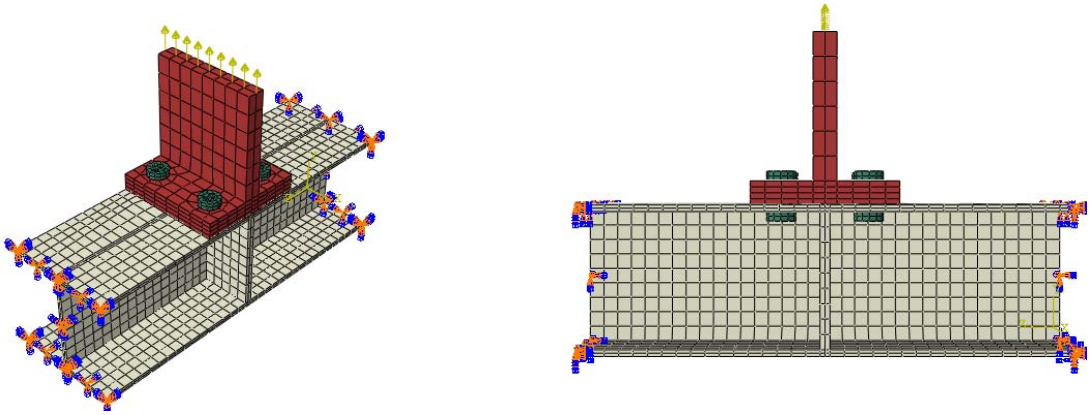

Figure 2.20: Numerical model for the numerical test T2.

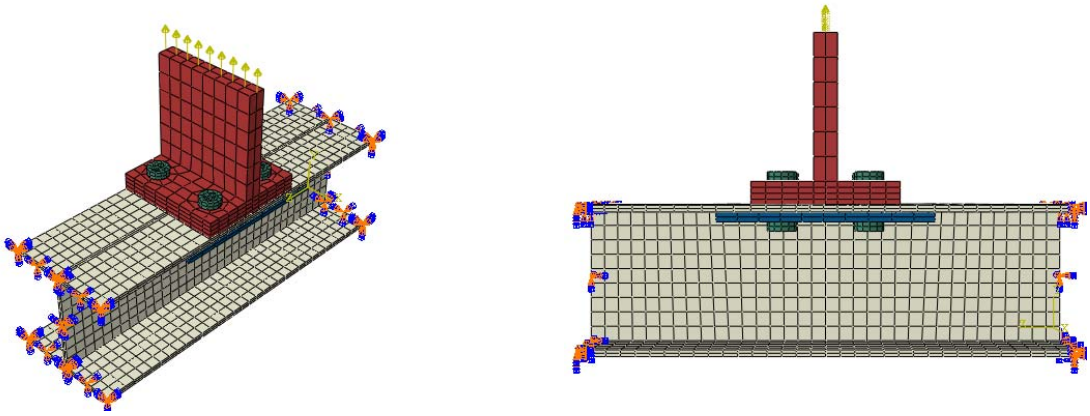

Figure 2.21: Numerical model for the numerical test T3.

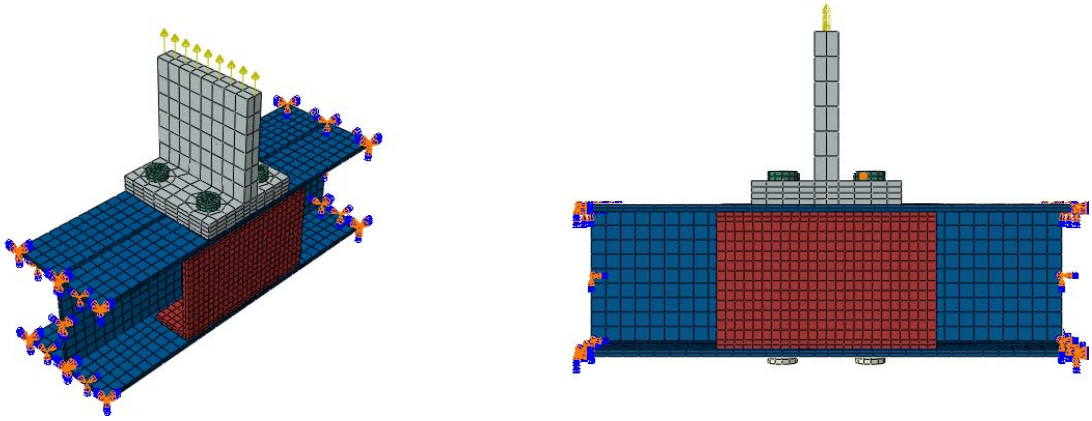

Figure 2.22: Numerical model for the numerical test T4.

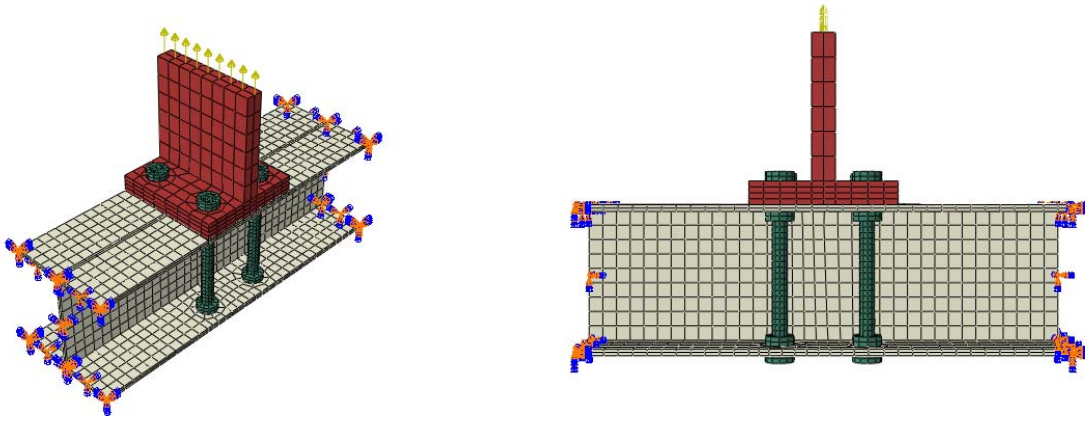

Figure 2.23: Numerical model for the numerical test T5.

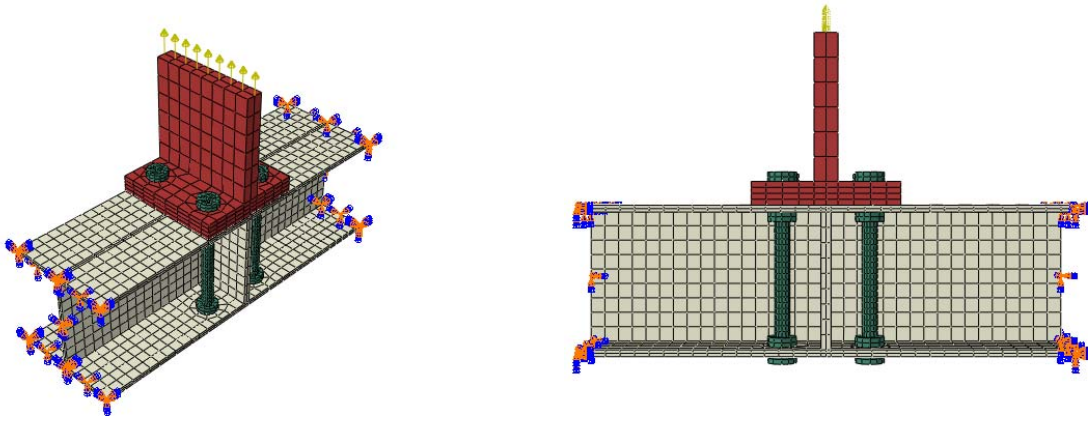

Figure 2.24: Numerical model for the numerical test T6.

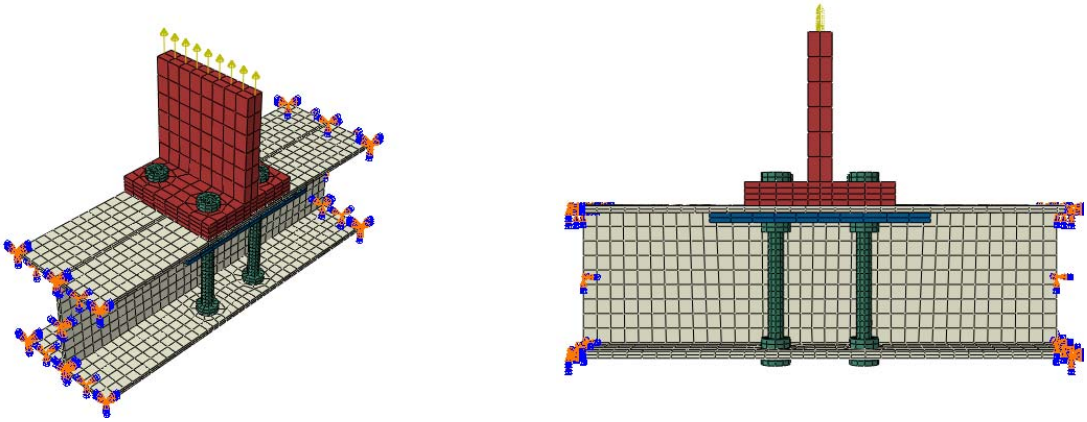

Figure 2.25: Numerical model for the numerical test T7.

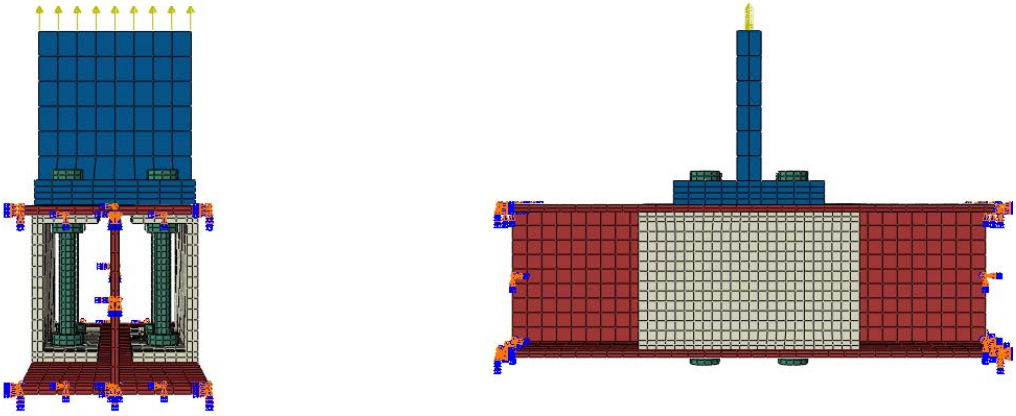

Figure 2.26: Numerical model for the numerical test T8.

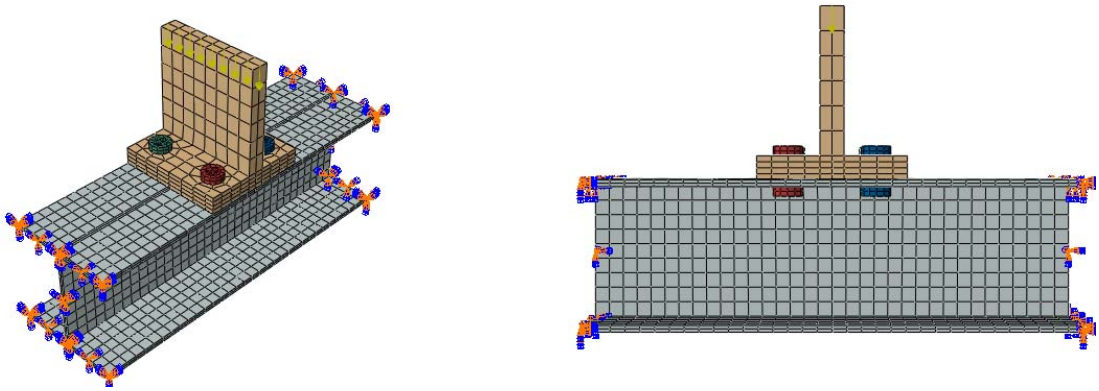

Figure 2.27: Numerical model for the numerical test C1.

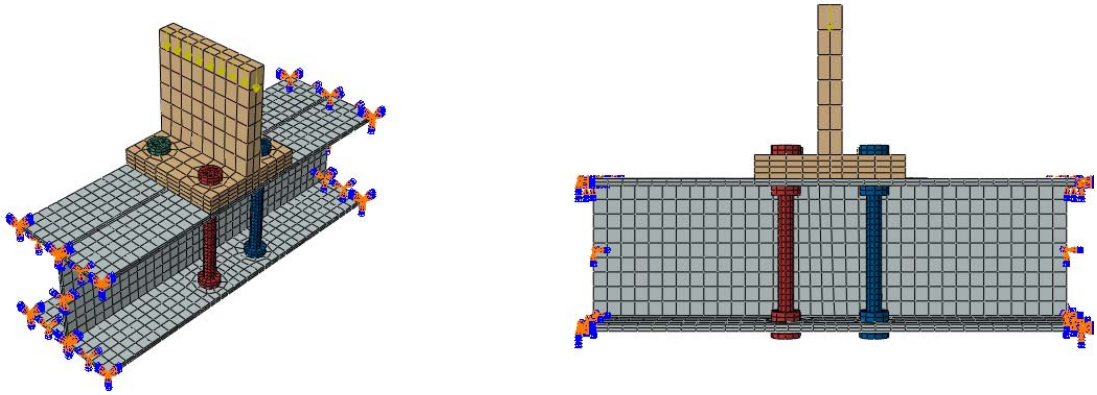

Figure 2.28: Numerical model for the numerical test C2.

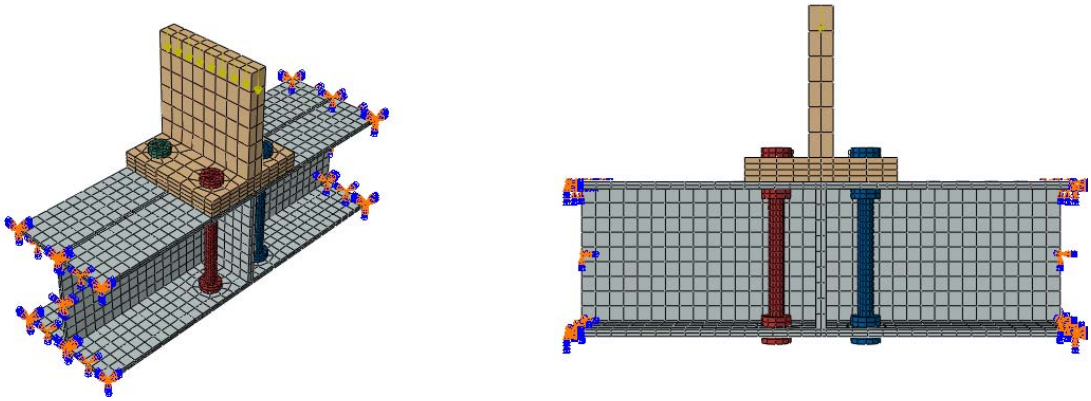

Figure 2.29: Numerical model for the numerical test C3.

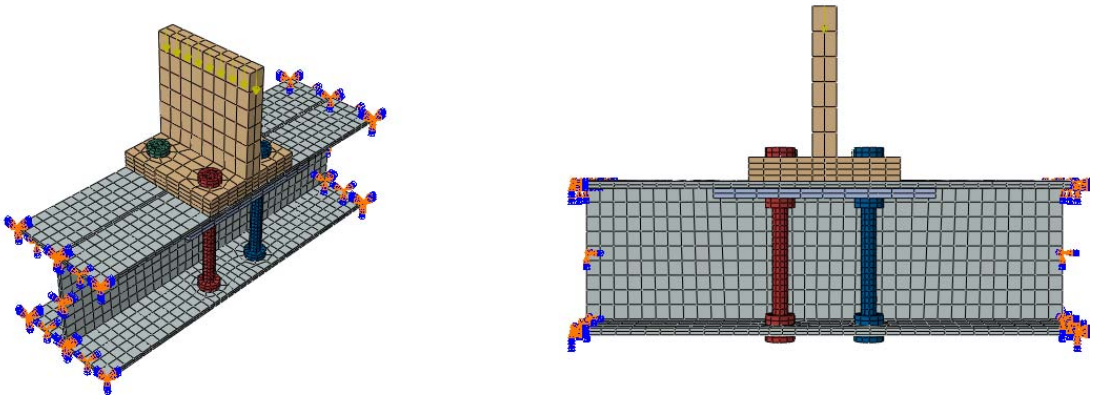

Figure 2.30: Numerical model for the numerical test C4.

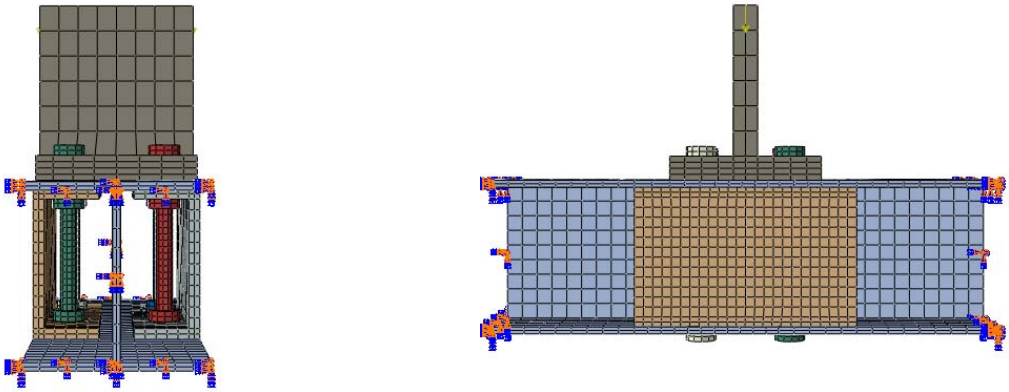

Figure 2.31: Numerical model for the numerical test C5.

All the results obtained are presented in chapter 4.

CHAPTER 3

THEORETICAL ANALYSIS

3.1 Introduction

Yield line theory was first introduced in the 1960's to analyze reinforced concrete slabs by Johansen in 1972. It is a powerful analysis method used to determine the flexural load at which a collapse mechanism will form in a flat plate structure [4].

A yield line is the continuous formation of plastic hinges along a straight or curved line. As a plate structure is loaded in flexure, yield lines will form when the flexural yield strength of the plate is exceeded. Collapse of the plate structure occurs when the formation of the yield lines produces a collapse mechanism [4].

The elastic deformations of the members are negligible compared to the plastic deformations at plastic hinges locations or yield lines. This allows the assumption that the plate structure is divided by the yield lines into a series of rigid plate regions. The outline of the rigid plate regions is commonly called the yield line pattern [4].

In this chapter yield line analysis is used to predict the t-subs yield strength by observing of type of reinforcement cited collapse mechanisms and of the column flange, and then the resistance load done by the finite element analysis from the second series of tests will be compared by those given by the yield line method.

3.2 Calculation method

Yield line analysis can be performed by two different methods: the virtual work or energy method, and the equilibrium method.

The virtual work method is the preferred method for analysis of steel plates. In the virtual work method, a small arbitrary displacement (virtual displacement) is applied to the structure in the direction of the applied loads. The external work is generated as the load passes through the small displacement. The internal work of the plate is generated by the rotation of the plate along the yield lines of the assumed yield line pattern to accommodate the small displacement [4].

To satisfy the conservation of energy principle, the internal work of the plate is set equal to the external work of the applied loads. The resulting equality can be solved to determine either the unknown failure load or the required plate flexural strength. This process of equating the internal and external work must be repeated for each assumed yield line pattern [4].

The application of yield line theory to determine the strength of an end plate requires three basic steps; assumption of a yield line pattern, generation of equations for internal and external work, and solution of internal and external work equality.

3.3 yield line patterns

In determining an assumed yield line pattern within a steel plate, the following guidelines have been established by Srouji and al. [4]:

- ✓ Axes of rotation generally lie along lines of support.
- ✓ Yield lines pass through the intersection of the axes of rotation of adjacent rigid plate segments.
- ✓ Along a yield line, the bending moment is assumed to be constant and equal to the plastic moment of the plate.

3.4 Collapse mechanism of end plate moment connections

The end plate goes through three different stages of behavior (Figure 3.1).

Where:

- ✓ Q is the prying force,
- ✓ B is the bolt resisting force,
- ✓ F is the loading.

During the first stage, plastic hinges have not developed and the plate is referred to as “thick”. The prying force is taken as zero in this stage.

When the plastic hinge forms at the beam flange, the plate becomes “intermediate” and the prying force is somewhere between zero and the maximum prying force that can occur.

The last stage begins when a second plastic hinge forms at the bolt line. The end-plate in that stage is called “thin” and the prying force is at its maximum.

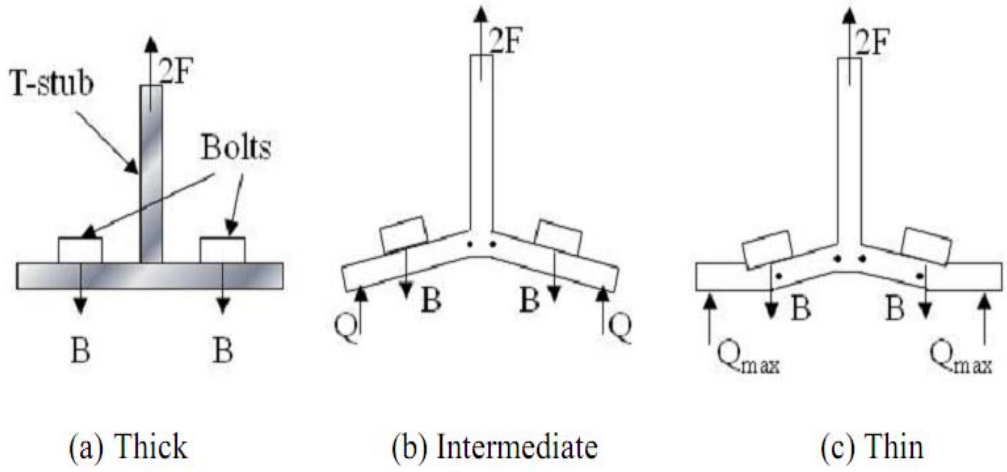

Figure 3.1: Three stages of end plate behavior.

3.5 Development of yield load formulas

In order to determine the mode of collapse for models T1 to T8, the deformed shape and the output of vertical displacement in the column flange for each model are presented.

It should be noted that all the yield line patterns used for these tests were referred to those proposed by **Packer and Morris** [8]**, Zoetemeijer** [9] and **Sethi** [9].

3.5.1 Unreinforced column flange

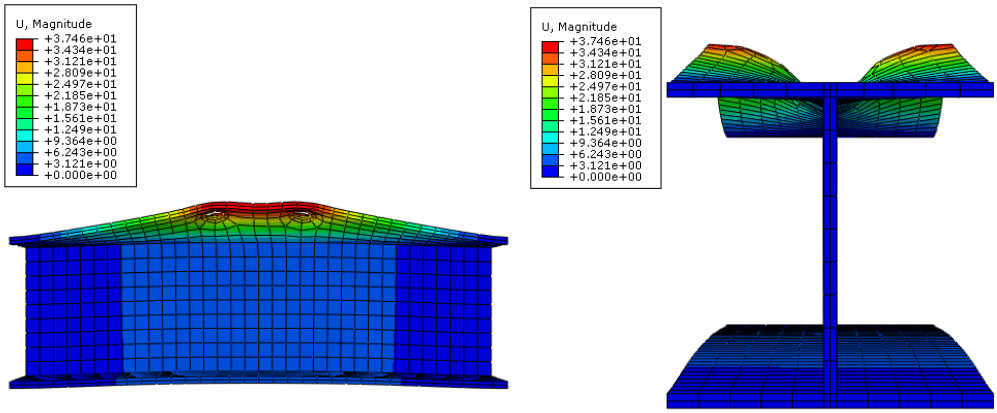

(a) (b)

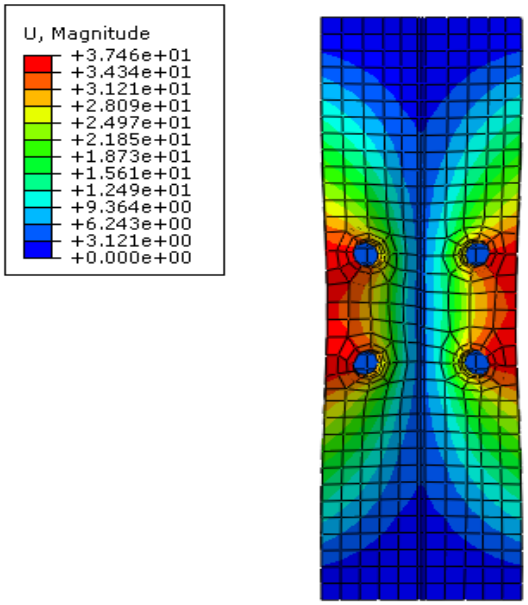

(c)

Figure 3.2: Column flange deformation for the unreinforced test.

The yield line pattern of the flange plate is shown in figure 3.3.

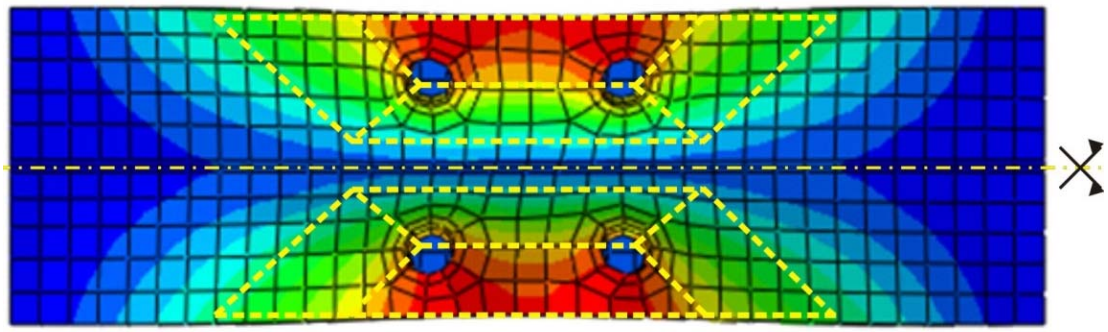

(a)

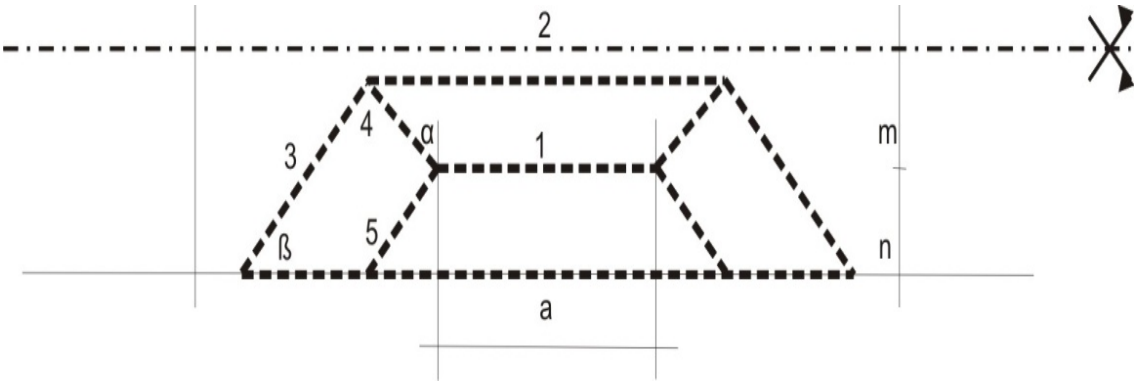

(b)

Figure 3.3: Yield line pattern for the unreinforced test.

The unknowns in this figure are α and β. The values of α and β which produce the smallest collapse loads are of interest.

To solve this problem, the internal dissipation of energy (ΔE) must be equal to the work done by the external loads (ΔT).

Yield line 1

The length of the yield line is:

$$L_1 = a$$

The rotation is:

$$\theta_1 = \frac{\Delta\delta}{m}$$

Thus

$$\Delta E_1 = \frac{\Delta\delta}{m}\ a\ m_p$$

Yield line 2

The length of the yield line is:

$$L_2 = a + 2m\tan\alpha$$

The rotation is:

$$\theta_2 = \frac{\Delta\delta}{m}$$

Thus

$$\Delta E_2 = \frac{\Delta\delta}{m}(a + 2mtg\alpha)m_p$$

Yield line 3

The length of the yield line is:

$$L_3 = \frac{m+n}{\sin\beta}$$

The rotation is:

$$\theta_3 = \frac{\Delta\delta cos\alpha}{mcos(\beta-\alpha)}$$

Thus

$$\Delta E_3 = 2\ m_p \frac{m+n}{m}\frac{\Delta\delta cos\alpha}{\sin\beta\ cos(\beta-\alpha)}$$

Yield line 4

The length of the yield line is:

$$L_4 = \frac{m}{\cos\alpha}$$

The rotation is:

$$\theta_4 = \frac{\Delta\delta \sin\beta}{mcos(\beta - \alpha)}$$

Thus

$$\Delta E_4 = 2m_p \frac{\Delta\delta \sin\beta}{\cos\alpha\, cos(\beta - \alpha)}$$

Yield line 5

The length of the yield line is:

$$L_5 = \frac{n}{\sin\beta}$$

The rotation is:

$$\theta_5 = \frac{\delta \cos\alpha}{m \cos(\beta - \alpha)}$$

Thus

$$\Delta E_5 = 2m_p \frac{n}{\sin\beta} \frac{\delta \cos\alpha}{m \cos(\beta - \alpha)}$$

The total energy dissipated internally is:

$$\sum_{i=1}^{5} E_i = 2\Delta\delta m_p \left(\left(\frac{a}{m} + \tan\alpha \right) + \frac{m + 2n}{m} \frac{\cos\alpha}{\sin\beta \cos(\beta - \alpha)} + \frac{\sin\beta}{\cos\alpha \cos(\beta - \alpha)} \right)$$

The work done by the external force F/2 is:

$$\Delta T = \frac{F}{2}\Delta\delta$$

Equating the external and the internal energy gives:

$$\frac{F}{2}\Delta\delta = 2\Delta\delta m_p \left(\left(\frac{a}{m} + \tan\alpha \right) + \frac{m + 2n}{m} \frac{\cos\alpha}{\sin\beta \cos(\beta - \alpha)} + \frac{\sin\beta}{\cos\alpha \cos(\beta - \alpha)} \right)$$

$$F = 4m_p\left(\left(\frac{a}{m}+\tan\alpha\right)+\frac{m+2n}{m}\,\frac{\cos\alpha}{\sin\beta\cos(\beta-\alpha)}+\frac{\sin\beta}{\cos\alpha\cos(\beta-\alpha)}\right)$$

The collapse load F is a minimum if the following conditions are satisfied:

$$\frac{\partial F}{\partial\alpha}=0$$

$$\frac{\partial F}{\partial\beta}=0$$

Carrying out the differentiations,

$$\frac{1}{4m_p}\frac{\partial F}{\partial\alpha}=\frac{1}{cos^2\alpha}+\frac{m+2n}{m}\left(\frac{-\sin\beta(\sin\alpha\cos(\beta-\alpha)+\cos\alpha\sin(\beta-\alpha))}{sin^2\beta cos^2(\beta-\alpha)}\right)$$
$$+\frac{\sin\beta}{cos^2\beta cos^2(\beta-\alpha)}(\sin\alpha\cos(\beta-\alpha)-\cos\alpha\sin(\beta-\alpha)) \quad = 0$$

$$\frac{1}{4m_p}\frac{\partial F}{\partial\alpha}=-\frac{m+2n}{m}\frac{sin^2\beta}{sin^2\beta cos^2(\beta-\alpha)}$$
$$+\frac{\sin\beta}{cos^2\beta cos^2(\beta-\alpha)}(2\sin\alpha\cos\beta\cos\alpha-\sin\beta(-\cos2\alpha))$$
$$+\frac{1}{cos^2\alpha} \quad = 0$$

$$\frac{1}{4m_p}\frac{\partial F}{\partial\alpha}=-\frac{m+2n}{m}\frac{1}{cos^2(\beta-\alpha)}$$
$$+\frac{cos^2(\beta-\alpha)+2\sin\alpha\cos\alpha\sin\beta\cos\beta+sin^2\beta(-\cos2\alpha)}{cos^2\beta cos^2(\beta-\alpha)} \quad = 0$$

$$\frac{1}{4m_p}\frac{\partial F}{\partial\alpha}=-\frac{m+2n}{m}\frac{1}{cos^2(\beta-\alpha)}$$
$$+\frac{\frac{1}{2}+\cos2(\beta-\alpha)+\frac{1}{2}\sin2\alpha\sin2\beta+\left(\frac{1}{2}-\frac{1}{2}\cos2\beta\right)(-\cos2\alpha)}{cos^2\beta cos^2(\beta-\alpha)} \quad = 0$$

$$\frac{1}{4m_p}\frac{\partial F}{\partial \alpha} = -\frac{m+2n}{m}\frac{1}{cos^2(\beta-\alpha)} + \frac{\frac{1}{2}+\cos 2(\beta-\alpha)+\frac{1}{2}\cos 2(\beta-\alpha)+sin^2\alpha}{cos^2\beta cos^2(\beta-\alpha)} = 0$$

$$\frac{1}{4m_p}\frac{\partial F}{\partial \alpha} = -\frac{m+2n}{m}\frac{1}{cos^2(\beta-\alpha)} + \frac{\cos 2(\beta-\alpha)+sin^2\alpha}{cos^2\alpha cos^2(\beta-\alpha)} = 0 \quad (1)$$

$$\frac{1}{4m_p}\frac{\partial F}{\partial \beta} = \frac{m+2n}{m}\frac{(-1)\cos\alpha}{sin^2\beta cos^2(\beta-\alpha)}[\cos\beta\cos(\beta-\alpha)+\sin\beta(-\sin(\beta-\alpha))] + \frac{\cos\beta\cos\alpha\cos(\beta-\alpha)-\sin\beta\cos\alpha(-\sin(\beta-\alpha))}{cos^2\alpha cos^2(\beta-\alpha)} = 0$$

$$\frac{1}{4m_p}\frac{\partial F}{\partial \beta} = \frac{m+2n}{m}\frac{cos^2\alpha(sin^2\beta - cos^2\beta)+2\sin\alpha\cos\alpha\sin\beta\cos\beta}{sin^2\beta cos^2(\beta-\alpha)} + \frac{1}{cos^2(\beta-\alpha)} = 0$$

$$\frac{1}{4m_p}\frac{\partial F}{\partial \beta} = \frac{m+2n}{m}\frac{sin^2\beta - cos^2(\beta-\alpha)}{sin^2\beta cos^2(\beta-\alpha)} + \frac{1}{cos^2(\beta-\alpha)} = 0 \quad (2)$$

From equation (1)

$$\frac{m+2n}{m} = \frac{\cos 2(\beta-\alpha)+sin^2\alpha}{cos^2\alpha} = \frac{\cos 2(\beta-\alpha)+1}{cos^2\alpha} - 1$$

$$\frac{m+n}{m}cos^2\alpha = cos^2(\beta-\alpha) \quad (3)$$

From equation (2)

$$\frac{1}{4m_p}\frac{\partial F}{\partial \beta} = \frac{m+2n}{m}\frac{sin^2\beta - cos^2(\beta-\alpha)}{sin^2\beta cos^2(\beta-\alpha)} + \frac{1}{cos^2(\beta-\alpha)} = 0$$

$$2\frac{(m+n)}{m+2n}sin^2\beta = cos^2(\beta-\alpha) \quad (4)$$

Substituting the result of equation (3) into equation (4) yields:

$$\frac{(m+n)}{m}cos^2\alpha = 2\frac{(m+n)}{m+2n}sin^2\beta$$

$$\cos\alpha = \sqrt{\frac{2m}{m+2n}}\sin\beta \quad (5)$$

Substituting the result of equation (5) into equation (4) yields:

$$\cos\beta = \frac{3}{4}\sqrt{\frac{m}{m+n}} \quad (6)$$

$$\sin\beta = \frac{1}{4}\sqrt{\frac{7m+16n}{m+n}} \quad (7)$$

Substituting the result of equation (7) into equation (4) and equation (5) yields:

$$\cos(\beta-\alpha) = \sqrt{\frac{7m+16n}{8(m+2n)}} \quad (8)$$

$$\sin\alpha = \sqrt{\frac{m(7m+16n)}{8(m+2n)(m+n)}} \quad (9)$$

If the expressions for $\sin\alpha$ and $\cos\beta$ are substituted into the equation for the collapse load, the following relation is found:

$$F = t_{fc}^2 f_{yc}\left(\frac{a}{m} + \sqrt{\frac{7m+16n}{m}}\right)$$

Where:

- ✓ f_{yc} : is the yield stress in the column flange.
- ✓ t_{fc} : is the thickness of the column flange.

3.5.2 Welded plates reinforced column

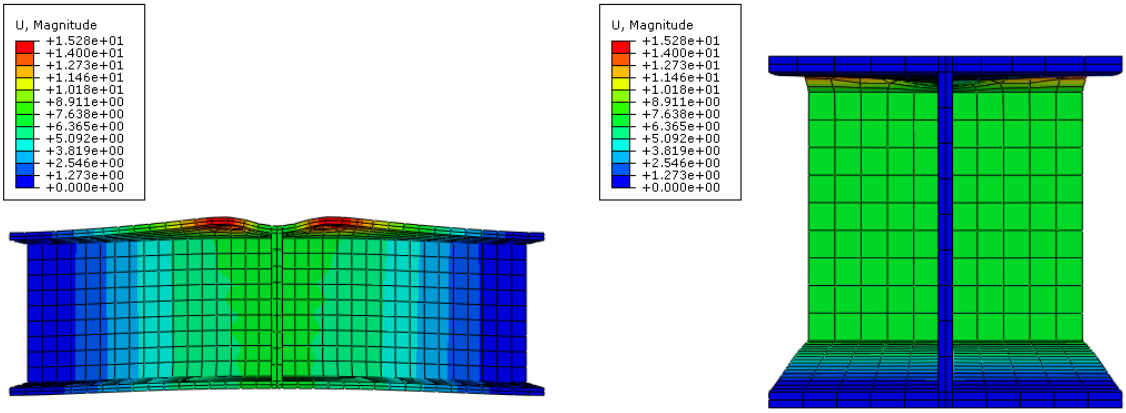

(a) (b)

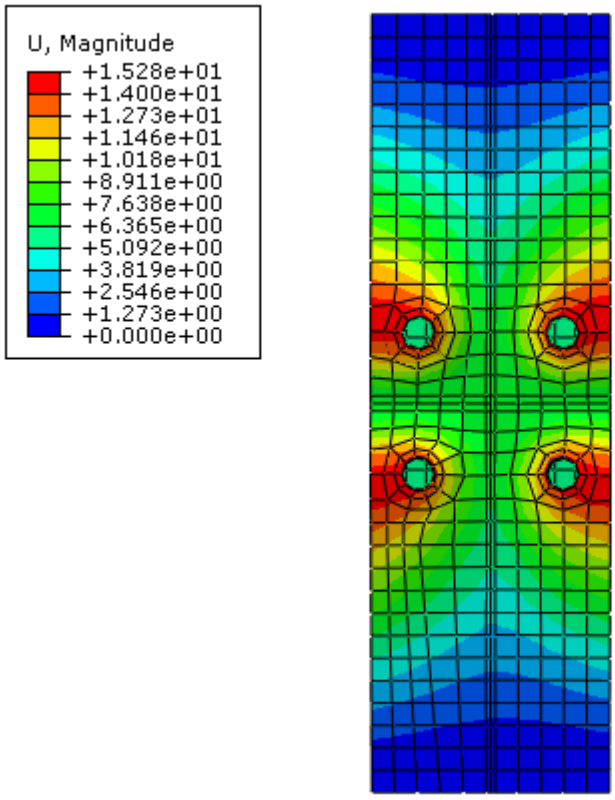

(c)

Figure 3.4: Column flange deformation for welded plates reinforced test.

The yield line pattern of flange plate is shown in figure 3.5.

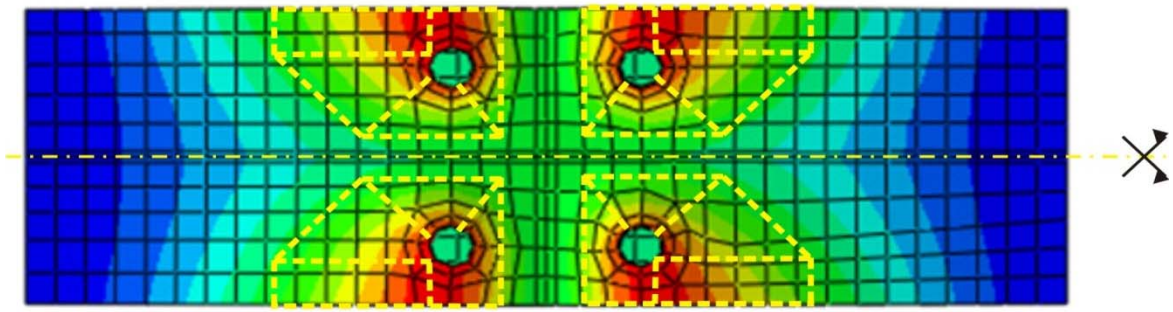

(a)

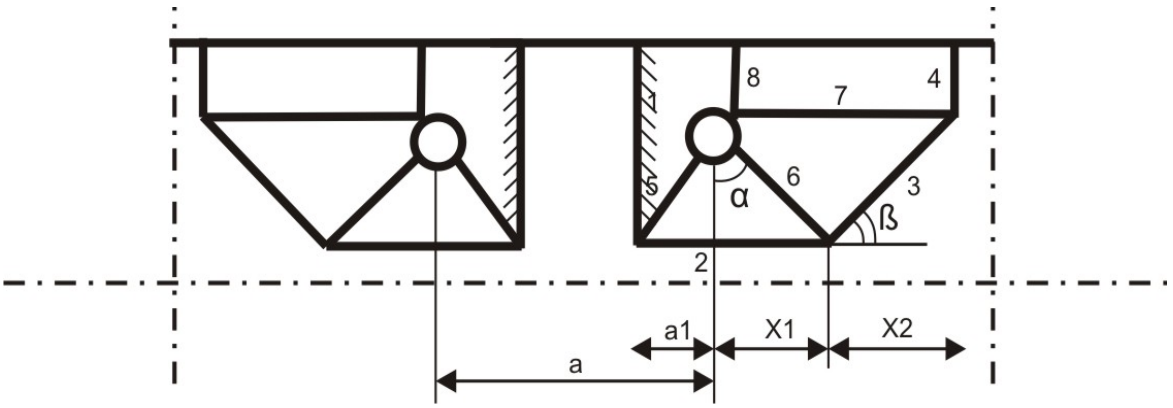

(b)

Figure 3.5: Yield line pattern for welded plates reinforced test.

Yield line 1

The length of the yield line is:

$$L_1 = m + n$$

The rotation is:

$$\theta_1 = \frac{\Delta\delta}{a_1}$$

Thus

$$\Delta E_1 = 2\,(m+n)\frac{\Delta\delta}{a_1}\;\; m_p$$

Yield line 2

The length of the yield line is:

$$L_2 = a_1 + X_1$$

The rotation is:

$$\theta_2 = \frac{\Delta\delta}{m}$$

Thus

$$\Delta E_2 = 2(a_1 + X_1)\frac{\Delta\delta}{m} m_p$$

Yield line 3

The length of the yield line is:

$$L_3 = \sqrt{m^2 + X_2^2}$$

The rotation is:

$$\theta_3 = \frac{\sqrt{m^2 + X_2^2}}{X_1 + X_2}\frac{\Delta\delta}{m}$$

Thus

$$\Delta E_3 = 2\,\frac{m^2 + X_2^2}{X_1 + X_2}\,\frac{\Delta\delta}{m}\,m_p$$

Yield line 4

The length of the yield line is:

$$L_4 = n$$

The rotation is:

$$\theta_4 = \frac{\Delta\delta}{X_1 + X_2}$$

Thus

$$\Delta E_4 = 2\,n\,\frac{\Delta\delta}{X_1 + X_2}\,m_p$$

Yield line 5

The length of the yield line is:

$$L_{5'} = m$$

$$L_{5''} = a_1$$

The rotation is:

$$\theta_{5'} = \frac{\Delta\delta}{a_1}$$

$$\theta_{5''} = \frac{\Delta\delta}{m}$$

Thus

$$\Delta E_5 = 2\, m_p\, \Delta\delta \left(\frac{m}{a_1} + \frac{a_1}{m}\right)$$

Yield line 6

The length of the yield line is:

$$L_6 = \sqrt{m^2 + X_1^2}$$

The rotation is:

$$\theta_6 = \frac{\sqrt{m^2 + X_1^2}}{X_1 + X_2} \frac{\Delta\delta}{m}$$

Thus

$$\Delta E_6 = 2\, \frac{m^2 + X_1^2}{X_1 + X_2} \frac{\Delta\delta}{m}\, m_p$$

Yield line 7

The length of the yield line is:

$$L_7 = X_1 + X_2$$

The rotation is:

$$\theta_7 = \frac{\Delta\delta}{m}$$

Thus

$$\Delta E_7 = 2\, (X_1 + X_2) \frac{\Delta\delta}{m}\, m_p$$

Yield line 8

The length of the yield line is:

$$L_8 = n$$

The rotation is:

$$\theta_8 = \left(\frac{1}{a_1} + \frac{1}{X_1 + X_2}\right)\Delta\delta$$

Thus

$$\Delta E_8 = 2\,n\left(\frac{1}{a_1} + \frac{1}{X_1 + X_2}\right)\Delta\delta\; m_p$$

The total internal energy will be:

$$\sum_{i=1}^{8} \Delta E_i = 2\,\Delta\delta\; m_p \left(\frac{2(m+n)}{a_1} + \frac{1}{m}(2a_1 + 2X_1 + X_2) + \frac{1}{\mathrm{m}(X_1 + X_2)}(2m^2 + {X_1}^2 + {X_2}^2 + 2mn)\right)$$

The work done by the external force F/2 is:

$$\Delta T = \frac{F}{2}\Delta\delta$$

Equating the external and the internal energy gives:

$$\frac{F}{2}\Delta\delta = 2\,m_p\,\Delta\delta\left(\frac{2(m+n)}{a_1} + \frac{1}{m}(2a_1 + 2X_1 + X_2) + \frac{1}{\mathrm{m}(X_1 + X_2)}(2m^2 + {X_1}^2 + {X_2}^2 + 2mn)\right)$$

$$F = 4\,m_p\left(\frac{2(m+n)}{a_1} + \frac{1}{m}(2a_1 + 2X_1 + X_2) + \frac{1}{\mathrm{m}(X_1 + X_2)}(2m^2 + {X_1}^2 + {X_2}^2 + 2mn)\right)$$

In order to find a minimum collapse load, the following conditions must be satisfied:

$$\frac{\partial F}{\partial X_1} = 0$$

$$\frac{\partial F}{\partial X_2} = 0$$

Carrying out the differentiations give:

$$\frac{\partial F}{\partial X_1} = 2(X_1 + X_2)^2 + 2X_1(X_1 + X_2) - (2m^2 + {X_1}^2 + {X_2}^2 + 2mn) = 0 \quad (1)$$

$$\frac{\partial F}{\partial X_2} = (X_1 + X_2)^2 + 2X_2(X_1 + X_2) - (2m^2 + {X_1}^2 + {X_2}^2 + 2mn) = 0 \quad (2)$$

From equation (1) and (2) it follows that:

$$(X_1 + X_2) + 2(X_1 - X_2) = 0$$

$$X_2 = 3X_1 \quad (3)$$

Substituting the result of equation (3) into equation (1) and equation (2) yields:

$$X_1 = \sqrt{\frac{m(m+n)}{15}} \quad (4)$$

$$X_2 = 3\sqrt{\frac{m(m+n)}{15}} \quad (5)$$

If the expressions for $X_1$and X_2 are substituted into the equation for the collapse load, the following relation is found:

$$F = t_{fc}^2 f_{yc}\left(\frac{2(m+n)}{a_1} + \frac{2a_1}{m} + \sqrt{\frac{15(m+n)}{m}}\right)$$

With:

$$a_1 = \frac{a - t_p}{2} - \frac{1}{5}t_w$$

Where:

- ✓ t_p: is the thickness of the welded plate,
- ✓ t_w: is the thickness of the fillet weld.

3.5.3 Backing plates reinforced column

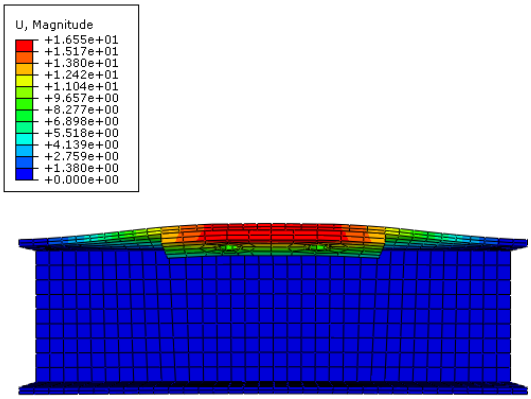

(a)

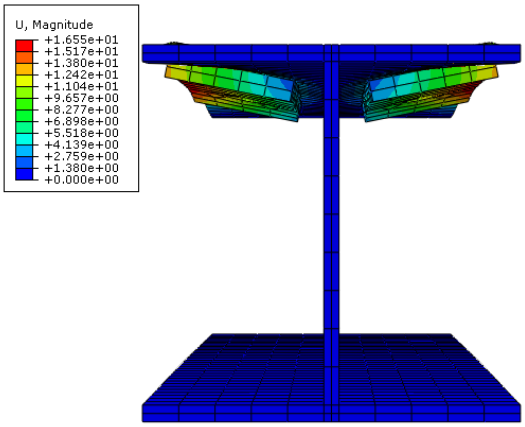

(b)

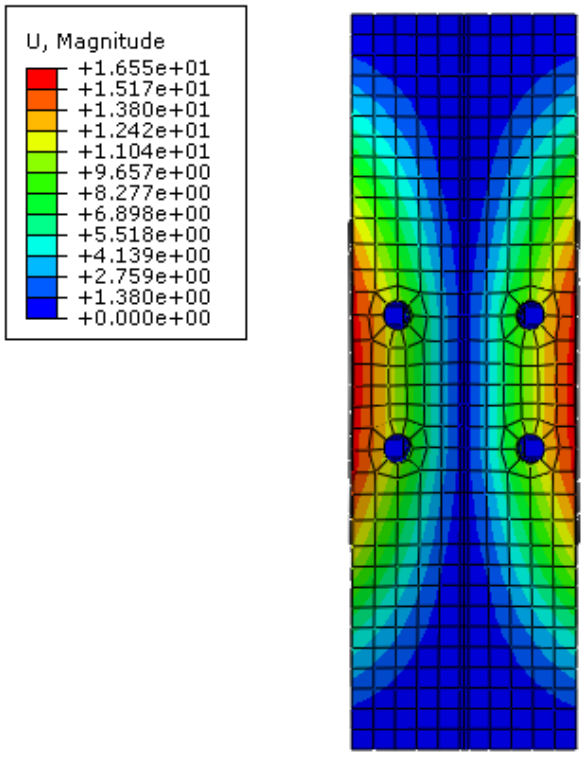

(c)

Figure 3.6: Column flange deformation for backing plates reinforced test.

The yield line patterns of the flange plate and the backing plate is shown in figure 3.7.

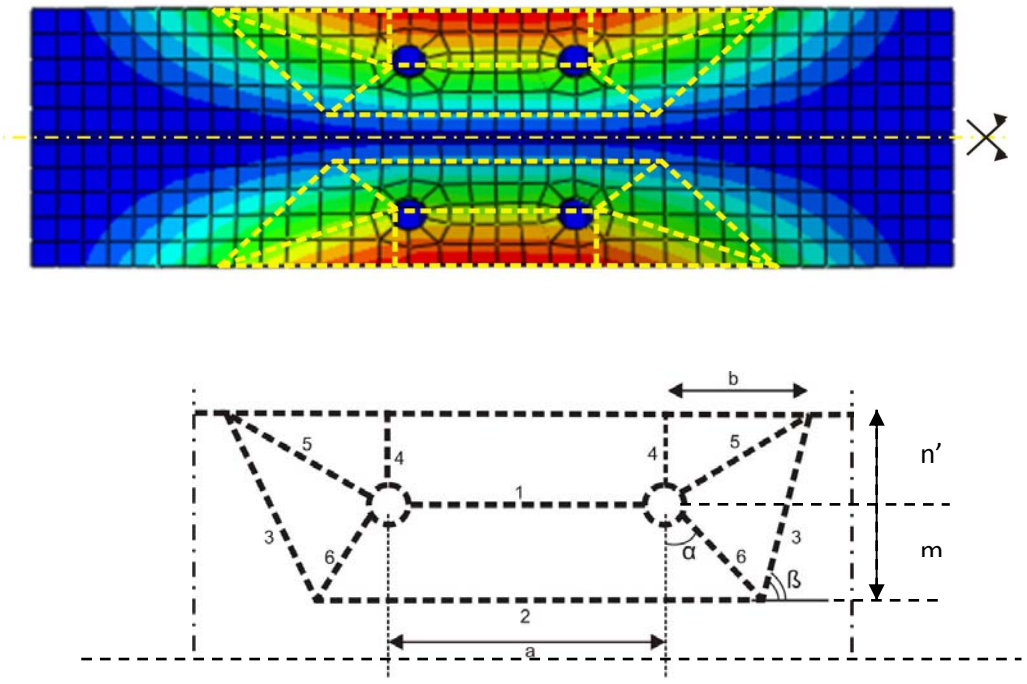

(a) Flange plate.

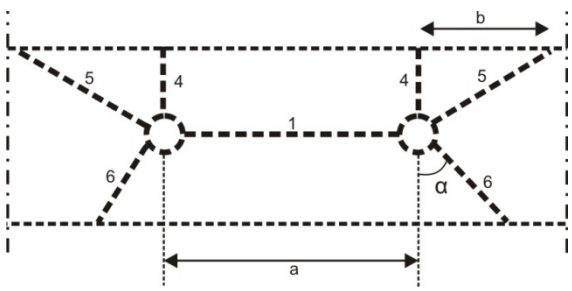

(b) Backing plate.

Figure 3.7: Yield line pattern for backing plates reinforced test.

Yield line 1

The length of the yield line is:

$$L_1 = a$$

The rotation is:

$$\theta_1 = \frac{\Delta\delta}{m}$$

Thus

$$\Delta E_1 = \frac{\Delta\delta}{m}\ a\ m_p$$

Yield line 2

The length of the yield line is:

$$L_2 = a + 2mtg\alpha$$

The rotation is:

$$\theta_2 = \frac{\Delta\delta}{m}$$

Thus

$$\Delta E_2 = \frac{\Delta\delta}{m}(a + 2mtg\alpha)m_p$$

Yield line 3

The length of the yield line is:

$$L_3 = \frac{m + n'}{\sin\beta}$$

The rotation is:

$$\theta_3 = \frac{\Delta\delta}{\frac{m}{cos\alpha}\cos(\beta - \alpha)}$$

Thus

$$\Delta E_3 = 2m_p\ \frac{m + n'}{\sin\beta}\ \frac{\Delta\delta}{\frac{m}{cos\alpha}\cos(\beta - \alpha)}$$

Yield line 4

The length of the yield line is:

$$L_4 = n'$$

The rotation is:

$$\theta_4 = \frac{\Delta\delta}{b}$$

Thus

$$\Delta E_4 = 2\, m_p\, n'\, \frac{\Delta\delta}{b}$$

Yield line 5

The length of the yield line is:

$$L_5 = \sqrt{b^2 + n'^2} = l$$

The rotation is:

$$\emptyset = \emptyset_1 - \emptyset_2 = \frac{\frac{S}{l}\Delta\delta}{y} - \frac{\Delta\delta - \frac{S}{l}\Delta\delta}{X'} = \Delta\delta\left(\frac{S}{ly} + \frac{S}{lX'} - \frac{1}{X'}\right)$$

$$\frac{S}{y} = \frac{C}{X} = \frac{C}{\frac{m}{cos\alpha}cos(\beta - \alpha)}$$

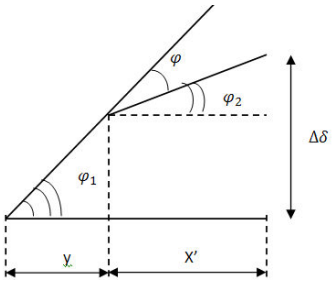

$$\frac{S}{X'} = \frac{b}{n'}$$

$$tg\gamma = \frac{L_4}{b} = \frac{n'}{b}$$

$$sin\gamma = \frac{X'}{b}\ and\ cos\gamma = \frac{b}{L_5} = \frac{b}{l}$$

$$tg\gamma = \frac{n'}{b} = \frac{X'}{b^2 l}$$

$$X' = \frac{n'b}{l}$$

Thus

$$\Delta E_5 = 2\, m_p\, \Delta\delta \left(ctg\beta + \frac{n'}{m} \frac{cos\alpha}{sin\beta\, cos(\beta - \alpha)} - \frac{n'}{b} \right)$$

Yield line 6

The length of the yield line is:

$$L_6 = \frac{m}{cos\alpha}$$

The rotation is:

$$\theta_6 = \frac{\Delta\delta\, sin\beta}{m \cos(\beta - \alpha)}$$

Thus

$$\Delta E_6 = 2\, m_p\, \frac{\Delta\delta\, sin\beta}{cos\alpha \cos(\beta - \alpha)}$$

Internal work of the column flange:

$$\sum_{i=1}^{6} \Delta E_i = 2\, \Delta\delta\, m_{p1} \left(\frac{a}{m} + tg\alpha + \frac{m + 2n'}{m} \frac{cos\alpha}{sin\beta \cos(\beta - \alpha)} + ctg\beta + \frac{sin\beta}{cos\alpha \cos(\beta - \alpha)} \right)$$

Internal work of the backing plate:

$$\sum_{i=1}^{6} \Delta E_i = 2\, \Delta\delta\, m_{p\,2} \left(\frac{a}{2m} + \frac{n'}{m} \frac{cos\alpha}{sin\beta \cos(\beta - \alpha)} + ctg\beta + \frac{sin\beta}{cos\alpha \cos(\beta - \alpha)} \right)$$

The work done by the external force F/2 is:

$$\Delta T = \frac{F}{2} \Delta\delta$$

Equating the external and the internal energy gives:

$$\frac{F}{2} \Delta\delta = 2\, \Delta\delta\, m_{p1} \left(\frac{a}{m} + tg\alpha + \frac{m + 2n'}{m} \frac{cos\alpha}{sin\beta \cos(\beta - \alpha)} + ctg\beta + \frac{sin\beta}{cos\alpha \cos(\beta - \alpha)} \right) + 2\, \Delta\delta\, m_{p\,2} \left(\frac{a}{2m} + \frac{n'}{m} \frac{cos\alpha}{sin\beta \cos(\beta - \alpha)} + ctg\beta + \frac{sin\beta}{cos\alpha \cos(\beta - \alpha)} \right)$$

$$\frac{F}{2} = 2\ m_{p1}\left(\frac{a}{m} + tg\alpha + \frac{m+2n'}{m}\frac{cos\alpha}{sin\beta\cos(\beta-\alpha)} + ctg\beta + \frac{sin\beta}{cos\alpha\cos(\beta-\alpha)}\right) + 2\ m_{p\,2}\left(\frac{a}{2m} + \frac{n'}{m}\frac{cos\alpha}{sin\beta\cos(\beta-\alpha)} + ctg\beta + \frac{sin\beta}{cos\alpha\cos(\beta-\alpha)}\right) \quad (1)$$

The collapse load F is a minimum if the following conditions are satisfied:

$$\frac{\partial F}{\partial \alpha} = 0$$

$$\frac{\partial F}{\partial \beta} = 0$$

Carrying out the differentiations give:

$$\frac{\partial F}{\partial \alpha} = 2\,m_{p1}\left(\frac{1}{cos^2\alpha} - \frac{m+2n'}{m}\frac{1}{cos^2(\beta-\alpha)} + \frac{\frac{1}{2}sin2\alpha\ sin2\beta - sin^2\beta\ cos2\alpha}{cos^2\alpha\ cos^2(\beta-\alpha)}\right) + 2\,m_{p\,2}\left(-\frac{n'}{m}\frac{1}{cos^2(\beta-\alpha)} + \frac{\frac{1}{2}sin2\alpha\ sin2\beta - sin^2\beta\ cos2\alpha}{cos^2\alpha\ cos^2(\beta-\alpha)}\right) = 0$$

$$\frac{\partial F}{\partial \alpha} = 2\,m_{p1}\left(\frac{\cos 2(\beta-\alpha) + sin^2\alpha}{cos^2\alpha.cos^2(\beta-\alpha)} - \frac{m+2n'}{m}\cdot\frac{1}{cos^2(\beta-\alpha)}\right) + 2\,m_{p2}\left(\frac{\frac{1}{2}\cos 2(\beta-\alpha) - \frac{1}{2}\cos 2\alpha}{cos^2\alpha.cos^2(\beta-\alpha)} - \frac{n'}{m}.\frac{1}{cos^2(\beta-\alpha)}\right) = 0 \quad (2)$$

$$\frac{\partial F}{\partial \beta} = 2\,m_{p1}\left(-\frac{1}{sin^2\beta} + \frac{m+2n'}{m}.\frac{-\cos\alpha(\cos\beta.\cos(\beta-\alpha) - \sin\beta.\sin(\beta-\alpha))}{sin^2\beta.cos^2(\beta-\alpha)} + \frac{\cos\beta.\cos\alpha.\cos(\beta-\alpha) - \sin\beta.\cos\alpha.(-\sin(\beta-\alpha))}{cos^2\alpha.cos^2(\beta-\alpha)}\right) + 2\,m_{p2}\left(-\frac{1}{\sin\beta^2} + \frac{n'}{m}.\frac{(-\cos\alpha.\cos(2\beta-\alpha))}{sin^2\beta.cos^2(\beta-\alpha)} + \frac{1}{cos^2(\beta-\alpha)}\right) = 0$$

$$\frac{\partial F}{\partial \beta} = 2\, m_{p1}\left(\frac{2(m+2n')}{m}.\frac{sin^2\beta - cos^2(\beta-\alpha)}{sin^2\beta.cos^2(\beta-\alpha)}\right) + 2\, m_{p2}\left(\frac{(m+2n')}{m}.\frac{sin^2\beta - cos^2(\beta-\alpha)}{sin^2\beta.cos^2(\beta-\alpha)}\right) = 0 \quad (3)$$

From equation (3)

$$\frac{1}{sin^2\beta.cos^2(\beta-\alpha)}.\frac{m+n'}{m}\left(sin^2\beta\left(4m_{p1}+2m_{p2}\right) - cos^2(\beta-\alpha)\left(4m_{p1}+2m_{p2}\right)\right) = 0$$

$$sin^2\beta.cos^2(\beta-\alpha) \neq 0$$

$$sin^2\beta\left(4m_{p1}+2m_{p2}\right) - cos^2(\beta-\alpha)\left(4m_{p1}+2m_{p2}\right) = 0$$

$$\sin\beta = \cos(\beta-\alpha) \quad (4)$$

Substituting the results of equation (3) into equation (1) yields:

$$\frac{1}{cos^2\alpha.sin^2\beta}\left(2.m_{p1}\left(2.sin^2\beta - \frac{2(m+n')}{m}cos^2\alpha\right) + 2.m_{p2}\left(sin^2\beta - \frac{(m+n')}{m}cos^2\alpha\right)\right) = 0$$

$$\frac{1}{cos^2\alpha.sin^2\beta}\left(sin^2\beta\left(4m_{p1}+2m_{p2}\right) - cos^2\alpha\frac{(m+n')}{m}\left(4m_{p1}+2m_{p2}\right)\right) = 0 \quad (5)$$

From equation (4) it follows that:

$$cos\alpha = \frac{sin\beta}{\sqrt{\frac{m+n'}{m}}} \quad (6)$$

$$cos\beta = 2\frac{sin\beta}{\sqrt{\frac{m+n'}{m}}} \quad (7)$$

$$sin\beta = \frac{1}{2}\sqrt{\frac{3m^2+4mn'}{m+n'}} \quad (8)$$

$$cos\alpha = \frac{1}{2}\sqrt{\frac{3m^2 + 4mn'}{m + n'}} \tag{9}$$

$$sin\alpha = \frac{1}{2}\frac{\sqrt{m^2 + 4n'^2 + 4mn'}}{m + n'} \tag{10}$$

Substituting the results of equations (6), (7), (8), (9) and (10) into equation (1) yields to the following relationship:

$$F = 2\left(\frac{4\,m_{p1} + 2\,m_{p\,2}}{m}\right)\left(\frac{a}{2} + \sqrt{3m^2 + 4mn'}\right)$$

$$\boxed{F = 2\left(\frac{t_{fc}^2 f_{yc} + \frac{1}{2}t_{bc}^2 f_{yb}}{m}\right)\left(\frac{a}{2} + \sqrt{3m^2 + 4mn'}\right)}$$

Where:

- ✓ f_{yc} : is the yield stress in the column flange.
- ✓ t_{fc} : is the thickness of the column flange.
- ✓ f_{bc} : is the yield stress in the backing plate.
- ✓ t_{bc} : is the thickness of the backing plate.

3.5.4 Channels reinforced column

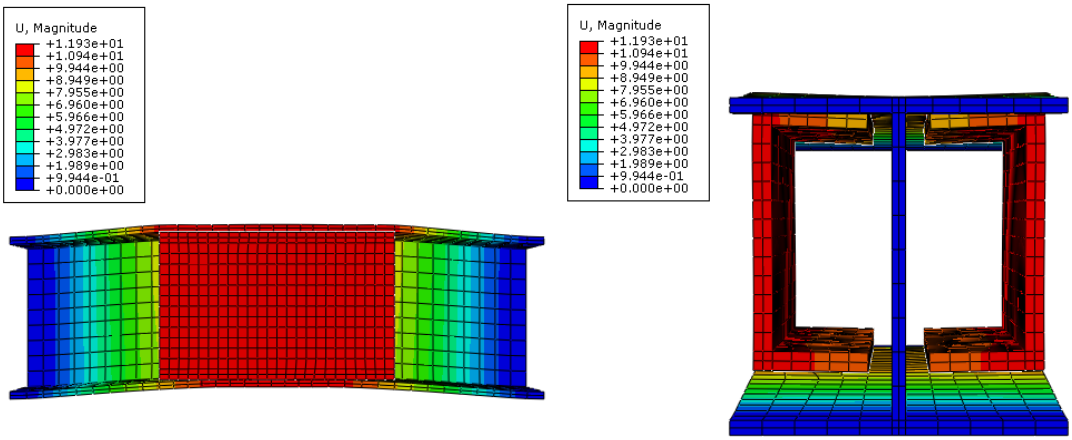

(a) (b)

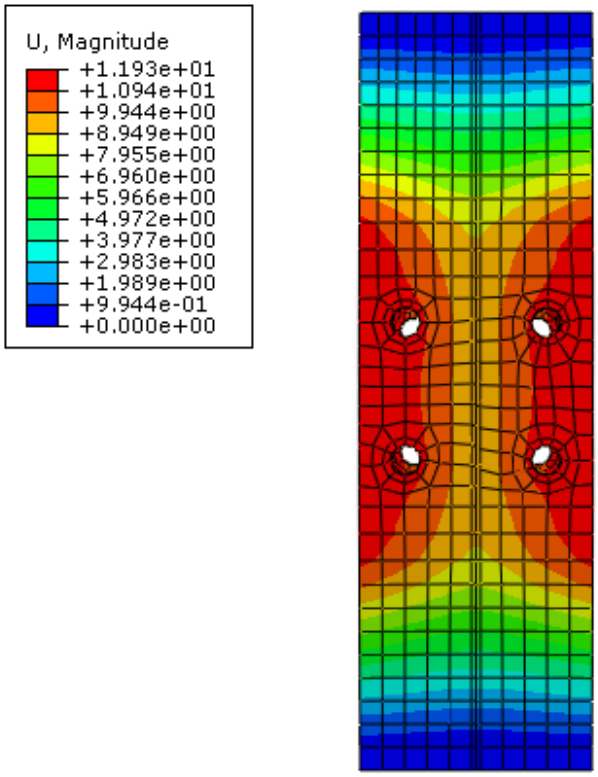

(c)

Figure 3.8: Column flange deformation for channels reinforced test.

The yield line pattern of the flange is shown in figure 3.11.

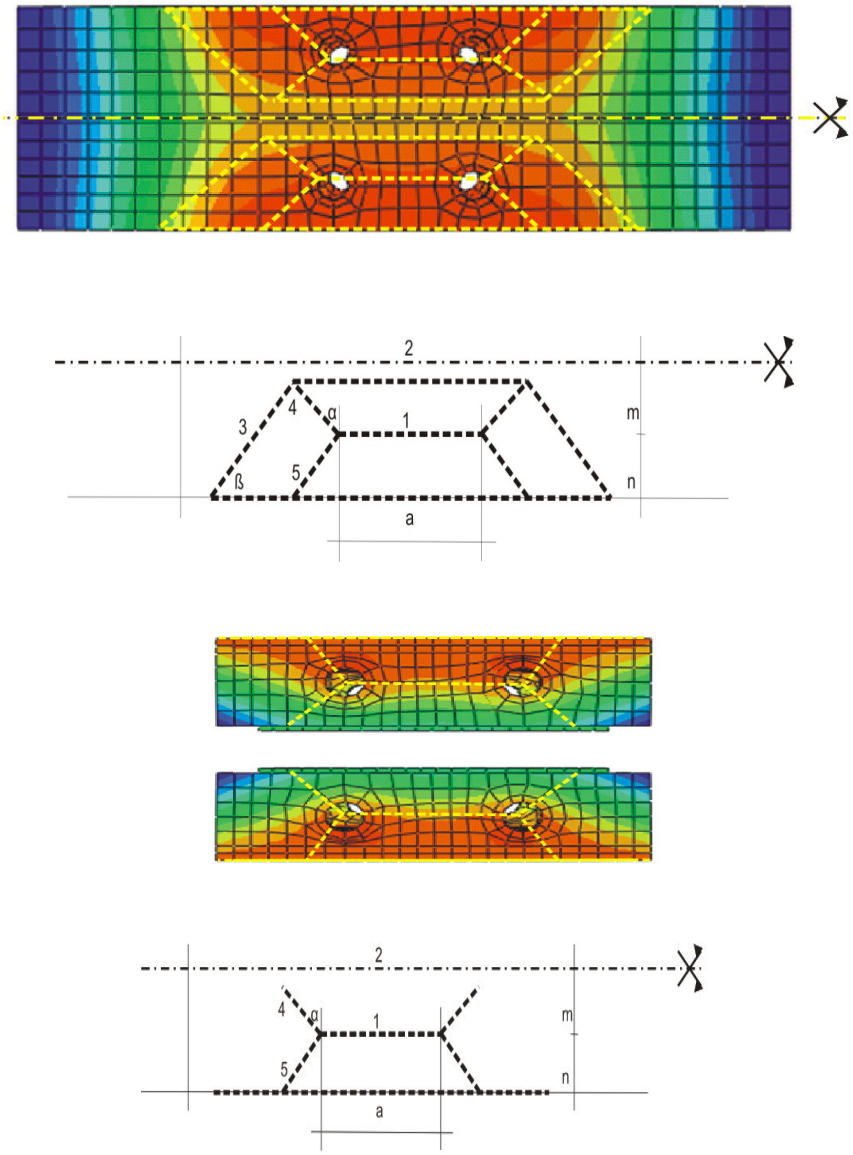

Figure 3.9: Yield line Pattern for channels reinforced test.

Carrying out the same analysis as in the case of the unreinforced tension zone . the following expression for the minimum collapse load is found.

$$F = \left(t_{fc}^2 f_{yc} + t_r^2 f_{yr}\right)\left(\frac{1}{m}\left(a + \sqrt{15(m^2 + mn)}\right)\right)$$

3.5.5 Threaded bars reinforced column

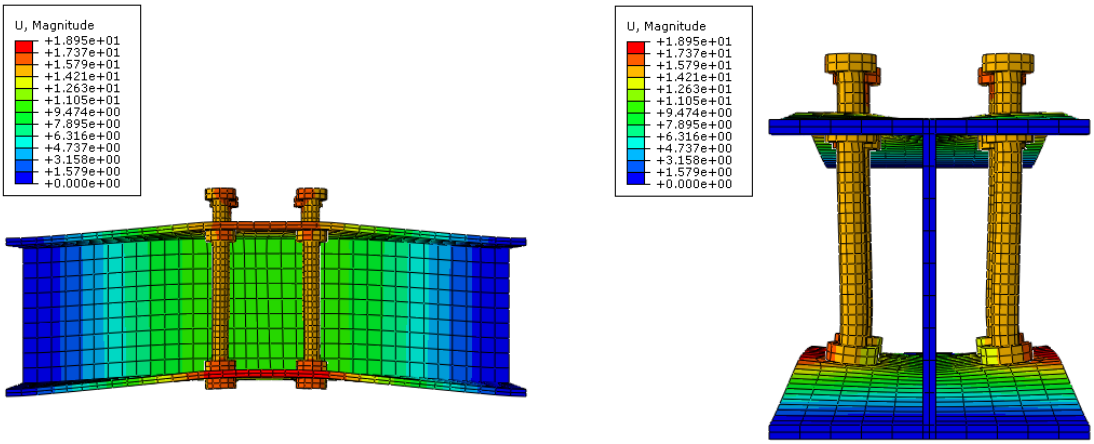

(a) (b)

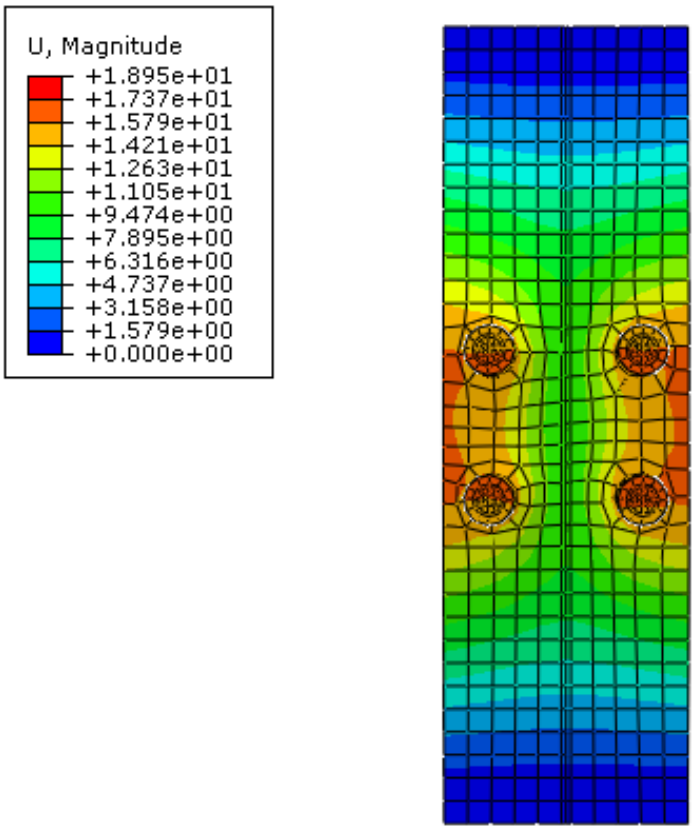

(c)

Figure 3.10: Flange deformation for threaded bars reinforced test.

The yield line pattern of the column flange is shown in figure 3.9.

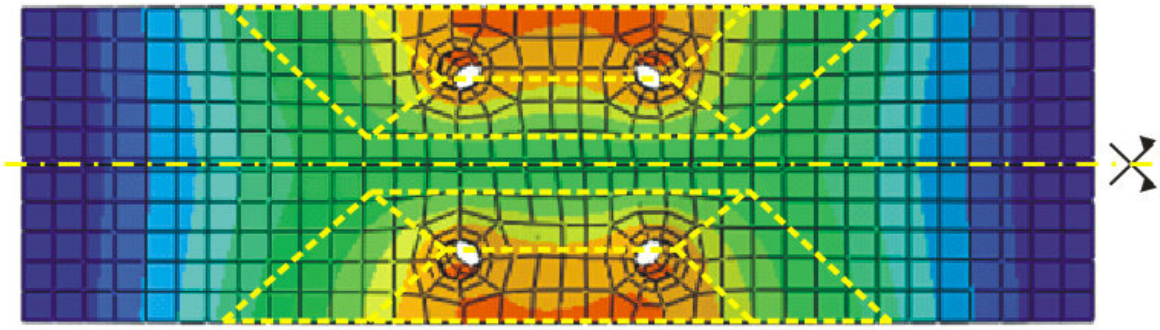

(a)

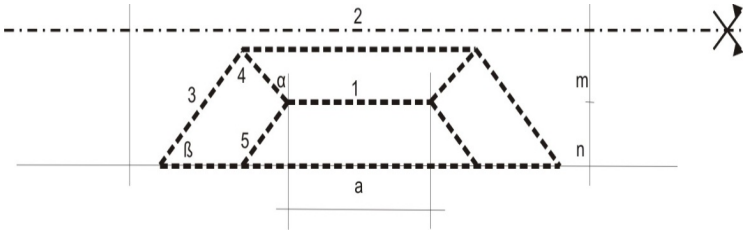

(b)

Figure 3.11: Flange deformation for threaded bars reinforced test.

The mode of collapse of the column flange was identical to the mode of collapse of channels reinforced test, and so:

$$F = \left(t_{fc}^2 f_{yc} + t_r^2 f_{yr}\right)\left(\frac{1}{m}\left(a + \sqrt{15(m^2 + mn)}\right)\right)$$

3.5.6 Threaded bars and welded plates reinforced column

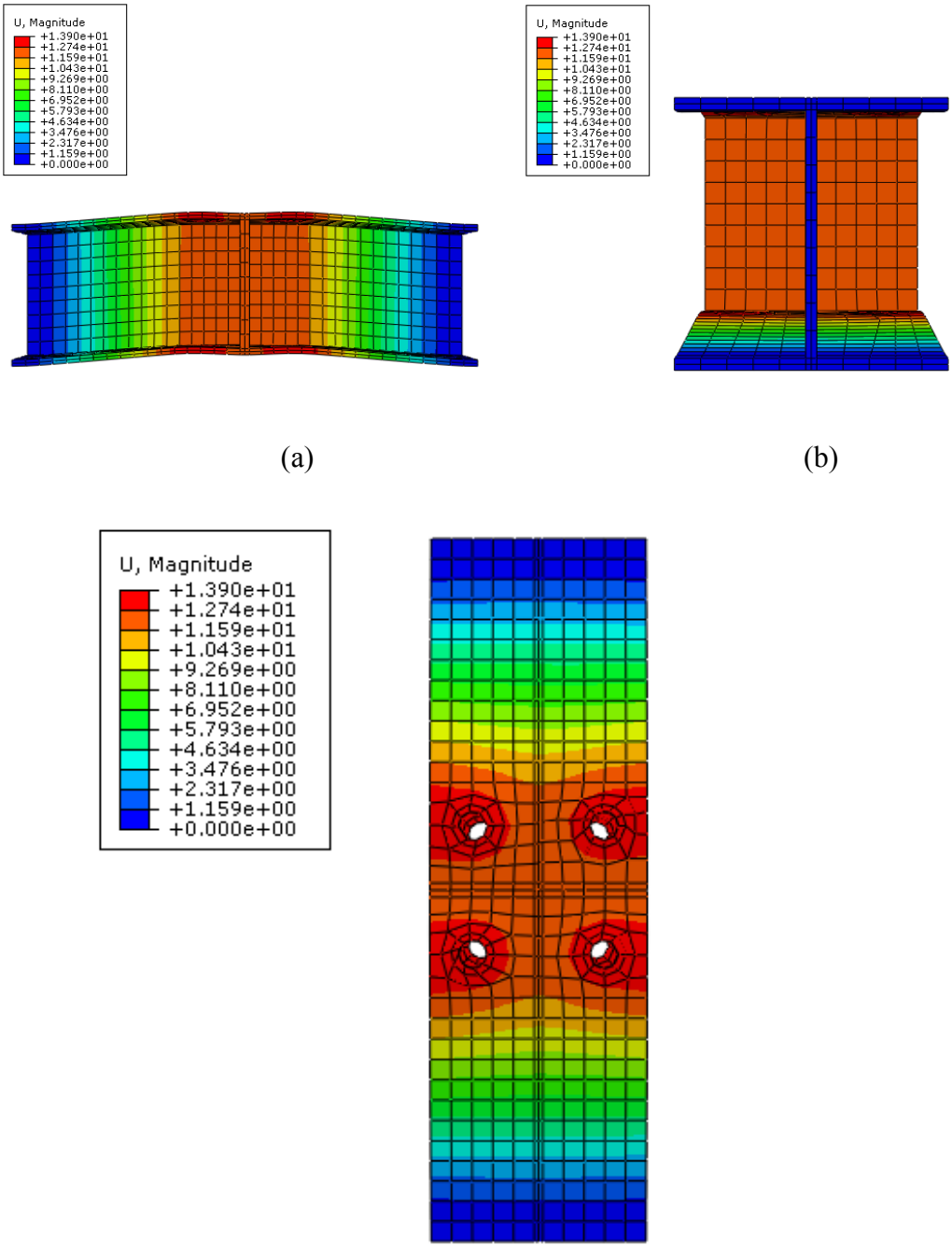

Figure 3.12: Column flange deformation for threaded bars and welded plates reinforced test.

The yield line pattern of the flange is shown in figure 3.13.

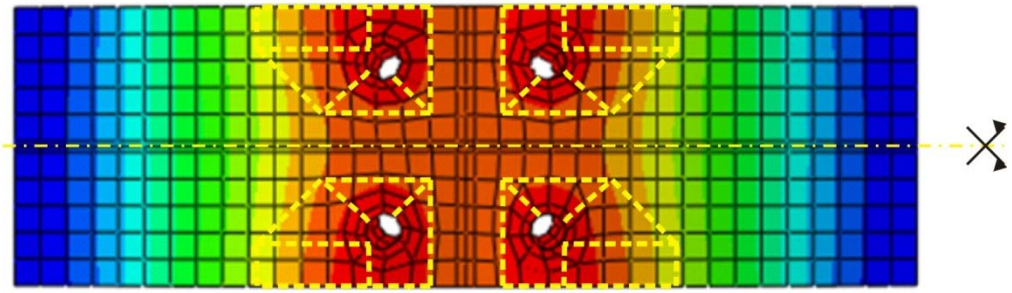

(a)

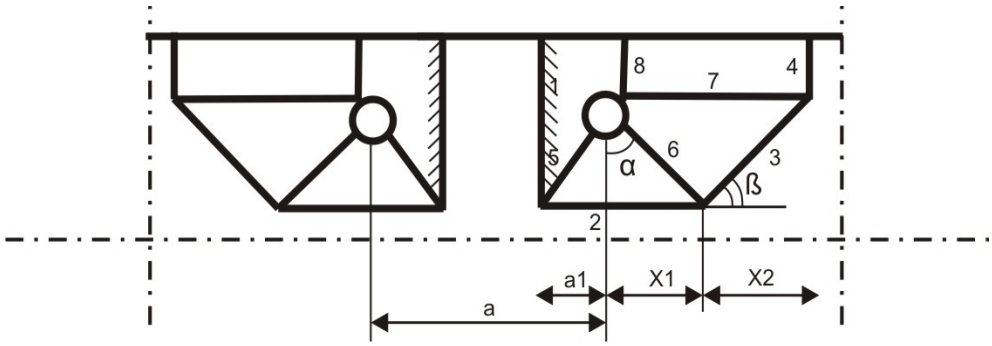

(b)

Figure 3.13: Yield line pattern for threaded bars and welded plates reinforced test.

The same formula as the test T2 was adopted.

$$F = t_{fc}^2 f_{yc} \left(\frac{2(m+n)}{a_1} + \frac{2a_1}{m} + \sqrt{\frac{15(m+n)}{m}} \right)$$

3.5.7 Threaded bars and backing plates reinforced column

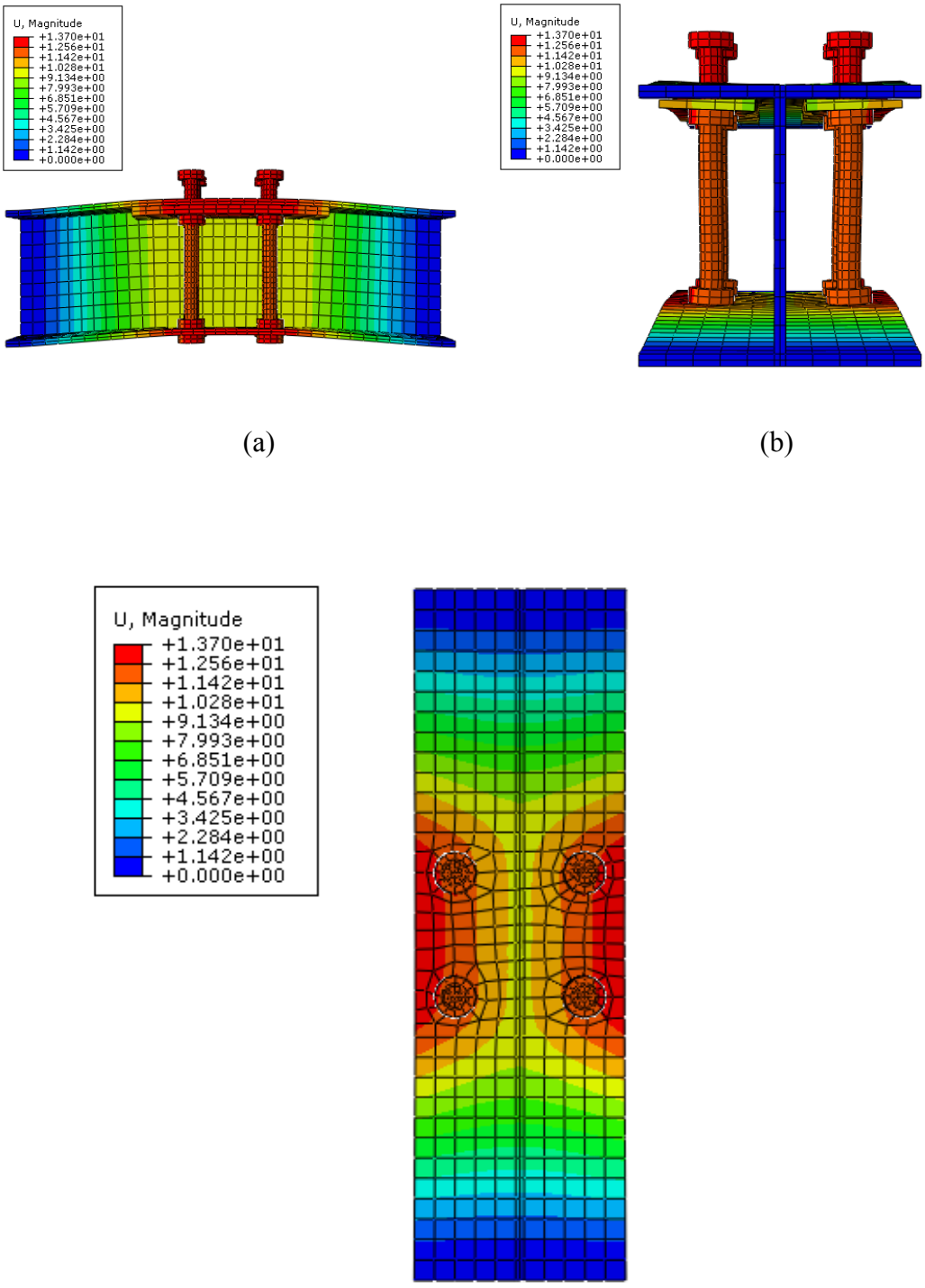

Figure 3.14: Flange deformation for threaded bars and backing plates reinforced test.

The yield line pattern of the column flange is shown in figure 3.15.

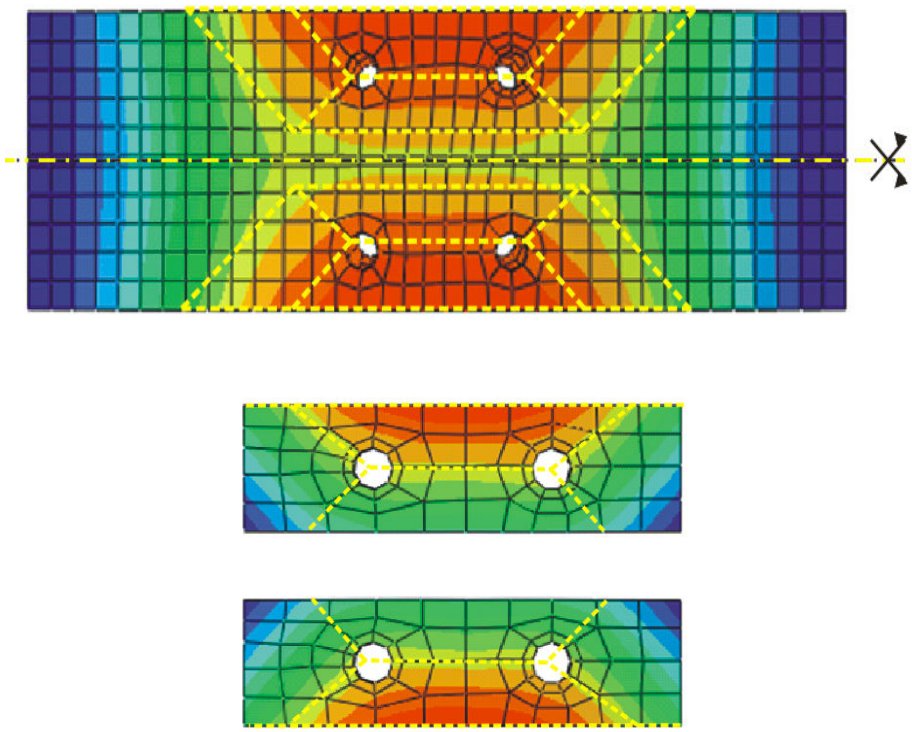

Figure 3.15: Yield line pattern For Test T7.

The mode of collapse of the column flange was identical to the mode of collapse of channel reinforced test, and so:

$$F = \left(t_{fc}^2 f_{yc} + t_r^2 f_{yr}\right)\left(\frac{1}{m}\left(a + \sqrt{15(m^2 + mn)}\right)\right)$$

3.5.8 Test T8

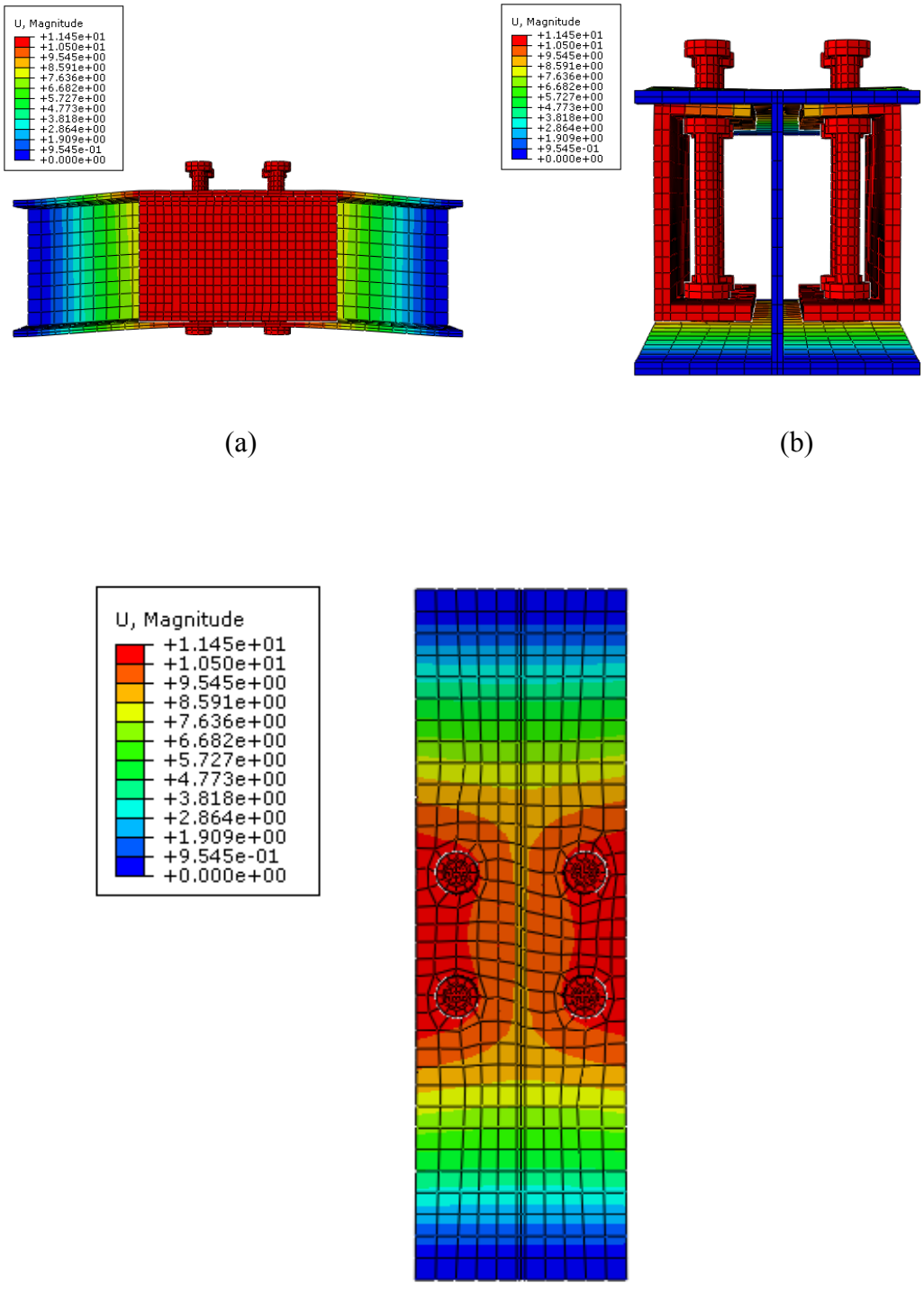

Figure 3.16: Column flange deformation for threaded bars and channels reinforced test.

The mode of collapse of the column flange is shown in figure 3.17.

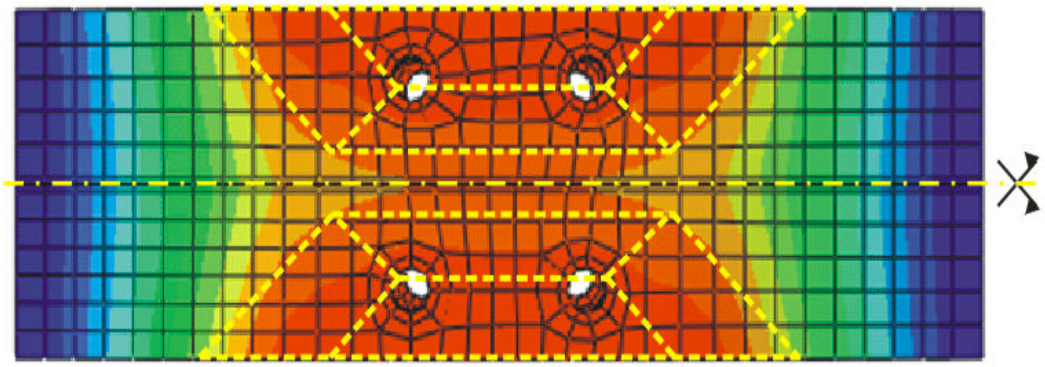

(a)

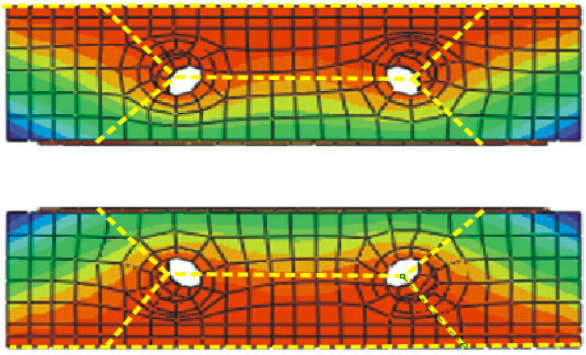

(b)

Figure 3.17: Yield line pattern for threaded bars and channels reinforced test.

The same formula as the test T4 was adopted.

$$F = \left(t_{fc}^2 f_{yc} + t_r^2 f_{yr}\right)\left(\frac{1}{m}\left(a + \sqrt{15(m^2 + mn)}\right)\right)$$

Summary

The next table summaried the reached yield load formulas.

Table 3.1: Yield load formulas.

Test	Yield load formula	Collapse mechanism
Test T1	$F = t_{fc}^2 f_{yc}\left(\frac{a}{m} + \sqrt{\frac{7m+16n}{m}}\right)$	flange
Test T2	$F = t_f^2 f_y\left(\frac{2(m+n)}{a_1} + \frac{2a_1}{m} + \sqrt{\frac{15(m+n)}{m}}\right)$	flange
Test T3	$F = 2\left(\frac{t_{fc}^2 f_{yc} + \frac{1}{2}t_b^2 f_{yb}}{m}\right)\left(\frac{a}{2} + \sqrt{3m^2 + 4mn'}\right)$	flange
Test T4	$F = \left(t_{fc}^2 f_{yc} + t_r^2 f_{yr}\right)\left(\frac{1}{m}\left(a + \sqrt{15(m^2 + mn)}\right)\right)$	flange
Test T5	$F = \left(t_{fc}^2 f_{yc} + t_r^2 f_{yr}\right)\left(\frac{1}{m}\left(a + \sqrt{15(m^2 + mn)}\right)\right)$	flange
Test T6	$F = t_f^2 f_y\left(\frac{2(m+n)}{a_1} + \frac{2a_1}{m} + \sqrt{\frac{15(m+n)}{m}}\right)$	flange
Test T7	$F = \left(t_{fc}^2 f_{yc} + t_r^2 f_{yr}\right)\left(\frac{1}{m}\left(a + \sqrt{15(m^2 + mn)}\right)\right)$	flange
Test T8	$F = \left(t_{fc}^2 f_{yc} + t_r^2 f_{yr}\right)\left(\frac{1}{m}\left(a + \sqrt{15(m^2 + mn)}\right)\right)$	flange

CHAPITRE 4

RESULTS AND ANALYSIS

4.1 Introduction

The behavior of the connections can be determined through experimental, analytical and numerical method. The experimental studies have, and still suitable to validate the results produced by the two approaches mentioned above.

In this project, the laboratory study affected by **Sethi** [16] was chosen. And so, a comparative study between that test and the numerical finite element analysis results of the validated test was to take in charge to determine the accuracy of the finite element analysis in predicting the nonlinear behavior of the t-stub end plate moment connection. The following comparisons are made:

- Load-displacement (f-δ) curve.
- Resistance load.
- Mode of failure.

Then a more detailed comparison will be given between the two rest series of tests in order to check the overall behavior of the connections in term of strength, stiffness and deformation capacity.

The comparison will be highlighted with the aid of graphs and diagrams.

4.2 Comparison between the experimental test and ABAQUS (First series of tests)

4.2.1 Comparison between the load-displacement curves

Figure 4.1 shows non-linear response curve obtained from the laboratory compared with the load-displacement curve obtained from ABAQUS.

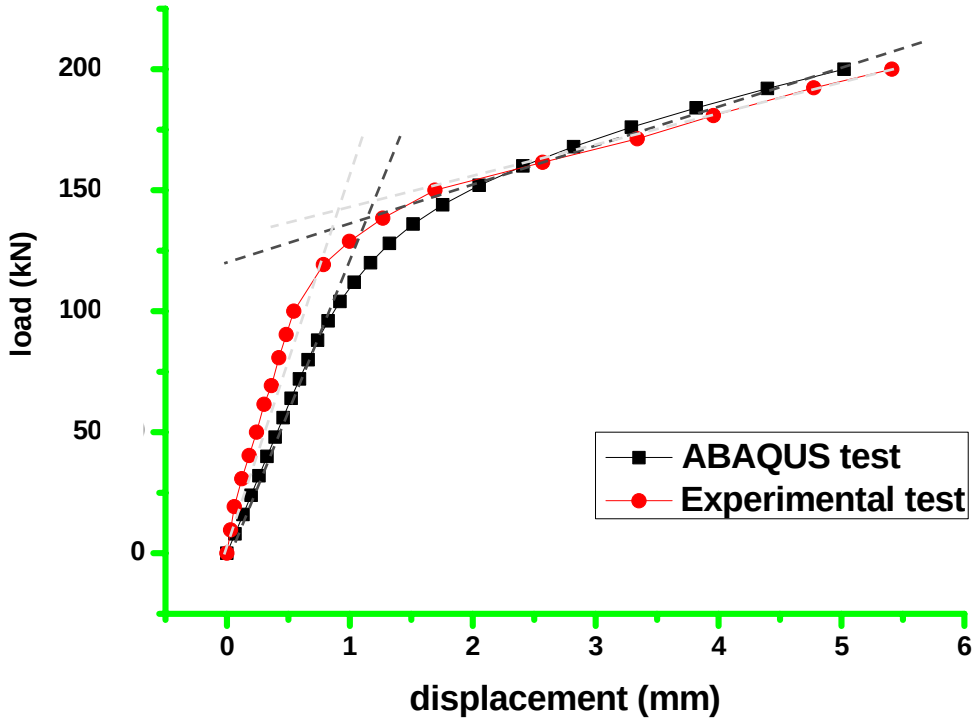

Figure 4.1: Load-Displacement curve for the test V1 and the test of **Sethi** [16].

The numerical results produced in ABAQUS are displayed as black while the loads and displacements, measured in experimental test are showed as red. By observing the two curves, it is apparent that the performance of the FE model was found to be in close agreement with the experimental test.

The trends of both the curves are similar although there was some difference in the initial elastic stage; the experimental test has lower displacement than the finite element model at the same load, which signifies that FE model is less stiffer than the experimental test. This may be the results of an inexactitude of the input materials properties and boundary conditions for the model.

4.2.2 Comparison of resistance loads

The comparison of the resistance loads between the experimental test and the finite element analysis is displayed in table 4.1. The percentage of difference is 3.70 %.

Table 4.1: Comparison of resistance loads between laboratory test and ABAQUS analysis.

Test identification	Resistance loads (kN)		Difference %
Test V1	Experimental test	ABAQUS test	3.70
	140	135	

4.2.3 Comparison on the mode of failure

Similar mode of failure was observed in both the experimental and the finite element analysis as mentioned in table 4.2.

Table 4.2: Comparison on the mode of failure between the experimental test and ABAQUS model.

Test identification	Mode of failure	
Test V1	Experimental test	ABAQUS test
	Bending of the column	Bending of the column

The failure mode of the finite element model occurred due to the bending of column, as shown in Figure 4.2.

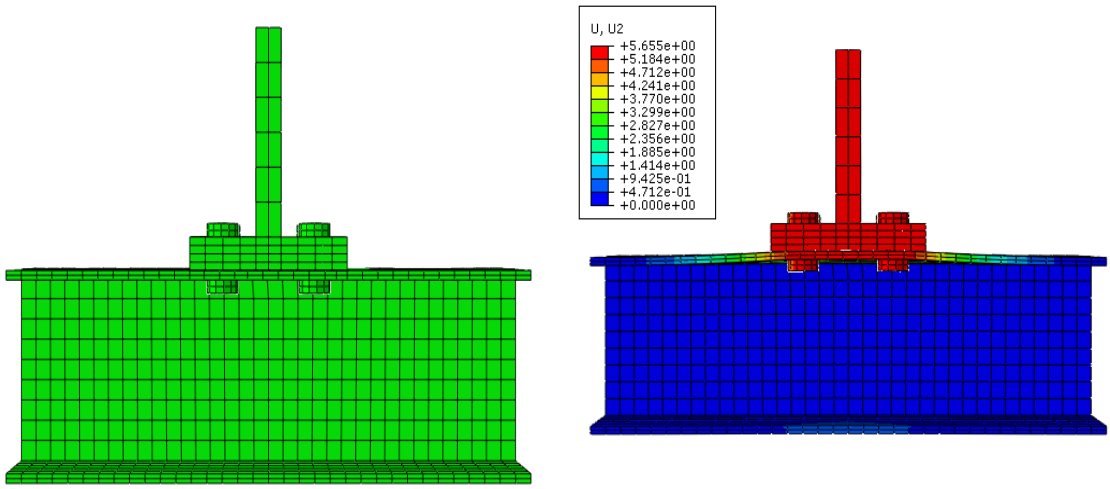

Figure 4.2: Finite element model for the test V1: Un-deformed and Deformed shape.

4.3 Comparisons on the second series tests

The deformed shapes of the finite element models and the relationship load versus displacement for the tests T1 to T8 are presented in the next figures.

✓ Numerical test T1

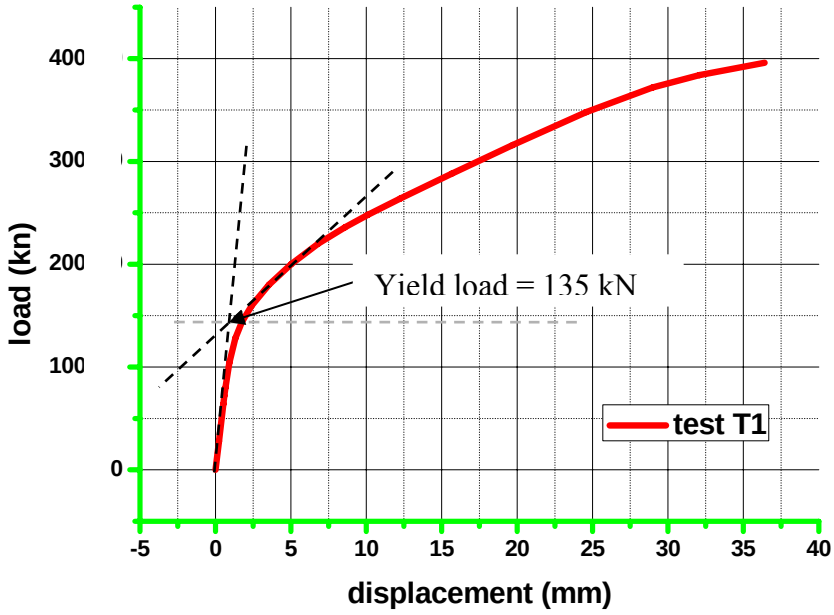

Figure 4.3 : Load-Displacement plot for the numerical test T1.

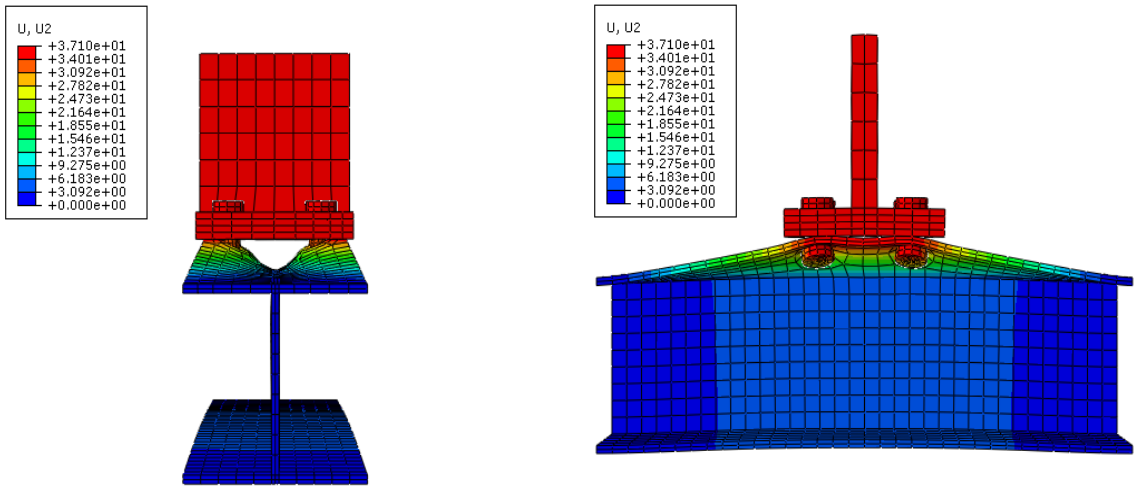

a. Elevation view. b. Plan view.

Figure 4.4 : Deformed shape for the numerical test T1.

✓ Numerical test T2

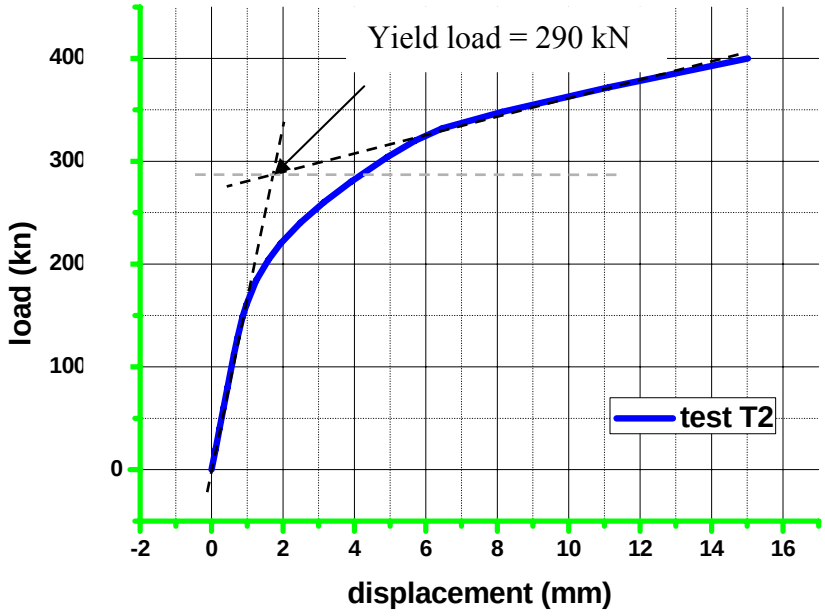

Figure 4.5: Load-Displacement plot for the numerical test T2.

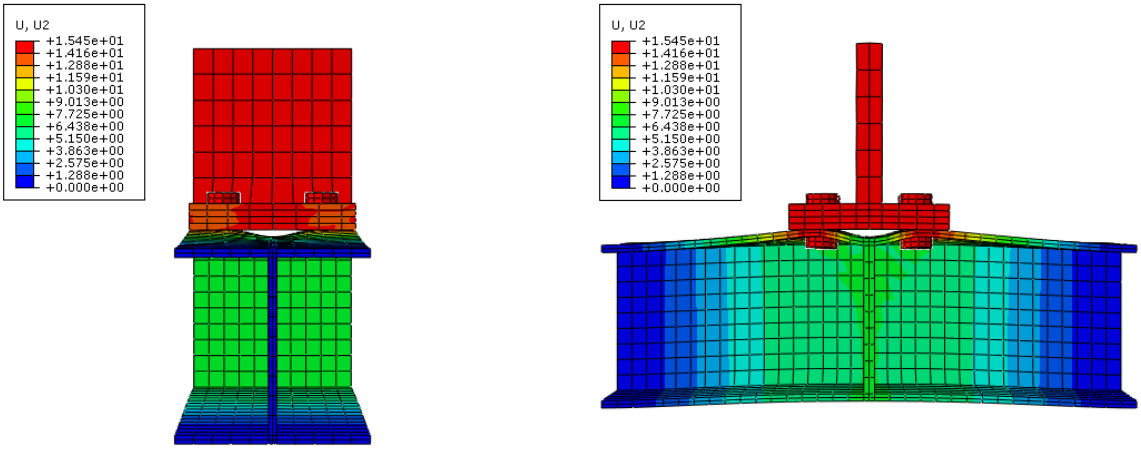

a. Elevation view. b. Plan view.

Figure 4.6 : Deformed shape of the numerical test T2.

✓ Numerical test T3

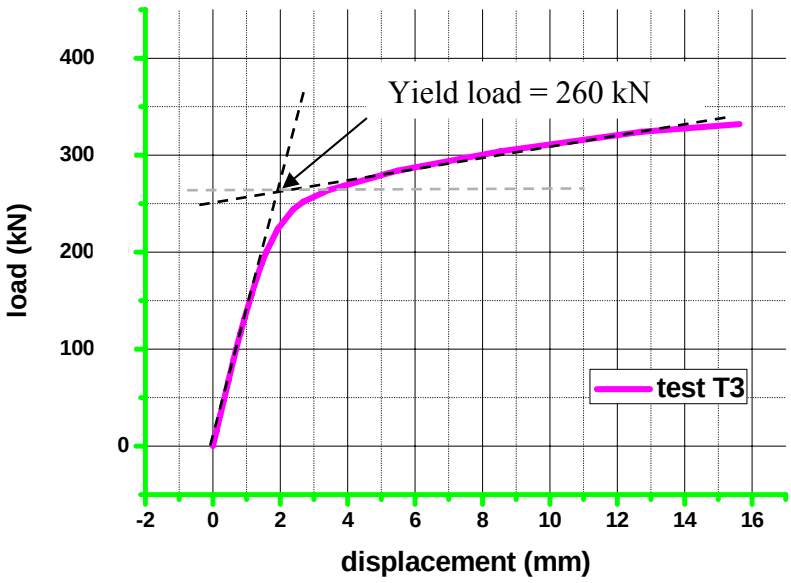

Figure 4.7: Load-Displacement plot for the numerical test T3.

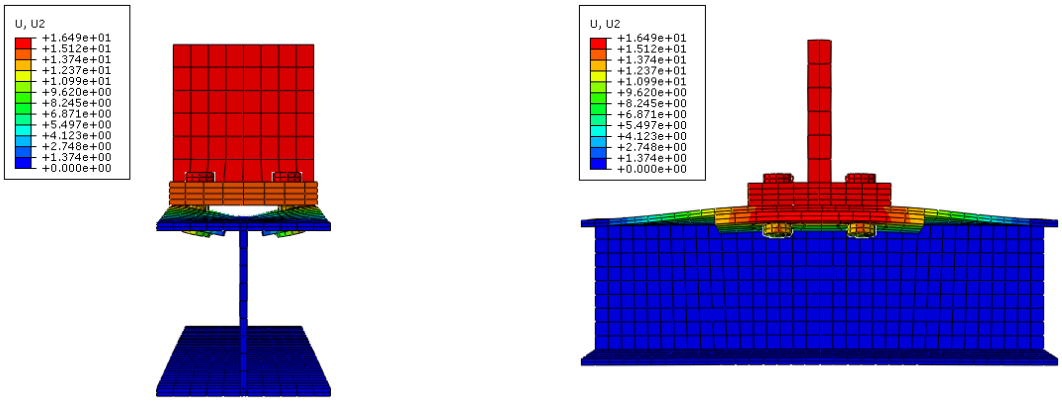

a. Elevation view. b. Plan view.

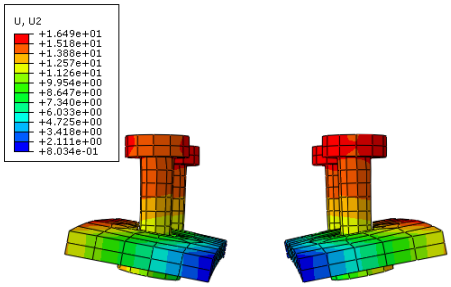

c. Deformed shape of the backing plate and the bolts.

Figure 4.8 : Deformed shape of the numerical test T3.

✓ Numerical test T4

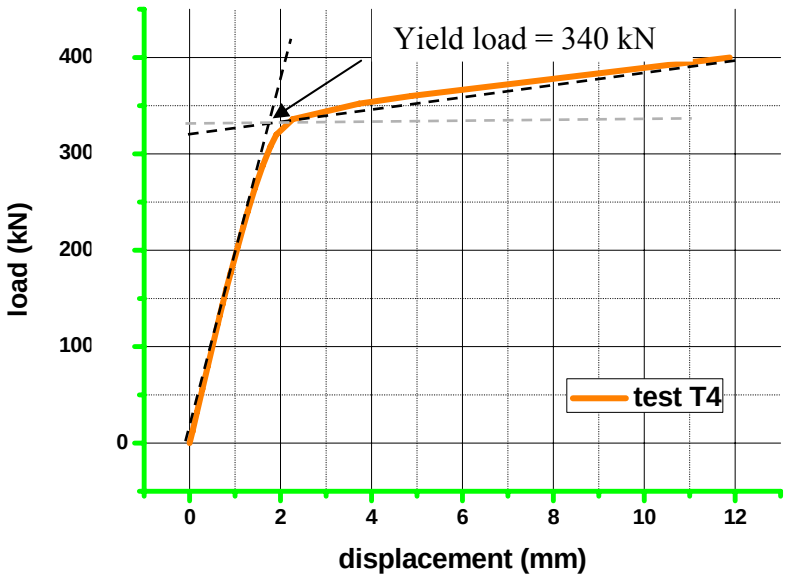

Figure 4.9: Load-Displacement plot for the numerical test T4.

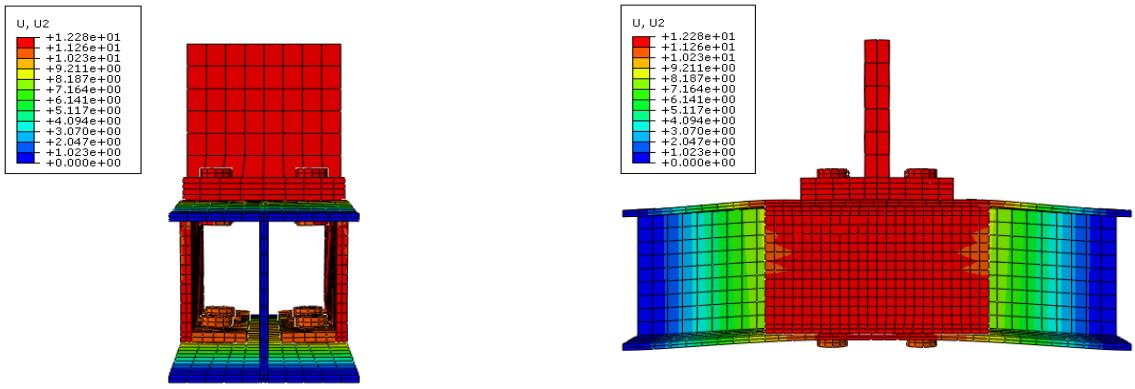

a. Elevation view. b. Plan view.

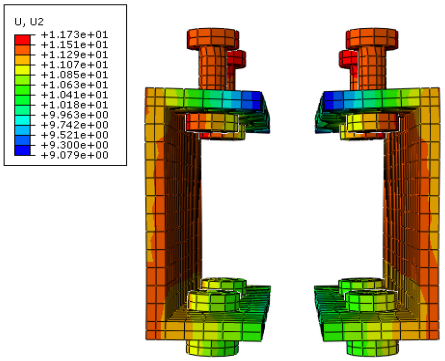

c. Deformed shape of the channels and the bolts.

Figure 4.10: Deformed shape of the numerical test T4.

✓ Numerical test T5

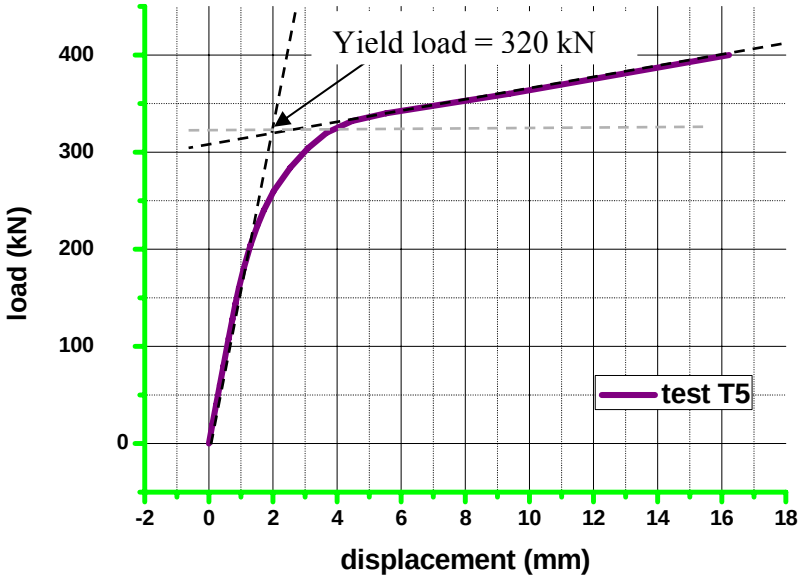

Figure 4.11: Load-Displacement plot for the numerical test T5.

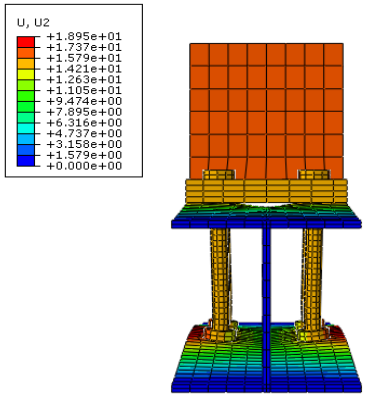

a. Elevation view.

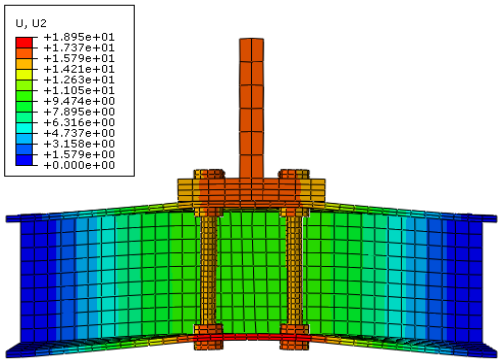

b. Plan view.

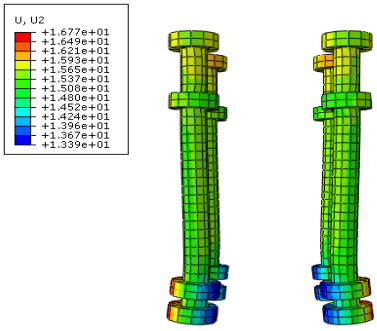

c. Deformed shape of the threaded bars.

Figure 4.12 : Deformed shape of the numerical test T5.

✓ Numerical test T6

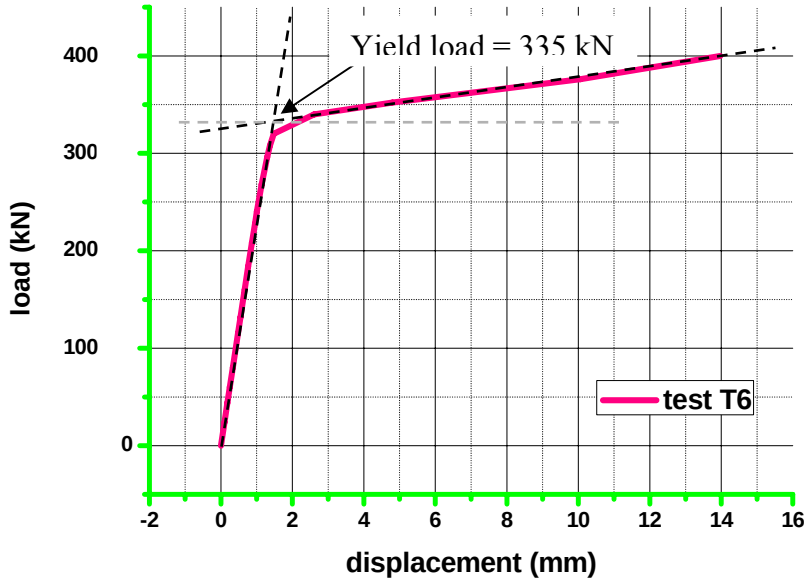

Figure 4.13: Load-Displacement plot for the numerical test T6.

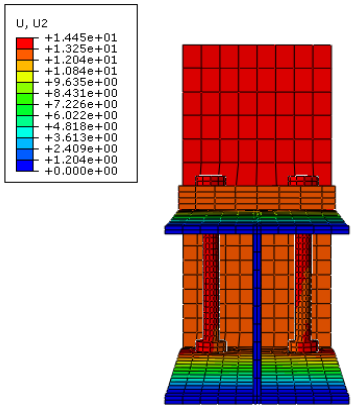

a. Elevation view.

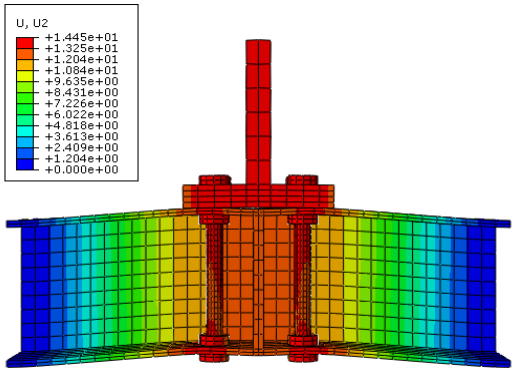

b. Plan view.

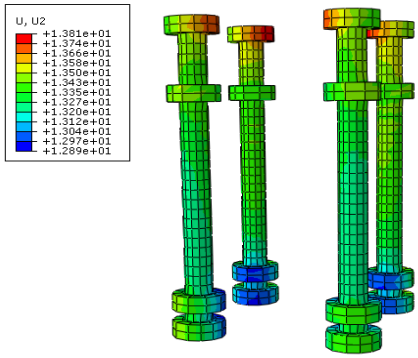

c. Deformed shape of the threaded bars.

Figure 4.14 : Deformed shape of the numerical test T6.

✓ Numerical test T7

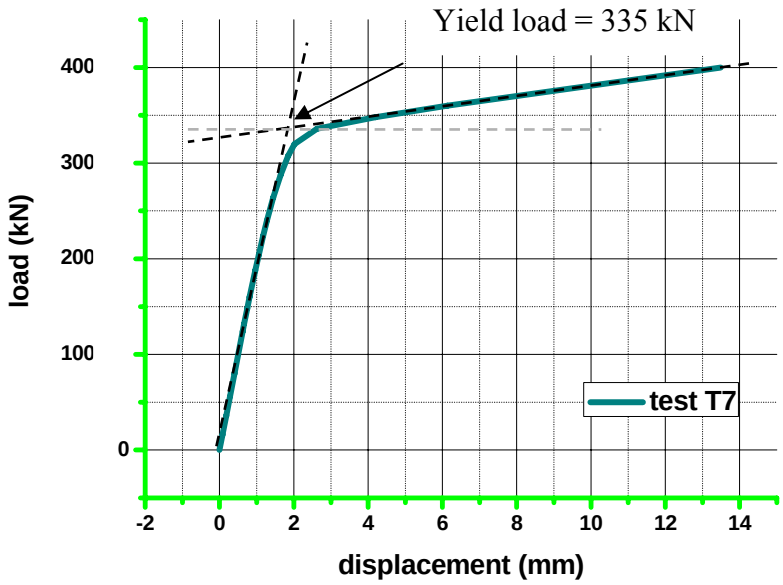

Figure 4.15: Load-Displacement plot for the numerical test T7.

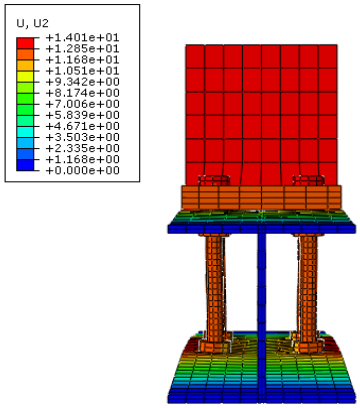

a. Elevation view.

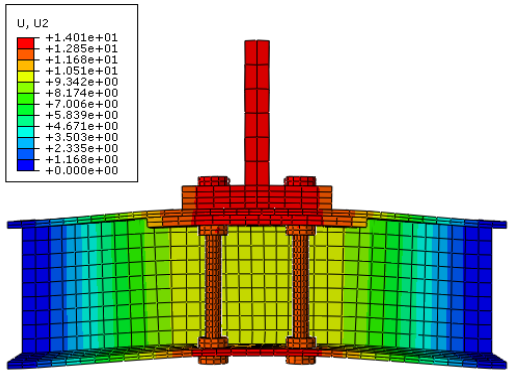

b. Plan view.

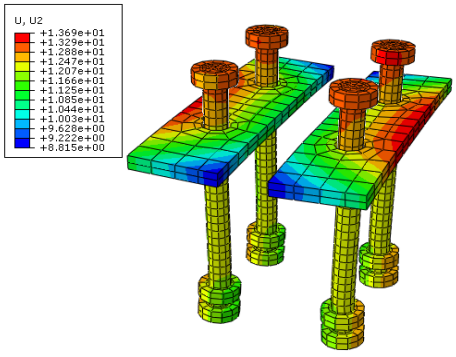

c. Deformed shape of the threaded bars and backing plates.

Figure 4.16 : Deformed shape of the numerical test T7.

✓ Numerical test T8

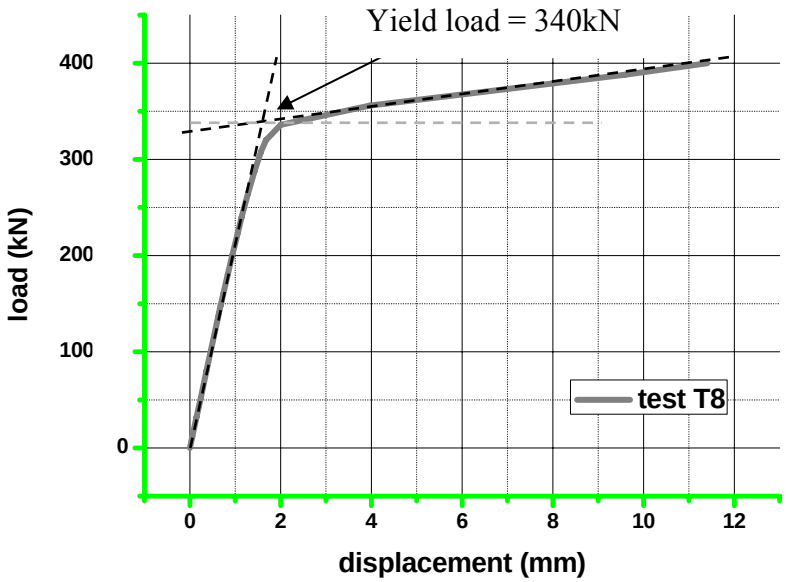

Figure 4.17: Load-Displacement plot for the numerical test T8.

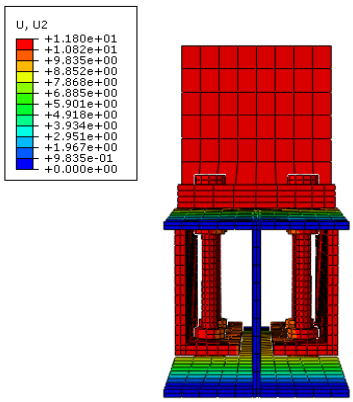

a. Elevation view.

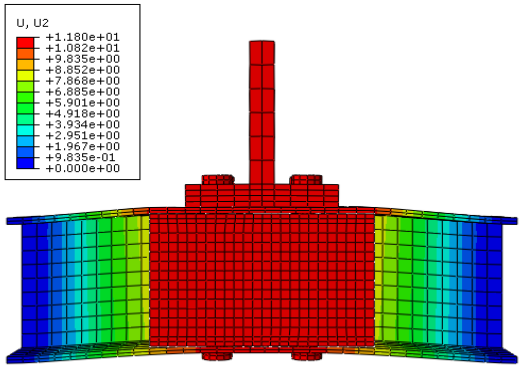

b. Plan view.

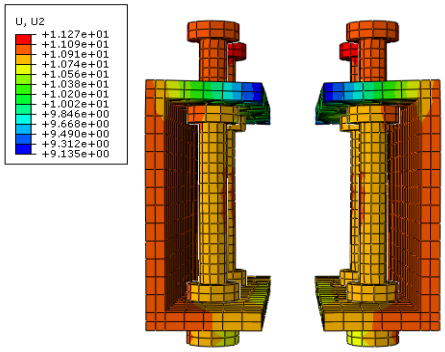

c. Deformed shape of the threaded bars and channels.

Figure 4.18 : Deformed shape of the numerical test T8.

From the graphs illustrated earlier, it can be observed that all the tests respond in the same way with increasing loads and have two dissimilar regions. At the beginning the curves are linear and while the load attain to a certain point become non-linear which give an idea that initially the connections behave elastically and when they achieve a resistance load the connection gradually lost stiffness and act as plastic.

The resistance load, called also the yield load, is the minimal value of the applied traction force on which the plastic hinges start to produce ; its value can be obtained by the intersection of the tangent lines traced on both linear and non-linear ranges as shown in the previous figures. The results obtained are summarized in the next table.

Table 4.3: The connections resistance load.

Identification Test	Yield load (Kn)	Reinforcement element
Test T1	135	Without
Test T2	290	Welded plates
Test T3	260	Backing plates
Test T4	340	Channels
Test T5	320	Threaded bars
Test T6	335	Threaded bars + welded plates
Test T7	335	Threaded bars + backing plates
Test T8	340	Threaded bars + Channels

For better understanding the behavior of the reinforced connections, a comparative study between such tests against the un-reinforced connection is necessary and will be discussed in the following sections.

4.3.1 Comparison on the reinforced tests against the un-reinforced test

✓ Numerical test T1 and T2

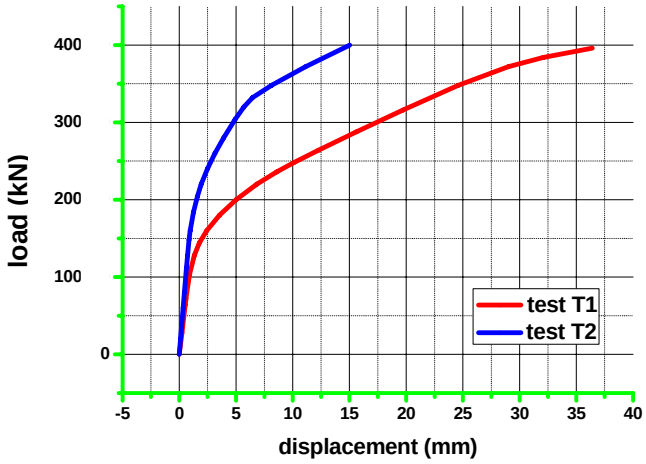

Figure 4.19: Typical applied load versus displacement for the numerical tests T1 and T2.

The comparison between the two curves shows that the use of the welded plate influenced the overall behaviour of the connection, the stiffness and the strength increase but the deformation capacity decreases.

✓ Numerical test T1 and T3

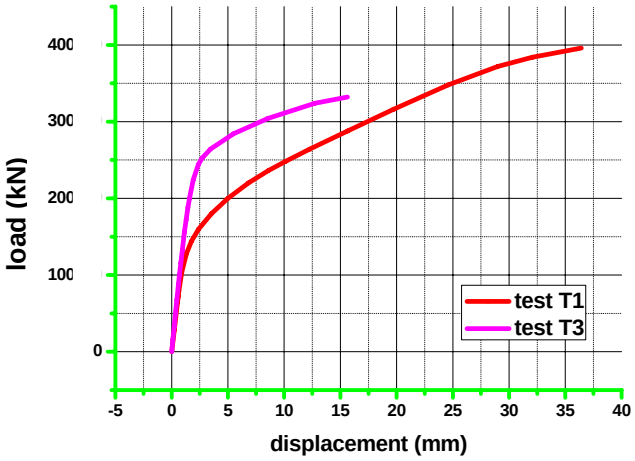

Figure 4.20: Typical applied load versus displacement for the numerical tests T1 and T3.

The same observation as previously cited was noted with the backing plate reinforced test. First yield occurred at about 260 kN. above this value a significant lost of stifness is observed.

✓ Numerical test T1 and T4

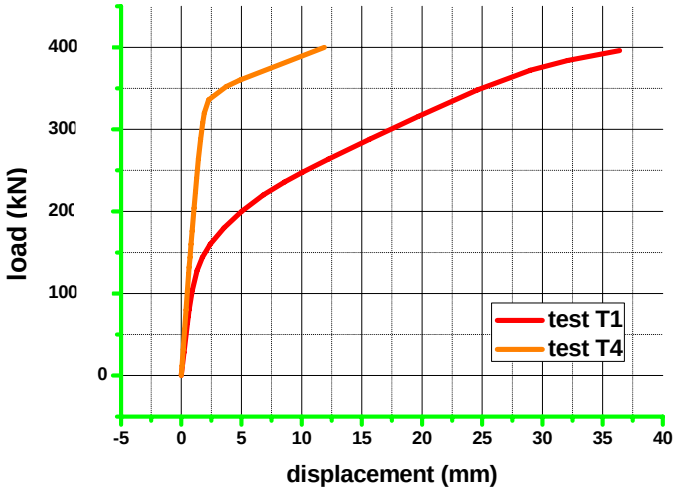

Figure 4.21: Typical applied load versus displacement for the numerical tests T1 and T4.

The Figure shows a significant divergence in term of stiffness between the two tests. The test T4 allowed contributing to an assembly whose load producing the beginning of the plastic hinges is approximately three times higher than the test T1.

✓ Numerical test T1 and T5

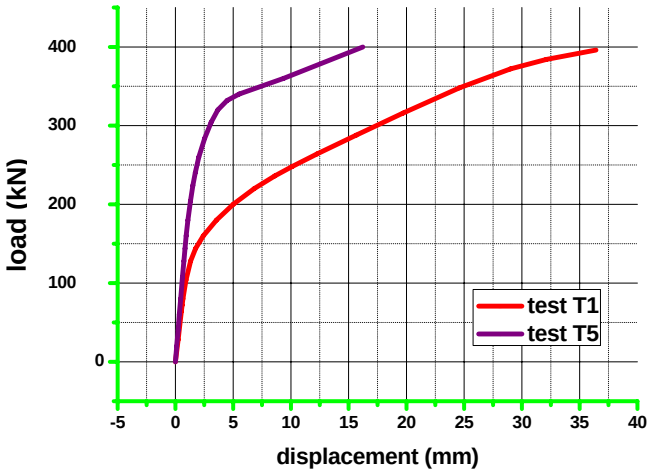

Figure 4.22: Typical applied load versus displacement for the numerical tests T1 and T5 .

The threaded bars strengthened test affords stiffer results than the reference test. The strength and stifness improve but the deformation capacity decreases .

✓ Numerical test T1 and T6

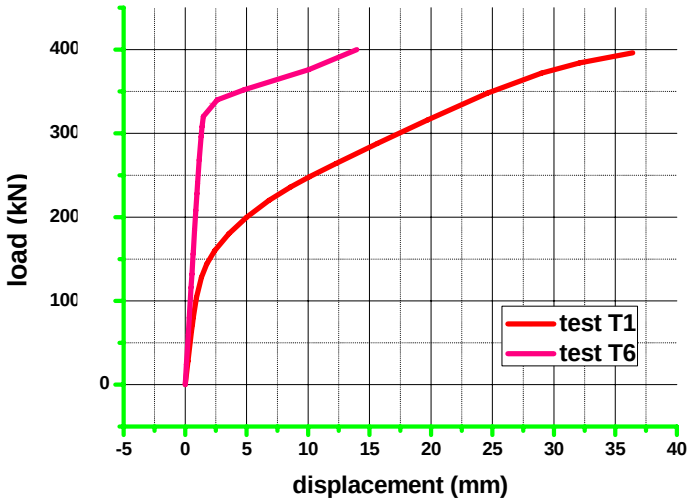

Figure 4.23: Typical applied load versus displacement for the numerical tests T1 and T6.

From the curves it was observed that the displacements plotted by the test T6 are less important than those plotted by the test T1at the same load.

✓ Numerical test T1 and T7

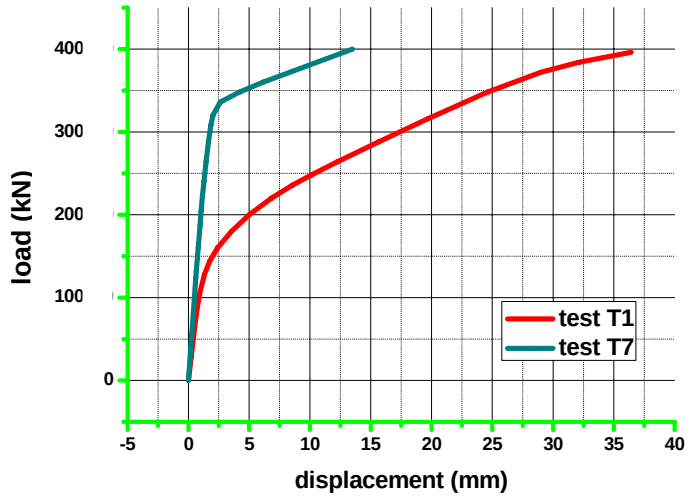

Figure 4.24: Typical applied load versus displacement for the numerical tests T1 and T7 .

The diagram shows test T7 carried out a higher resistance load than test T1. It shows also that test T7 is more stiffer and had a lower deformation capacity than the test T1.

✓ Numerical test T1 and T8

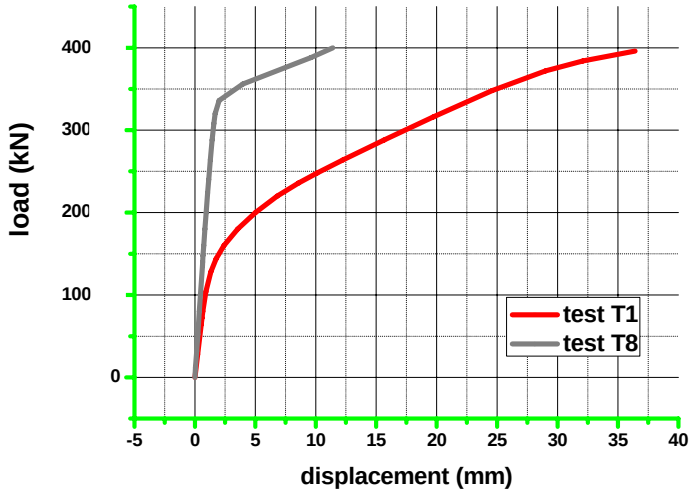

Figure 4.25: Typical applied load versus displacement for the numerical tests T1 and T8.

As can be observed, the comparison of the behaviour of both connections leads to the same previous notes.

For summarizing, the previous numerical results comparaisons can be exposed in the figure 4.26.

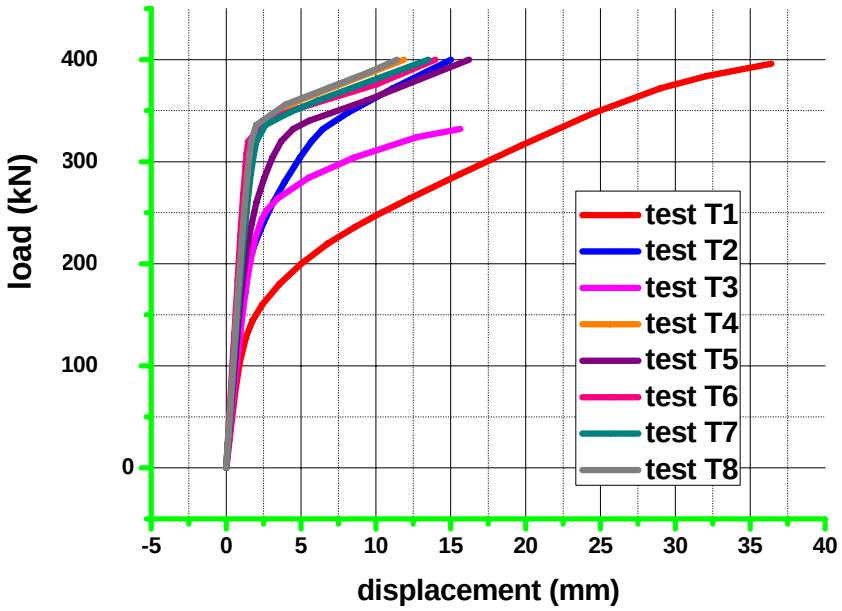

Figure 4.26: Comparison among stiffened connections versus the un-stiffened connection.

Of the results examination, it seems to be reasonable to say that in term of the overall behavior , the load-displacement curves were affected by the employing of the stiffners .

By increasing in the load the deformation capacity reduces for all stiffened connections however a negligible difference is also must to be noted for the tests T2,T4,T5,T6,T7,T8.

The initial stiffness increase and it is more important for the tests T4,T6,T7,T8. In the plastic region, the stiffness is approximately the same for all the connections, an exception was observed for the backing plate reinforced test when a lower stiffness against the other stiffened connections occured.

A remarkable improvement in the strength is necessary to cite and it is practically the same for the tests T4, T6,T7,T8 as referred in the next diagram.

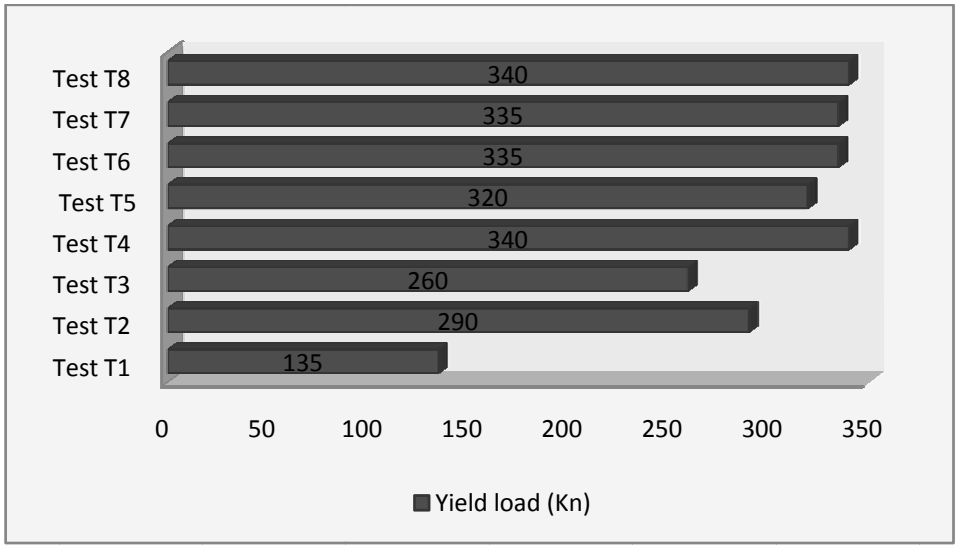

Figure 4.27: Comparison of strength improvement between stiffened connectios versus the un-stiffened connection.

The aim of this dissertation is to study the behavior of the threaded bars as a new type of reinforcement and check their influence on the amelioration of the behavior of the whole conection,therefore a more detailed comparison focused on such a stiffner will be presented as following.

4.3.2 Comparaison on the threaded bars stiffened tests

✓ Numerical tests T2,T5,T6

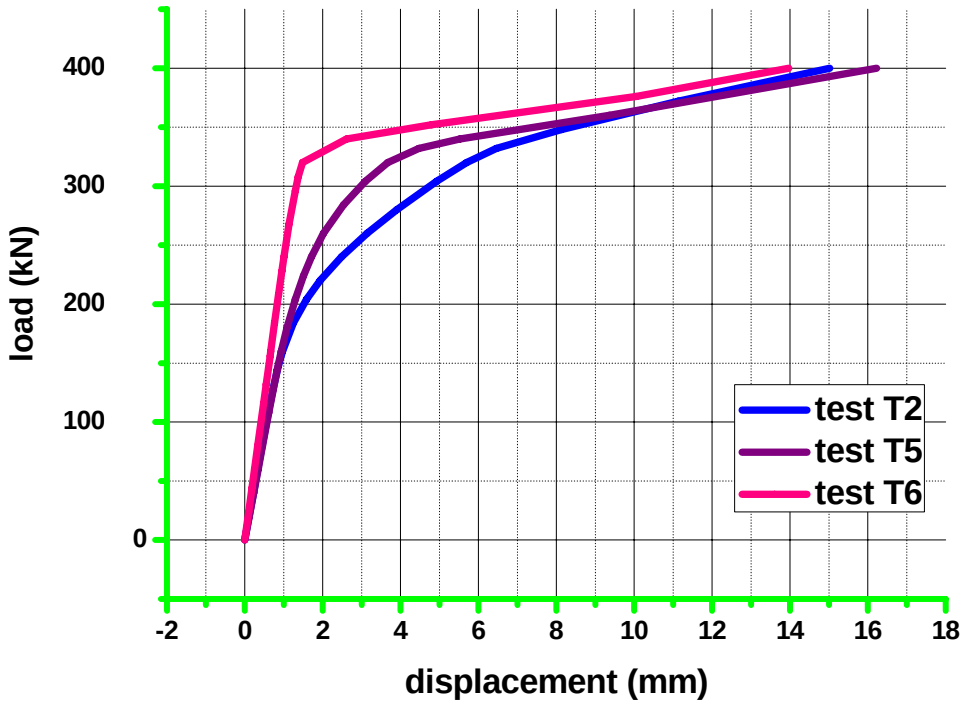

Figure 4.28: Load-displacement comparison for the numerical tests T2,T5,T6.

It is apparent from the figure that the using of the threaded bars and the welded plate together yields to more stiffer and strengthened connection. The improvement of the strength is 17.24 % compared to the test T2 and 6.25% compared to the test T5.

The behavoir of the the test T2 and T5 is identical in term of stiffness, the difference arises in the strength .

A negligeble difference in the deformation capacity is also observed for the three tests.

✓ Numerical tests T3,T5,T7

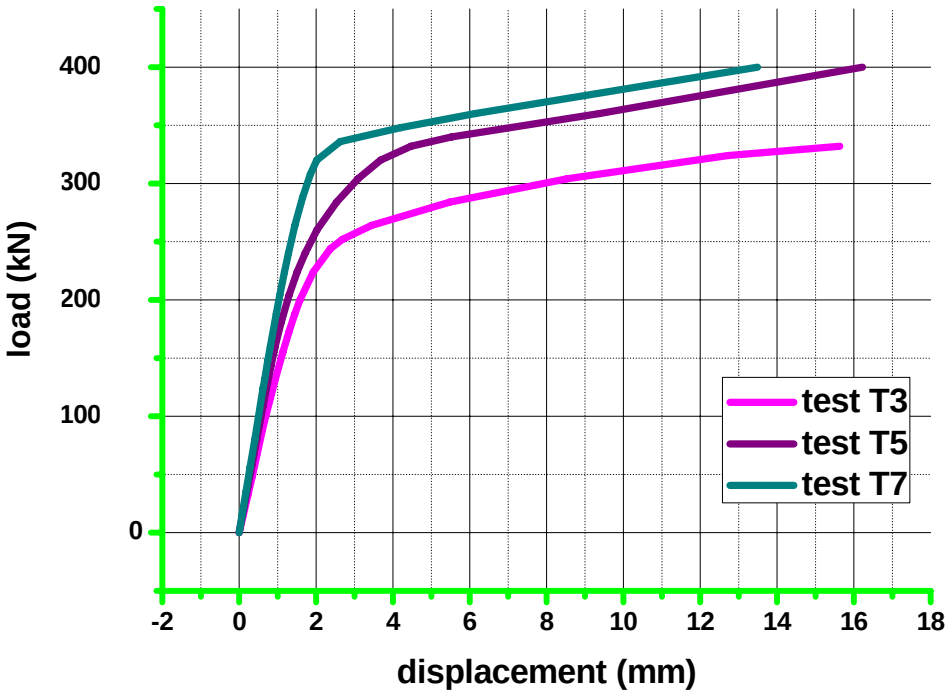

Figure 4.29: Load-displacement comparison for the numerical tests T3,T5,T7.

The tests clearly yield differente responses. The comparison between the load-displacement curves of the connections shows that test T7 is stiffer than the test T5, which is by itself more stiffer than the test T3.

Although the maximum applied load for the test T3 is 320 kN , but it is shown from the trend of the curve that the deformation capacity of the connections was reduced significantly from the test T3 to T7.

It shoud be also noted that the resistance load of the test T7 is higher than both the other tests.

✓ Numerical tests T4,T5,T8

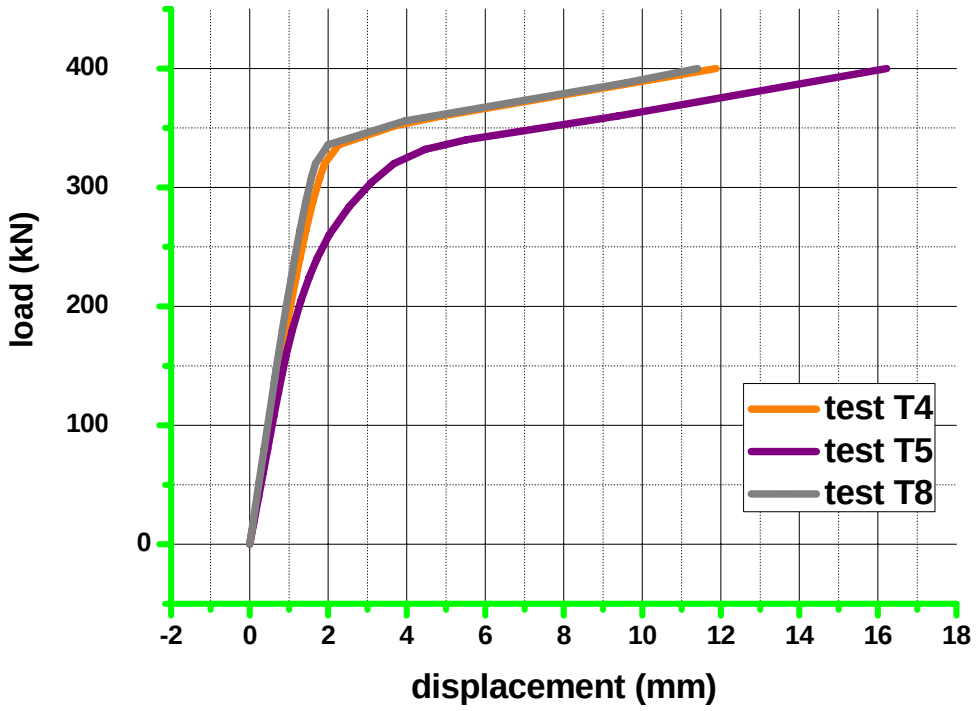

Figure 4.30: Load-displacement comparison for the numerical tests T2,T5,T6.

The numerical results plotted by the test T4 and those plotted by the test T8 are extremely coincident and they are similar in term of stiffness, strength and deformation capacity.

Although the test T5 is less stiffer than both the tests T4 and T8 but it is still has the higher deformation capacity.

The percentage of difference for the strength of the test T5 against the tests T4 and T8 is in order of 6.25%.

4.3.3 Comparison between the results of the finite element method and the yield line method

Different yield line patterns were used to predict the yield load done by each test based on the results done by the finie element analysis. Table 4.4 cited a percentage of strength improuvement achieved .

Table 4.4: Strength improvement of stiffend tests.

Test identification	Type of reinforcement	Yield load (kN)	Strength improvement
Test T1	Without	135	-
Test T2	Welded plates	290	0.46
Test T3	Backing plates	260	0.52
Test T4	Channels	340	0.40
Test T5	Threaded bars	320	0.42
Test T6	Threaded bars + welded plates	335	0.41
Test T7	Threaded bars + backing plates	335	0.41
Test T8	Threaded bars + Channels	340	0.40

The table shows a slightly difference between the tests T4, T7, T8 stiffened by channels, threaded bars +backing plates and threaded bars +channels respectively and the test T5 stiffened by threaded bars .

So, by comparing a strength increasing of the tests T4, T7, T8 and the test T5, it can be conclude that the use of backing plates and channels with the threaded bars to act as one element didn't contribute in the total internal work of the whole connection. And this is why the same yield line pattern was adopted for those tests.

The same remark was reached by comparing the test T4 and the test T5. The channel element didn't give a remarkable differnce against threaded bar element in term of internal energy, and by observing the deformation plot of the test T5, it was also decided to adopted the same yield line pattern of the test T4.

The same remark was reached by comparing the test T2 and T6.

The following sections illustrate the results obtained.

4.3.3.1 Yield line results

The geometrical characteristics of the tests whose used to predict their resistance load using the yield line method are displayed in the next table. The predicted resistanse load is displayed in table 4.6.

Table 4.5: Dimensions of the Yield Line Patterns.

Test	t_f (mm)	n (mm)	m (mm)	n' (mm)	a(mm)
Test T1	6.8	30	37.79	30	90
Test T2	6.8	30	37.79	30	90
Test T3	6.8	30	37.79	30	90
Test T4	6.8	30	37.79	30	90
Test T5	6.8	30	37.79	30	90
Test T6	6.8	30	37.79	30	90
Test T7	6.8	30	37.79	30	90
Test T8	6.8	30	37.79	30	90

Table 4.6:Yield Line Results.

Test identification	Type of reinforcement	Predicted yield load (kN)
Test T1	Without	100
Test T2	Welded plates	159
Test T3	Backing plates	239
Test T4	Channels	380
Test T5	Threaded bars	380
Test T6	Threaded bars + welded plates	159
Test T7	Threaded bars + backing plates	380
Test T8	Threaded bars + Channels	380

4.3.3.2 Comparison with finite element results

The next table illustrates the results value of both methods used to predict the yield load.

Table 4.7: Comparison between the predicted and finite element yield load.

Test	Type of reinforcement	Predicted yield load (kN)	F.E. yield load (kN)	Predicted /F.E.
Test T1	Without	100	135	0.74
Test T2	Welded plates	159	290	0.55
Test T3	Backing plates	239	260	0.92
Test T4	Channels	380	340	1.12
Test T5	Threaded bars	380	320	1.19
Test T6	Threaded bars + welded plates	159	335	0.47
Test T7	Threaded bars + backing plates	380	335	1.13
Test T8	Threaded bars + Channels	380	340	1.12

It can be noted for the unreinforced test T1the yield load pattern gives a lower load than the finite element. The yield load predicted is within 26%.

The yield load predicted for the welded stiffened test is under-estimated; the range of difference is within 45%. The same observation should be highlighted in the case of the test T6 when 53 % of dissimilarity was found.

For the backing reinforced test, the results showed good agreement between the predicted and finite element yield load. The differentiation is within 8%.

The comparison of the finite element load for the tests T4, T5, T7, and T8 with the predicted yield load gives12%, 19%, 13%, and 12% of divergence respectively.

4.4 Comparison on the third series of tests

The deformed shapes of the finite element models and the relationship load versus displacement for the tests C1 to C5 are presented in the next figures.

✓ Numerical test C1

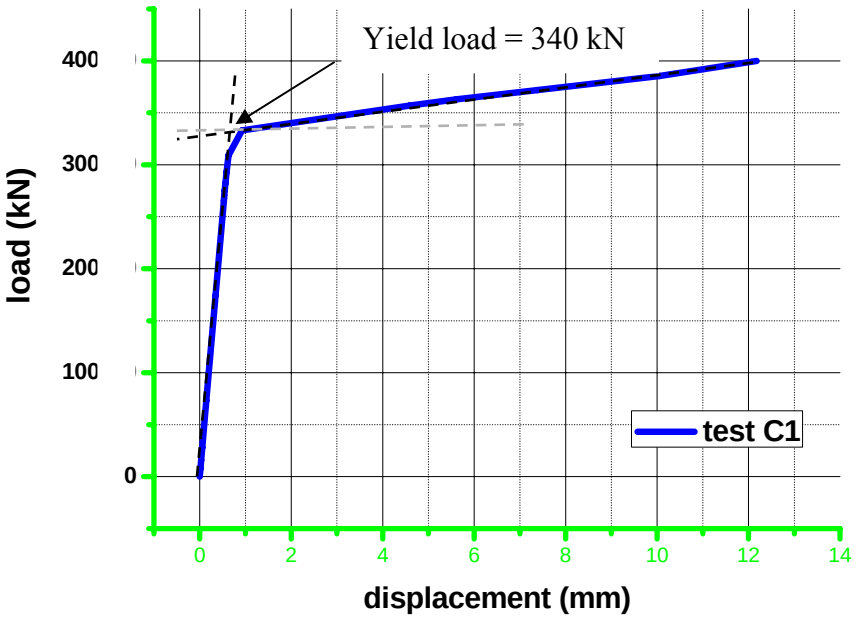

Figure 4.31 : Load-Displacement plot for the numerical test C1.

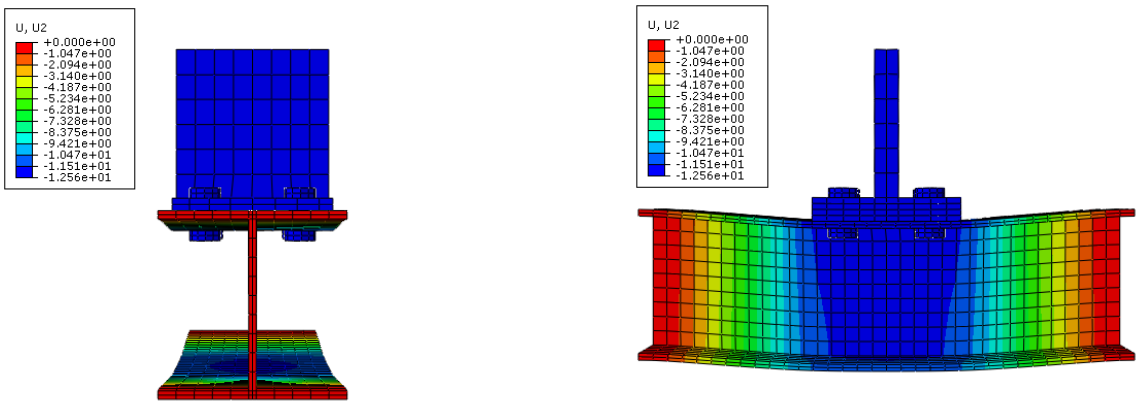

a. Elevation view. b. Plan view.

Figure 4.32 : Deformed shape for the numerical test C2.

✓ Numerical test C2

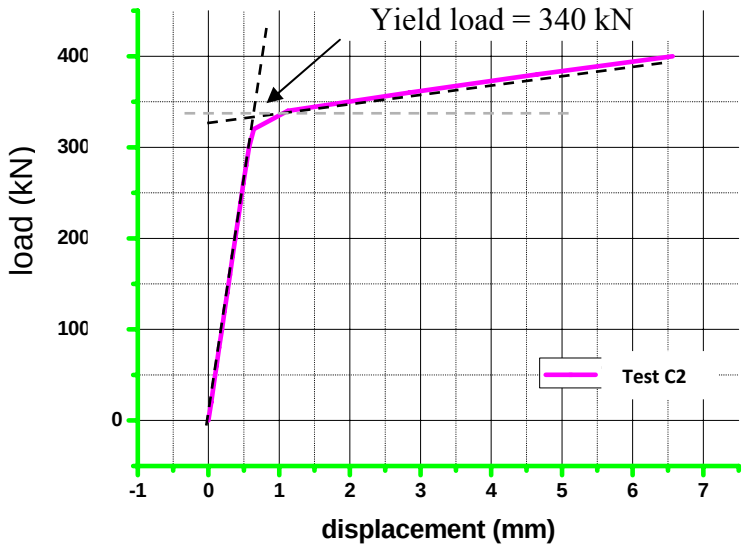

Figure 4.33: Load-Displacement plot for the numerical test C2.

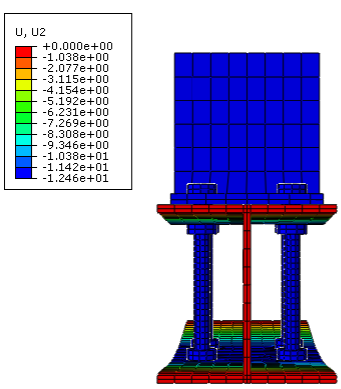

a. Elevation view.

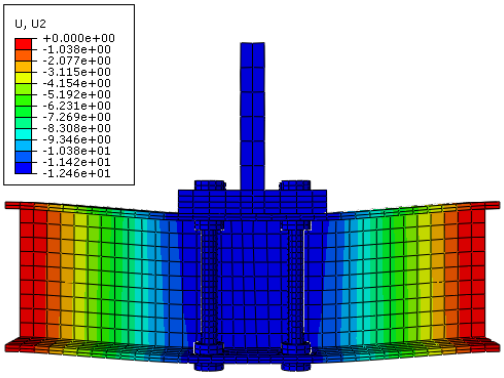

b. Plan view.

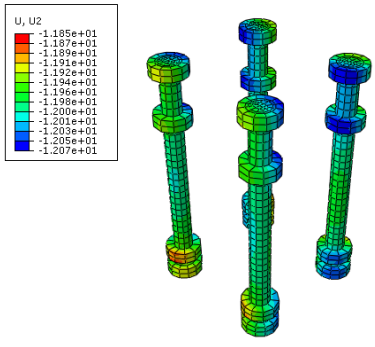

c. Deformed shape of the threaded bars.

Figure 4.34 : Deformed shape for the numerical test C2.

✓ Numerical test C3

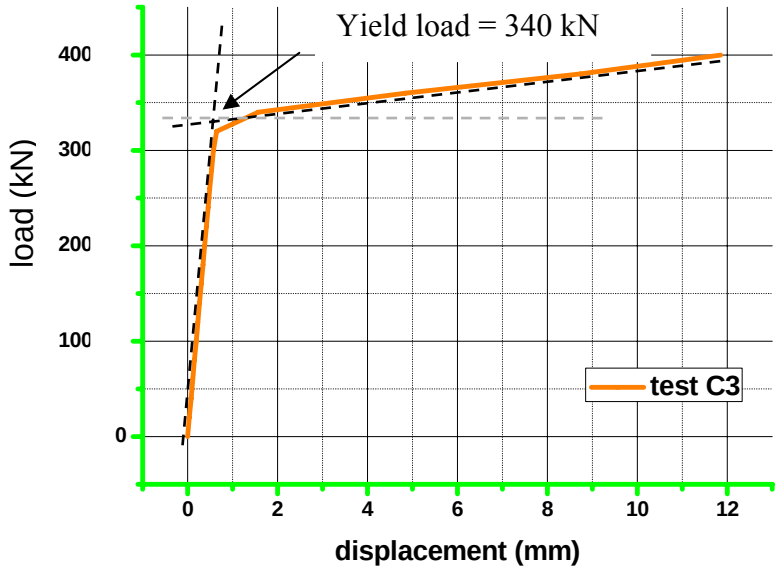

Figure 4.35 : Load-Displacement plot for the numerical test C3.

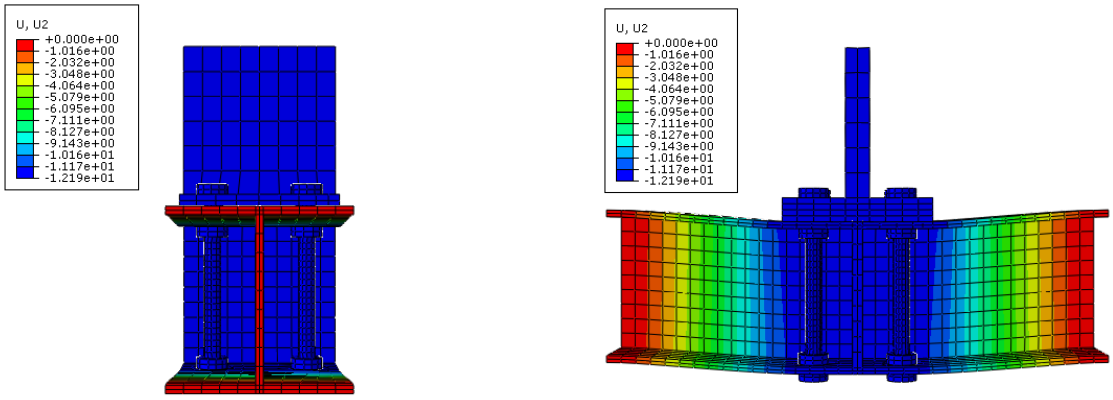

a. Elevation view. b. Plan view.

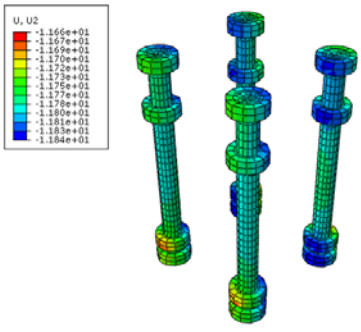

c. Deformed shape of the threaded bars.

Figure 4.36 : Deformed shape for the numerical test C3.

✓ Numerical test C4

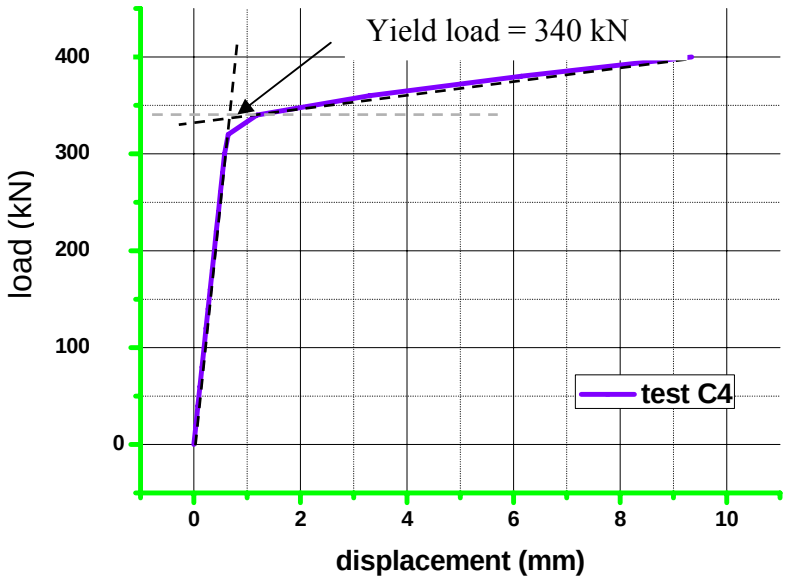

Figure 4.37 : Load-Displacement plot for the numerical test C4.

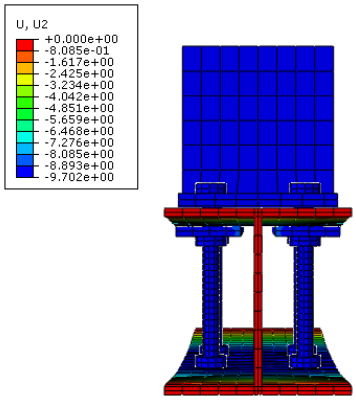

a. Elevation view.

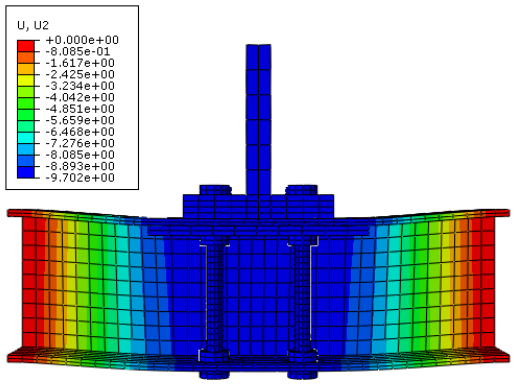

b. Plan view.

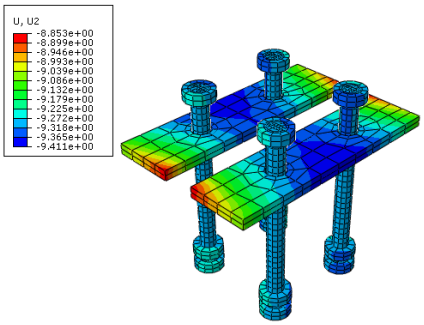

c. Deformed shape of the threaded bars and the backing plate.

Figure 4.38 : Deformed shape for the numerical test C4.

✓ Numerical test C5

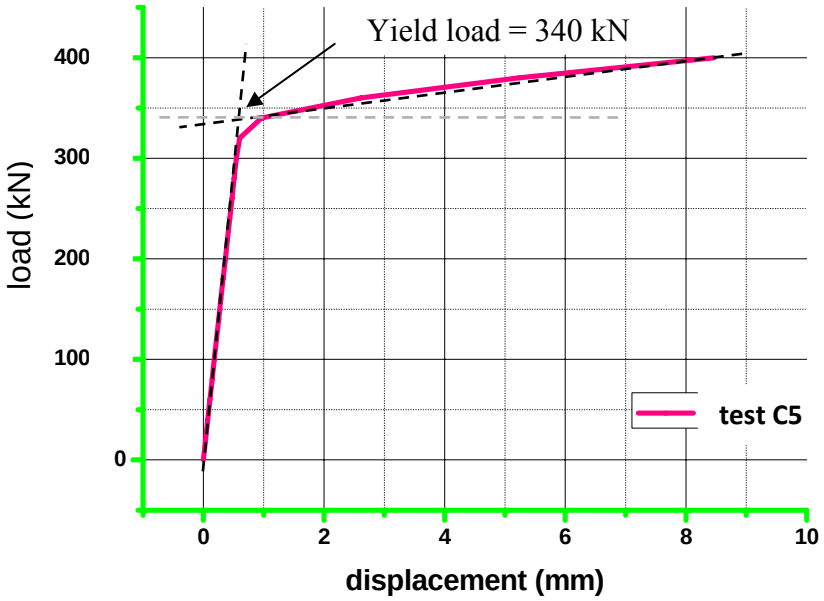

Figure 4.39 : Load-Displacement plot for the numerical test C5.

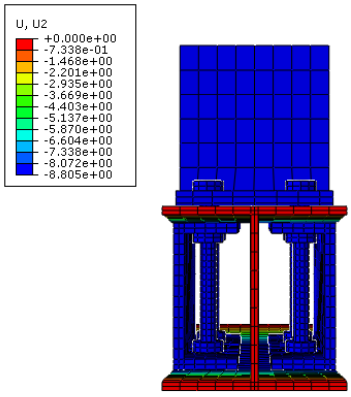

a. Elevation view.

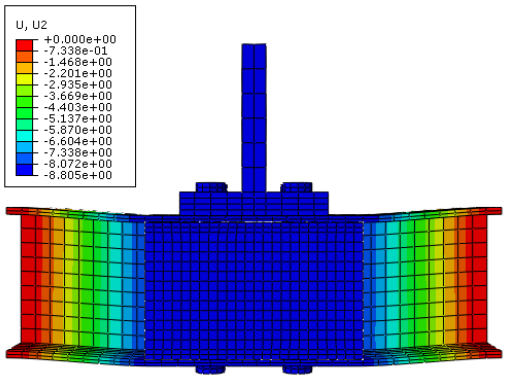

b. Plan view.

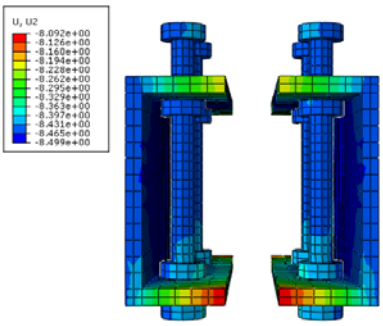

c. Deformed shape of the threaded bars and the channels.

Figure 4.40 : Deformed shape for the numerical test C5.

For summarizing, the previous numerical results can be exposed in the next figure.

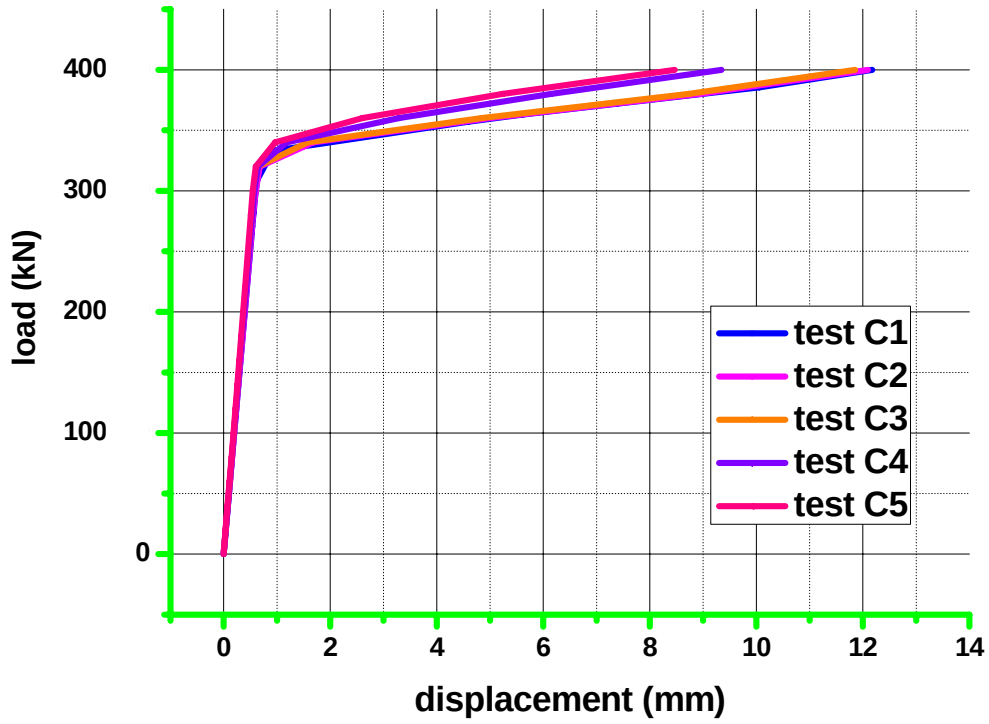

Figure 4.41: Comparison among the stiffened connections versus the un-stiffened connection.

It can be seen from figure 4.41 that the load-displacement curves of all the t-stub connection are almost linear when the load is less than 340 kN, when the connections passed that value behaved non-linearly.

The resistance load for all the connections is approximately the same and it is equal to 340kN.

It can be shown also from the figure 4.41, the stiffness in the plastic region for test C1, C2 and C3 is extremely the same. The same observation should to be noted for the test C4 and C5.

A negligible difference in the deformation capacity is established.

4.5 Conclusion

From the results discussed in this chapter, it can be observed that the behavior of the t-stub connections differs from test to other and this due to the different reinforcement elements added.

For the three series of tests, the curves load-displacement had two different regions, the first refer to the elastic behavior of the materials, as well as the second region refer to the plastic behavior of the materials.

The effect of the different element of reinforcement on the overall behavior of the connection is more important in term of strength, stiffness and capacity deformation for the second series of tests than the third series of tests.

The results of the yield patterns used varied from underestimate, reasonable to overestimate results.

CONCLUSION & RECOMMENDATION

CONCLUSION

Based upon the numerical and theoretical research conducted, the primary conclusions can be summarized as follows:

- A series of fourteen t-stubs to column connections are undertaken to study the behavior of the threaded bars in compression and tension zone. The fourteen tests are divided into three series tests.

- A t-stub to column connection was experimentally tested to study its force-deformation behaviour by **Sethi** [16]. The experimental behaviour was compared with built up finite element model.

- A finite element connection model was successfully constructed and developed using ABAQUS finite element program. The C3D8R element type used in the modeling was found to be suitable for use in nonlinear analysis of the t-stub to column connections.

- The load-displacement curve plotted from ABAQUS analysis results had shown a similar trend as that of the experimental load-displacement curve. The percentage of difference of resistance moment between the laboratory test and the finite element analysis was acceptable. Besides, mode of failure of the finite element model also matched the experimental mode of failure.

- The yield line method was used to develop formulas that can predict the minimum collapse load on which a plastic hinge starts to produce.

- The comparison between the yield line method and the finite element method conducted to say that some yield line patterns were conservative and other were overestimate.

- The different element of reinforcement added for the second series of tests were improved the strength and the stiffness of the connections but decrease the deformation capacity. This was contrary for the third series of tests when a negligible variation on the post stiffness and the deformation capacity was shown.

- A special focus was considered on the behavior of the threaded bars, the following conclusions can be noted:

  - Resistance improvement was shown if using the threaded bars and the welded plate together and it was more important than using the welded plate alone. The same remark was noted for the use of the threaded bars and the backing plate together.

  - For the test T8, it wasn't useful to apply the threaded bars and the channels together because using these two reinforcement element didn't bring any improvement in term of overall behavior of the connection.

  - For the compression tests, the use of the threaded bars had a negligible effect on the behavior of the connection although, **Nip and Surtees** [13] had proved an increasing in the strength of connections used in their studies.

- Finite element analysis can be used as analysis tool to predict the nonlinear behaviour of t-stub to column connections.

The finite element analysis can be seen to provide advantages in terms of time and expense over full scale testing and can produce a more complete picture of stress, strain and force distributions.

RECOMMENDATION

Some recommendations are suggested for future research. The recommendations are explained as below:

- The amelioration of the validated numerical model by taking in account the existence of the welds.

- Standard tensile test should be carried out on the bolts and the reinforcement element. The data such as initial yield stress is required in defining the nonlinearity behavior of the connection.

- The plastic material properties should be assigned as accurate as possible to ensure good correlation between finite element analysis and laboratory test.

- Mesh refinement and convergence test should be performed in future analysis to obtain more reliable results, by using other finite element analysis programs.

- The moment-rotation relationship should be taken into consideration, if is it available, when comparing the finite element analysis with the experimental tests for more insure the degree of accuracy of finite element analysis.

- The sensitivity analysis of reinforced T-stubs connection to various parameters such as the thickness of the reinforcement plates and the pretension force should be taken in charge.

- The evolution of the bolt load and the contact pressure due to the prying force effect can be studied.

- More works can be performed on the effect of reinforcement of the end-plate moment connections in compression and tension zone with full scale test rather than t-stubs models.

- The effect of reinforcement on the strong columns must be also taking into consideration.

- Amelioration in the yield line patterns.

REFERENCES

1. H B Kaushik and Dr D C Rai "An Insight into the flexibility of light beam-to-column connections" , February 2006.

2. Sumner, E. A "Unified design of extended end-plate moment connections subject to cyclic Loading", Ph.D. Dissertation, Virginia Polytechnic Institute and State University, Blacksburg, June 2003.

3. Wong Jyie Yiee. "Finite Element Analysis of Flush End Plate beam to column bolted steel Connection on Minor axis using Lusas software" , University of Malysia, 2007.

4. Chemin Lim. "Low cycle fatigue life prediction of four bolt extended unstiffened end plate moment connections" Ph.D. Dissertation, North Carolina State University, 2009.

5. Ana M. Girão Coelho; Luís Simões da Silva; and Frans S. K. Bijlaard "Finite-element modeling of the nonlinear behavior of bolted T-Stub connections", Journal of structural engineering © ASCE . June 2006.

6. "Design of fully restrained moment connections", AISC LRFD 3rd Edition , course online, 2001.

7. Tapan Sabuwala. "Finite element analysis of steel beam to column connections subjected to blast loads", The Pennsylvania State University, August 2001.

8. Packer,J.A. and Morris,L.J.,"A Limit state design method for the tension region of bolted beam column connections", The Structural Engineer Vol 55, Oct.1977.

9. Zoetemeijer,P,"A design method for the tension side of statically loaded bolted beam to column connections", Heron Vol 20(1),1974.

10. D.B. Moore and P.A.C. Sims, "'Preliminary Investigations into the Behaviour of Extended End-Plate Steel Connections with Backing Plates", Journal of Constructional Steel Research 7(1987) 297-310.

11. W. Grogan , J.O. ," Experimental behaviour of end plate connections reinforced with bolted backing angles Surtees", Journal of Constructional Steel Research 50 (1999) 71–96

12. Z. Al-Khataba, A. Bouchair , "Analysis of a bolted T-stub strengthened by backing-plates with regard to Eurocode 3", Journal of Constructional Steel Research 63 (2007) 1603–1615

13. T. F. Nip and J. O. Surtees , "threaded bar compression stiffening for moment connections", School of Civil Engineering, University of Leeds, Leeds LS2 9JT, UK. 2001

14. T. F. Nip and J. O. Surtees ,"Use of threaded rod compression stiffening in end plate connections", the structural engineer Vol 79/N0 11 June 2011.

15. Tagawa and Gurel," Strength evaluation of bolted moment connections stiffening with channels"

16. Sethi A. "Non-welded reinforcement in bolted steel beam/column connections". Doctoral dissertation, University of Leeds, 1989.

17. Aliane Yasmina," Renforcement non soudée dans le cas d'un assemblage Poteau pouter avec platine '', Magistere thesis, University of Saad Dehlab of Blida,2003

18. ABAQUS 6.9, "Getting Started with Abaqus".

19. ABAQUS 6.9," Analysis user manual".

20. P.Prabha, S.Seetharaman, S.Arul Jayachandran and V. Marimuthu," Mimicking expensive experiments by Abaqus", Scientists, Structural Engineering Research Centre, CSIR campus, Taramani, Chennai - 600 113.

21. K.S. Al-Jabri a ,A.Seibi b ,A.Karrechc," Modelling of unstiffened flush end-plate bolted connections in fire ",Journal of Constructional Steel Research 62 (2006) 151–159

22. Jeon Kim, Joo-Cheol Yoon, Beom Soo Kang,"Finite element analysis and modeling of structure with bolted joints",Applied mathematical modeling 31 (2007) 895 911

23. Ying Hu, Buick Davison, Ian Burgess and Roger Plank," Multi-Scale Modelling of Flexible End Plate Connections under Fire " , The Open Construction and Building Technology Journal, 2010, 4, 88-104